THE ROLE OF SURFACE FREE ENERGY IN THE COMPACTION OF POWDERS

A THESIS SUBMITTED TO
THE UNIVERSITY OF MANCHESTER
FOR THE DEGREE OF
DOCTOR OF PHILOSOPHY

IN THE
FACULTY OF SCIENCE
OCTOBER 1988

BY

MANEE LUANGTANA-ANAN B.Pharm.

DEPARTMENT OF PHARMACY
UNIVERSITY OF MANCHESTER

ProQuest LLC
789 East Eisenhower Parkway
P.O. Box 1346
Ann Arbor, MI 48106 - 1346

DEDICATED TO

MY PARENTS

DECLARATION

The author hereby declares that no portion of the work referred to in this thesis has been submitted in support of an application for another degree or qualification of this or any other university or other institution of learning.

CONTENTS

PART 2

ACKNOWLEDGEMENTS

I wish to express my profound gratitude to my supervisor, Dr. John T. Fell for his advice, kindness and endless help throughout the course of this study.

Sincere thanks are due to the following:

Professor A. Tallentire for the provision of research facilities in the Department of Pharmacy.

The Royal Pharmaceutical Society of Great Britain for the award of a scholarship , The Manchester Pharmaceutical Association Scholarship.

The University of Manchester for the award of a scholarship , Alfred Lucas Blain Memorial Scholarship in Pharmacy.

Lt. S. Jai-In (RTN) for the advice on computing matters.

Mrs M. Davies and Belinda for providing a happy home and a companionship during my study in Manchester.

Finally my thanks are due to my parents for their encouragement and financial support, without them this work would not have been possible.

ABSTRACT

Contact angle measurements have been used to determine the surface free energies of solids in powder form. As contact angle measurements on powders are determined indirectly, an initial study was undertaken to compare materials available in both sheet and powder form. Polytetrafluoroethylene, (PTFE) polymethylmethacrylate (PMMA)and polyhexamethylene adipamide (Nylon 66) were chosen as model materials which are insoluble in most solvents. Contact angles of both powder and sheet forms of these materials showed good agreement using the h-ϵ and tilting plate methods. The surface free energies of the materials were calculated from contact angles determined with pairs of liquids of known dispersion and polar forces. Liquid pairs which gave a wide difference in contact angles were found to give the most reliable results.. Surface free energies calculated from powder and sheet forms of the materials were in agreement indicating that the pressure applied to the powder prior to contact angle measurement had no effect on surface characteristics. These results are also in accordance with contact angles determined by liquid penetration on tablets and powders. Therefore the surfaces of compressed tablets can be representative of the original powder.

The surface free energies obtained were then used in a study of bonding mechanisms in compacts. The magnitude of bond strength was calculated from a knowledge of the surface free energy. Relationships between estimated strength, measured in terms of Hamaker constants and experimentally measured tensile strengths were obtained. Van der Waals attractive forces were found to be involved in every type of compact studied. Polymers were chosen as model materials for this study and the work was extended to some pharmaceutical powders and to binary systems.

LIST OF TABLES

Chapter 3

LIST OF FIGURES

Chapter 3

PART 2

CHAPTER 1

CHAPTER 2

CHAPTER 3

LIST OF SYMBOLS

A	=	Hamaker constant
b	=	fulcrum distance
C	=	correction factor
c	=	constant
d	=	diameter
d_o	=	distance of separation
F	=	downward force
ΔF	=	Van der Waals energy
g	=	gravitational force
H	=	Hysteresis
h	=	Plank's constant
h_m	=	maximum drop height
ht	=	drop height
L	=	length of the displacement at three phase line
l	=	penetrated distance
$\frac{dl}{dt}$	=	rate of penetration
P	=	applied pressure
P_z	=	applied pressure along an axial axis
ΔP	=	pressure difference
ΔP_{cap}	=	capillary pressure
ΔP_{ext}	=	external pressure
p	=	perimeter of the plate
q	=	number of atoms per unit volume

r	=	capillary radius
r_m	=	mean capillary radius
S	=	area fraction of solid
T	=	thickness
t	=	time
V	=	volume
V_n	=	natural recovery velocity
w	=	ratio of true area and geometric surface area
θ	=	contact angle
θ_a	=	advancing angle
θ_r	=	receding angle
θ_o	=	intrinsic contact angle
θ_{app}	=	apparent contact angle
θ_{por}	=	contact angle of liquid on the saturated porous fraction
θ_{solid}	=	contact angle on solid fraction
γ	=	surface free energy
γ_S	=	solid surface free energy
γ_L	=	liquid surface free energy
γ_{SL}	=	solid-liquid interfacial energy
γ_{SV}	=	solid-vapour interfacial energy
γ_{LV}	=	liquid-vapour interfacial energy
γ_S^d, γ_L^d	=	solid, liquid dispersion energy
γ_S^p, γ_L^p	=	solid, liquid polar energy
γ_c	=	critical surface tension
ρ	=	liquid density

ρ_g	=	true density of solid
ρ_B	=	bulk density of solid
Π_e	=	surface pressure
τ	=	relaxation time
ε_S	=	surface porosity
ε_V	=	volume porosity
η	=	liquid viscosity
Σ	=	dielectric constant
α	=	polarizability of atom
β	=	van der Waals constant
υ	=	electron frequency at ground state
$\overline{h\omega}$	=	Lifshitz-Van der Waals constant
σ	=	tensile strength
σ_z	=	axial tensile strength
ϕ	=	interaction parameter

GENERAL INTRODUCTION

The surface free energy of solid is an important characteristic for all powders and is involved in many pharmaceutical processes such as tabletting, disintegration, dissolution etc. A knowledge and understanding of this parameter should play a crucial role in leading to better dosage forms. This research work is divided into two major areas. Firstly, a study of the methods available for determining the surface free energies of powders and secondly, on the application of these results to the process of tabletting.

Since contact angle measurements have been well established to determine the surface free energy of solids available with smooth surfaces, the initial project will be involved with techniques for the measurement of contact angles. A comparison will be made among different methods and an appropriate technique will be chosen for the surface free energy determination of powders. Further studies will be related to the application of the surface free energy to bonding mechanisms in tablets since tablets are the most commonly used dosage form. A prediction of this bond strength will be made as the strength of bonds is a property required to give an acceptable tablet for handling and finally biological processes. The studies will be performed in air and in liquid media because wetted tablets are the actual condition for drug release to take place . Finally disintegration tests will be examined using some of the liquids studied previously.

The thesis is divided into two parts each with its own introduction, materials, results and discussion and conclusion. General conclusions are drawn at the end of the thesis.

PART 1

CHAPTER 1

INTRODUCTION

1.1 CONTACT ANGLE STUDIES

When a drop of liquid is placed on a solid surface, it can exhibit different types of behaviour, depending on the balance of the cohesive forces of the liquid and the adhesive forces between the liquid and solid surface. A finite angle will form when the cohesive forces are greater than the adhesive forces. The liquid will spread i.e. form a layer of zero angle when the adhesive forces are greater than the cohesive forces. On the other hand, the liquid drop will form a sphere ($\theta = 180^{\circ}$) when the adhesive force is absent. The contact angle is the angle formed by the balance of forces at the interface. Fig 1.1 shows different angles formed at different balance of forces. These forces are interfacial tensions between solid and vapour (γ_{sv}) , solid and liquid (γ_{sL}) and liquid and vapour (γ_{Lv}) respectively. The contact angle (θ) can be defined by Young's equation.

$$\cos\theta = \frac{\gamma_{sv} - \gamma_{sL}}{\gamma_{Lv}} \qquad \ldots 1.1$$

There is a great deal of controversy over the validity of Young's equation. The measured angle may not be an equilibrium angle due to the effect of hysteresis (Neumann 1974) which is discussed in detail in 1.1.2. Therefore Young's equation can not be applied. However, Johnson and Dettre (1969) found that the equation is valid when the angle is in equilibrium on a smooth and homologous solid surface.

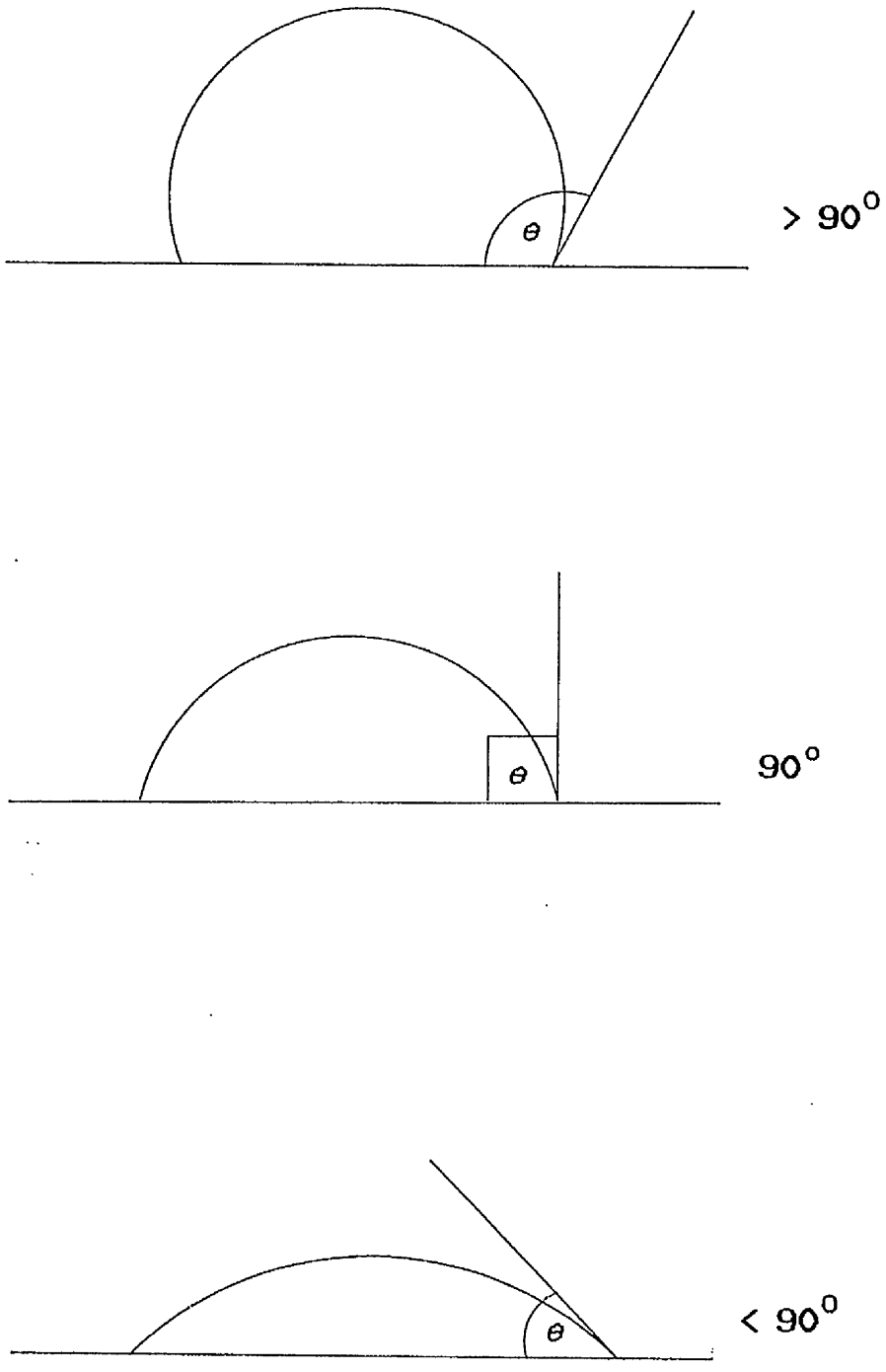

FIG. 1.1 BALANCE OF γ_{LV}, γ_{SV}, γ_{SL} FOR SURFACES WITH DIFFERENT FORCES, GIVING A RANGE OF VALUES FOR θ.

1.1.1 CONTACT ANGLE DETERMINATIONS

The choice of method for measuring contact angles depends very much on the geometry of the system. The accuracy and reproducibility obtained is usually within ± 3°. For a flat solid plate, a variety of techniques can be used which give reproducible and speedy results, whereas for pharmaceutical materials available as powders, the choice becomes restricted.

1.1.1.1 MEASUREMENTS ON A FLAT PLATE

1. Sessile drop method

The direct measurement of the contact angle from the drop profile is the most widely used technique. The angle can be detected by many procedures such as photography, projection of the image of the drop on a screen or using an eyepiece protractor fitted to a microscope. The angle is then determined by drawing a tangent at the contact point. The problem of this method is the difficulty in locating the point of contact and constructing a tangent line. An alternative to direct measurements is to calculate the angle from the drop dimensions (Bartell and Zuidema, 1936 and Mack, 1936). If it is assumed that the drop is small, such that gravity will not alter the shape, the drop can be regarded as a segment of a sphere. By measuring the height (ht) and the base length (d) the following equation applies:

$$\tan \theta/2 = \frac{2ht}{d} \qquad \ldots 1.2$$

2. Tilting plate method

This method was first introduced by Huntington (1906) and devised by Wenzel (1936). The apparatus consists of a microscope and a small glass container on a vertical movable support. A flat smooth sheet of the test material is connected to a protractor scale and immersed into the test liquid in the glass container, forming a concave or convex menicus which is observed through a microscope. The plate is then tilted until the menicus becomes flat, as shown in Fig. 1.2. The angle formed between the plate and the horizontal is the contact angle.

3 Wilhelmy Plate Method

When a smooth thin plate is brought into contact with a liquid, a downward force exerted on this plate can be expressed as:

$$F = p\gamma_{Lv}\cos\theta \qquad \ldots 1.3$$

where F is the downward force, p is perimeter of the plate. If the depth of immersion is not zero, so that a volume V of liquid is displaced, then equation 1.3 will be:

$$F = p\gamma_{Lv}\cos\theta - V\rho g \qquad \ldots 1.4$$

where ρ is the liquid density and g is the gravitational force

Measurement of the immersion or withdrawal forces and knowledge of the other parameters leads to a value of the contact angle.

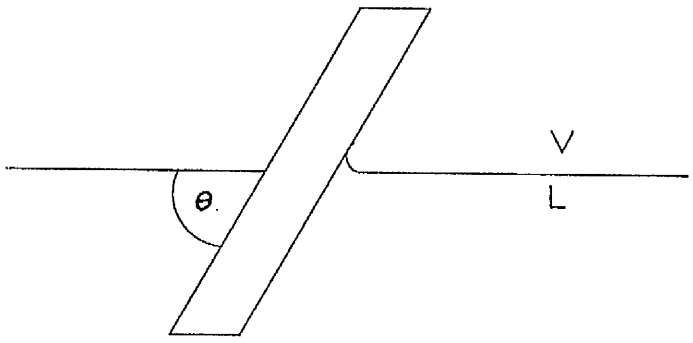

FIG. 1.2 CONTACT ANGLE OBTAINED FROM TILTING PLATE METHOD

1.1.1.2 MEASUREMENTS ON POWDERS

Contact angle measurements on powders are most important but the particle size of most powders of interest is too small to allow the asessment by direct methods. Many attempts have been made to find alternative methods giving an indirect determination of cos θ.

1. h-ϵ METHOD

This method was first introduced by Kossen and Heertjes (1965). The contact angle of a liquid drop on a solid surface can be determined by measuring the maximum height (h_m) a drop attains as its volume is increased and applying the following equations of Padday (1957) and Poynting and Thomson (1905).

$$\cos\theta = 1 - \frac{\rho g h_m^2}{^2\gamma_{Lv}} = 1 - Bh_m^2 \quad \ldots 1.5$$

where B is the constant which is equivalent to $\rho g/2\gamma_{Lv}$

This equation is valid for a smooth flat solid surface. However, for porous surfaces a porosity factor (ϵ_s) is introduced. The measured angle which is an apparent contact angle (θ_{app}) has a relationship with the true angle:

$$\cos\theta_{app} = \epsilon_s \cos\theta_{por} + (1-\epsilon_s)\cos\theta_{solid} \quad \ldots 1.6$$

where cos θ_{por} is the angle of the liquid on the saturated porous fraction which is 1 and θ_{solid} is the angle on saturated fraction.

Combining equation 1.5 and 1.6 gives

$$\cos\theta = 1 - \frac{Bh_m^2}{1-\varepsilon_s} \qquad \ldots 1.7$$

Since ϵ_s can not be measured directly, Kossen and Heertjes (1965) calculated this value in terms of the measurable volume porosity (ϵ_v) on the assumption that the particles were spherical, of uniform particle size and the number of particles per unit surface area (n) was equal to the number of particles per unit area in any flat plane in the porous mass. The surface porosity could then be derived from the volume porosity and the following equation used to determine the contact angle.

for $\theta < 90$

$$\cos\theta = 1 - \sqrt{\frac{Bh_m^2}{3(1-\varepsilon_v)(1-Bh_m^2/2)}} \qquad \ldots 1.8$$

for $\theta > 90$

$$\cos\theta = -1 + \sqrt{\frac{2}{3(1-\varepsilon_v)}\left(\frac{2}{Bh_m^2} - 1\right)} \qquad \ldots 1.9$$

Equations 1.8 and 1.9 are valid in the case of a completely smooth surface. Witvoet(1971) derived new equations to deal with rough surface .

for $\theta < 90$

$$\cos\theta = 1 - \sqrt{\frac{2}{3(1-\varepsilon_v)} Bh_m^2} \quad \ldots 1.10$$

for $\theta > 90$

$$\cos\theta = -1 + \sqrt{(2-Bh^2)\frac{2}{3(1-\varepsilon_v)}} \quad \ldots 1.11$$

A liquid drop is formed on a powder which is compressed into a smooth compact. A maximum drop height is detected by a telemicroscope and the contact angle is calculated by the application of equation 1.10 or 1.11.

Since the porosity is involved in the determination of the contact angle and is directly affected by the compaction pressure. A study of the effect of pressure on the porosity and contact angle is neccessary to evaluate the validity of Witvoet's equations. Lerk et al. (1976) studied the contact angle of Aspirin compacts prepared at different porosity and found that they gave a constant angle. An agreement was also observed in the work of Mohammad (1983). He found that after a certain limit an increase in pressure gave a constant contact angle on Corvic and PEM compacts whereas below this pressure the angle was lower. These results may be due to liquid penetrating through wide pores in the compact produced at lower pressures and exuding from the compact or due to the rough surfaces produced at low pressures.

Much work has been carried out on pharmaceutical materials by this technique (Lerk et al.1976, 1978; Fell and Efentakis 1978, 1979). In general it was found that the h-ϵ method could be used successfully on pharmaceuticals and gave reproducible results. The contact angle of compressed discs can also be detected by direct measurement, constructing a tangent line on to a liquid drop (Zografi and Tamn, 1976) or by a photographic method (Stamm et al., 1984).

These methods are open to criticism since pressure is applied to the powder to form a smooth compact. This may result in plastic deformation at the uppermost surface of the compact which is then likely to have properties different to that of the powder form (Buckton and Newton 1986). Fell and Efentakis (1979) compared the angle of compressed compacts using the h-ϵ and direct method, and good agreement was obtained. Efentakis (1979) found that the contact angle of salicylic acid did not change according to the pressure.

2. LIQUID PENETRATION METHOD

This method is based on the Washburn theory (1921) and it is the only method available for determining the contact angle of powders without treatment. Washburn considered the penetration of liquid through a powder bed, which is assumed to be composed of a bundle of parallel capillary tubes of a constant radius (r) with the powder structure staying homogeneous throughout the period of penetration. The rate of penetration of liquid under laminar constant flow through a tube is given according to Poiseuille's law:

$$\frac{dV}{dt} = \frac{\Delta P r^4 \Pi}{8\eta l} \qquad \ldots 1.12$$

where dV is the volume of liquid which in the time dt flows through any cross section of the capillary (dl) which is equal to $\Pi r^2 dl$, ΔP is the pressure difference across the length of the tube (l) which causes the motion of liquid and η is the liquid viscosity. Substituting for dV into equation 1.12 gives:

$$\frac{dl}{dt} = \frac{\Delta P r^2}{8\eta l} \qquad \ldots 1.13$$

ΔP can be divided into a capillary and an external pressure as belows:

where $\Delta P_{cap} = 2\gamma_{Lv} \cos\theta / r$

ΔP_{ext} is the total external pressure

If P_{ext} is negligible in comparison with the capillary pressure, substitution of the capillary pressure into equation 1.13 and integrating gives:

$$l^2 = \frac{r\gamma_{Lv}\cos\theta t}{2\eta} \qquad \ldots 1.14$$

This is known as Washburn's equation for the penetration of liquid across regular circular cross section capillaries while in the case of irregular cross section , the term of r_m^2/c is introduced, where r_m is the mean radius and c is the constant depending on the cross sectional shape. Therefore equation 1.14 will be :(Carli and Simioni, 1977)

$$l^2 = \frac{r_m^2}{c} \frac{\gamma_{Lv} \cos\theta t}{2\eta} \quad \ldots 1.15$$

From the Washburn equation the contact angle of a liquid on a powder can be obtained provided the capillary radius is known. However, this value can not be measured directly. Studebaker and Snow (1955) derived the Washburn equation on the basis of the relative wettability of one liquid to another. One liquid was treated as a perfectly wetting liquid, and the other as a non wetting test liquid. Therefore the Washburn equation will be as the follows:

for perfectly wetting liquid

$$l_1^2 = \frac{r\gamma_{Lv_1} t_1}{2\eta_1} \quad \ldots 1.16$$

for non wetting liquid

$$l_2^2 = \frac{r\gamma_{Lv_2} \cos\theta t_2}{2\eta_2} \quad \ldots 1.17$$

Dividing equation 1.17 by equation 1.16 gives:

$$\cos\theta = \frac{\gamma_{Lv_1} \eta_2 t_1 l_2^2}{\gamma_{Lv_2} \eta_1 t_2 l_1^2} \quad \ldots 1.18$$

or

$$\cos\theta = \frac{\gamma_{Lv_1} \eta_2 \text{gradient}_2}{\gamma_{Lv_2} \eta_1 \text{gradient}_1} \quad \ldots 1.19$$

where suffixes 1,2 refer to the perfectly wetting liquid and non wetting liquid, respectively, and the gradient is of a graph of the square of penetration length as a function of time.

The contact angle of a test liquid on a powder bed or compact can be investigated. The liquid penetration rate of the test and standard liquid which gives zero contact angle are measured. The contact angle is calculated by the application of equation 1.19.

An alternative method of liquid penetration method was suggested by Bartell and Osterhof (1927). The method is based on the measurement of the applied pressure which impedes the capillary driving pressure into a capillary bed. This method is rather tedious and constant radius is not obtained. Therefore the Studebaker and Snow method is adopted in most studies.

However, the method has some drawbacks which are explained in detail in 1.1.4. The technique has been used to evaluate several pharmaceutical powder systems. Buckton (1985) determined the wettability of barbiturate powders, using a series of alcohols, ethanol-water mixtures and propanol-water mixtures. The disintegration and dissolution process has been studied widely by this technique. Van Kamp et al (1986a) studied the volume uptake of different types of lactose. They gave different rates of penetration, volume uptakes and consequently disintegration times. The technique is also useful for a multicomponent system. Wan and Choong (1986) formulated phenacetin tablets with different ratios of PVP (as a binder) and

starch (disintegrant). The higher concentration of starch at a constant PVP concentration gave a higher water uptake and higher penetration rate and hence shorter disintegration time. Similar studies have been carried out by other authors with different products (Nagami et al.,1969; Ganderton, 1969; Ganderton and Selkirk, 1970; Ganderton and Fraser, 1970; Lerk et al,1979; Fukuoka et al. 1983; Van Kamp,1986b).

1.1.2 CONTACT ANGLE HYSTERESIS

For an ideal solid surface ie. plane, uniform, non defomable and homogenous, the liquid drop will exhibit only one equilibrium contact angle, the Young contact angle. In practice, however, a number of stable angles are obtained. The highest angle is called an advancing contact angle (θ_a), the lowest angle is called a receding contact angle (θ_r) (Fig 1.3). The difference between the two angles is called the hysteresis (H).

$$H = \theta_a - \theta_r \qquad ..1.20$$

The advancing and receding angles can be obtained by increasing or decreasing the volume of a liquid drop. They can be also measured by tilting a plate at different angles. The contact angles obtained at the lowest and the highest point where the drop is in contact with the solid are then, respectively, the advancing and receding contact angles.

The causes of hysteresis are mainly due to roughness and heterogeneity as described below:

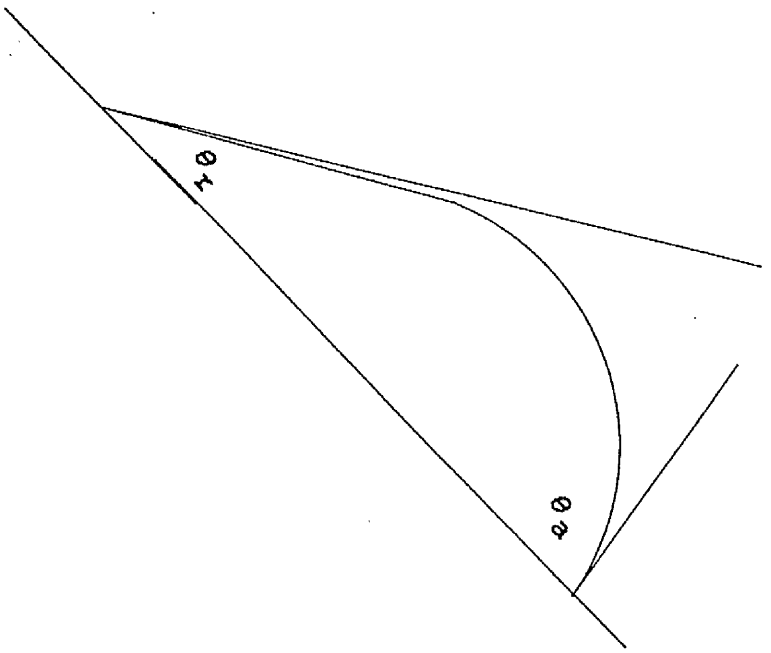

FIG. 1.3 A DROP ON A TILTED SURFACE, SHOWING AN ADVANCING AND RECEDING CONTACT ANGLE.

1.1.2.1 SURFACE ROUGHNESS

The Young angle is derived from a consideration of a smooth solid surface, but the roughness cannot be avoided in normal materials and especially for powder compacts. Wenzel (1936) introduced an equation to account for rough surfaces:

$$\cos\theta_{app} = w\cos\theta_0 \quad ...1.21$$

where w is true area/geometric area, θ_{app} is the measured angle on the rough surface and θ_0 is the intrinsic contact angle (the angle on the ideal solid).

The true area is always larger than the geometric area since it takes account of peaks and valleys in the surface. According to Wenzel's equation, the roughness affects the contact angle depending on the intrinsic angle. If the intrinsic angle is below 90° the roughness will decrease the contact angle while in the case of angles over 90° the inverse effect will be expected.

Much work has been carried out to study the effect of roughness on the contact angle . Johnson and Dettre (1964a) suggested that advancing and receding angles are determined by a balance between the vibrational energy of the drop and the heights of the energy barriers which impede the movement of the liquid drop. They found that surface rugosities can act as capillaries in the surface, above a critical rugosity a liquid will spread spontaneously along the grooves in the surface as given by:

$$w = 1/\cos\theta_0 \quad ..1.22$$

Ray and Bartell (1953) studied the effect of roughening a paraffin surface. The advancing angle was found to increase whereas the receding angle decreased. Zografi and Johnson (1984) found that roughness produced a significant hysteresis by affecting the receding angle much more than the advancing angle on paraffin, polytetrafluoroethylene (PTFE) and polymethylmethacrylate (PMMA). Therefore the use of advancing contact angles as an estimation of the equilibrium intrinsic angle gives a more reliable result than the receding angle. However a knowledge of the receding angle is useful to indicate the degree of surface roughness.

1.1.2.2 SURFACE HETEROGENEITY

Surface heterogeneity can occur in two conditions. Firstly when there is an area in which the atomic or molecular composition differs from other areas and secondly when different crystallographic planes of a pure, single crystal give different energies, densities and contact angles.

Cassie and Baxter (1944) extended Wenzel's equation to apply to heterogenous surfaces as follows:

$$\cos\theta = s_1\cos\theta_1 + s_2\cos\theta_2 \quad ...1.23$$

where s_1 and s_2 represent the area fractions of solid one and two which have contact angles θ_1 and θ_2 respectively as intrinsic angles, and θ is the contact angle on the heterogeneous surface. The heterogeneity causes the different energy in each configuration. Pease (1945) suggested that the advancing angle should be more associated with the low energy part of the surface (non polar surface) while the receding angle is more characteristic of the high energy part (polar portion). Therefore for heterogeneous surfaces, advancing and receding angles can be used as Young's contact angle when the former is for the low energy component and the latter is for the high energy component. Johnson and Dettre (1964b) also determined the hysteresis effect of heterogeneous surfaces in the same way as rough surfaces ie. the determination of a balance between the vibrational energy of a drop and the heights of the energy barriers between allowed metastable states.

Both surface roughness and heterogeneity can cause significant contact angle hysteresis. Johnson and Dettre (1969) found that the heterogeneity can cause more serious effects than surface roughness unless the rugosity is more than 0.5 mm.

Particle size has an effect on contact angle studies. An increased particle size would be expected to lead to higher roughness. Mohammad (1983) studied the contact angle of Corvic. Within the size range studied (53-180 μm) particle size had no effect on the contact angle. Similar results were observed by Lerk et al.(1976) on the angle of aspirin within the size range 125-850 μm.

1.1.2.3 MISCELLANEOUS

The cleanliness of both solid and liquid phases may cause a tremendous variation in contact angle since the contamination will decrease the surface tension of the liquid (Adam, 1964).

The penetration of liquid during the period of advancing contact angle measurement will leave a wet surface when the receding angle is measured. Adam (1964) suggested that the left over liquid will cause an increase in its attraction, therefore the advancing angle is always higher than the receding one. To prevent this effect, either the solid surface is pre-wet or a larger molecular size of liquid, which can not penetrate into the pores, is used.

1.1.3 THE DYNAMIC CONTACT ANGLE

A static contact angle is formed at a stationary liquid front, determined by the equilibrium of interfacial energies, whereas a dynamic contact angle is formed at a moving liquid front, determined by the balance of interfacial driving forces and viscous retarding forces.

The dynamic angle can be obtained by many methods. The most commonly used technique is liquid penetration. Other methods are a capillary rise method and the spreading of a liquid drop towards an equilibrium shape assessed by photography.

The dynamic angle is not constant but varies with velocity during capillary flow. The work of Hansen and Miotto (1959), Elliott and Riddiford (1967) and Phillips and Riddiford (1972) found that the angle varied with the velocity, arising from lagging of molecular relaxation behind the impressed motion. The relaxation time, τ, which is required for the slowest relaxing molecule in the periphery to reach its equilibrium position, and L the displacement length at three phase line is related to the natural recovery velocity, V_n as follows:

$$Vn = L/\tau \qquad \ldots 1.24$$

If the interfacial velocity, V, is lower than V_n, then the molecule will have sufficient time to recover from the imposed displacement, hence all boundary tension operating at the periphery should be equilibrium tensions. In this case the dynamic angle is independent of the interfacial velocity and identical to the static angle (Elliott and Riddiford, 1967; Lowe and Riddiford, 1970; Phillips and Riddiford, 1972 and Cain

et.al,1983). If $V >> V_n$,then at least the most slowly relaxing molecules are disoriented at the line of contact, and the boundary tension , hence γ_{sL} is increased above the equilibrium value, depending on the degree of disorientation. According to Young's equation, the angle will thus be higher. Lowe and Riddiford (1970) suggested that below the critical rate the relaxation times of the non polar and polar forces are short enough for them both to be operative, whereas above this point, dipole relaxation lags behind and only the dispersion forces can operate. Elliott and Riddiford (1967) found that at a velocity below 1mm/min. the contact angle of water-polyethylene and water-silicone glass were independent of velocity, whereas above this point the angle changed with velocity. Cain et al.(1983) studied the dynamic angle of a glass microscope slide, using a capillary rise technique. The angle increased significantly when the immersion rate changed from 0 to 0.2 mm/min. An angle independent of rate was observed between velocities of 0.2-0.5 mm/min. Beyond this point, the angle increased with the rate again.

1.1.4 SOME PROBLEMS OF THE WASHBURN THEORY

Problems associated with this method have been discussed by Yang and Zografi (1986). The Washburn equation may be inadequate as it assumes that the media consists of a bundle of constant radius cylindrical tubes. However, the

interconnectedness of the porous net work and the irregular shapes of the pores can lead to a change in the curvature at the liquid air interface. Consequently, a jumping movement can be observed rather than continuous motion.

Further problems are the geometric contribution which is not the same in different liquids exhibiting different contact angles in the same media (Ayala et al. 1987) therefore the comparison cannot be made between the dissimilar states. In addition to fulfil the Washburn condition, all voids behind the wetting liquid should be saturated with the penetrated liquid. This is difficult due to an entrapped air and can lead to hysteresis. In addition the technique is valid for a spontaneous penetration (positive capillary driving force; $\theta < 90^{\circ}$).

According to the Washburn equation a plot between the square of the length of penetration against time should give a straight line. Since the penetrated volume (V) is directly proportional to the length of penetration, the Washburn equation can be written in a simplified form as:

$$V^2 = k_1 l^2 = k_2 t \qquad \ldots 1.25$$

or

$$V = k_1^m \, l = k_2^m \, t^m \qquad \ldots 1.26$$

where k_1 and k_2 are constant and m is equal to 0.5, according to the Washburn equation to yield a straight line.

However it has been shown that m can vary from 0 to 1 (Carli and Simioni,1979 and Carli et al.,1981). m varies according to the pore size distribution, apparently related to the particle size. Lower values of m were observed for larger particle sizes. Carli et al. (1981) also found that m changes according to the applied pressure, high pressures giving low m and k values which is related to a very wide pore size distribution shifted towards smaller pores. They suggested that the deviation of m may be due to the assumption of the capillaries being parallel, but are in practice interconnected.

Fukuoka (1981,1983) and Lerk et al.(1979) found that plots of penetrated volume against time for crystalline cellulose exhibited a straight line instead of the normal Washburn plot. This was due to cracking and swelling of the compacts.

With regard to the above problems, the contact angle obtained from liquid penetration studies may not give the appropriate value, even though linearity of the plot between the square of liquid uptake against time is obtained.

1.2 THE CRITICAL SURFACE TENSION

Fox and Zisman (1950) introduced the concept of critical surface tension as an empirical method of determining the wettability of a solid surface by plotting cos θ of liquids on the solid surface against surface tension of the liquids. The point which gives cos θ = 1 is called the critical surface tension. This plot is generally described by the following equation.

$$\cos\theta = 1+b(\gamma_c - \gamma_L) \quad \ldots 1.27$$

where b is the slope of the line. Liquids with lower surface tensions than the critical value will spread along the surface while above this point, the liquids will form a finite contact angle. In other words the critical surface tension of a solid can be defined as the point at which liquid just spreads on the surface. Zisman (1963) found that the critical surface tension value could be used as an indicator of the chemical structure of a solid surface. It has also been used in work on the film coating process. An increase in the γ_c of the tablet surface resulted in a better and more rapid wetting of the tablet surface, and increased the effective area of contact, consequently increasing the strength of the adhesive bond (Wood and Harder, 1970)

Despite the usefulness of the critical surface tension, there are some defects in the interpretation of this empirical value. Dann (1970a,b) found γ_c varied according to the liquid used. High polar liquids such as a series of alcohols gave lower values of critical surface tension than a non homologous series of hydrocarbon liquids. Mohammad and Fell (1983) also found the critical surface tension of mixtures of phenobarbitone and Emcompress and mixtures of PEM and Corvic were lower when isopropylalcohol-water mixtures were used than polyethylene glycol-glycerol mixtures. The reason for this discrepancy was said to be due to the incompleteness of the Fowkes equation (1964) in not taking account of polar forces (Kaeble, 1970 and Dann 1970b). Murphy (1972) found that the adsorption of methanol occured at the solid-liquid and the solid-vapour interfaces, the hydroxyl group of the alcohol orientated towards the solid surface, leaving the hydrocarbon chain directed into the liquid surface. Therefore the outer group of the adsorbed film would be responsible for the critical value, instead of the solid surface. In support to the work of Murphy, Fell and Effentakis (1978) studied the critical surface tension of salicylic acid, acetylsalicylic acid, phenacetin and paracetamol, using a series of mixtures of methanol and water and found that despite large difference in initial contact angle from 59 to 103 degrees all the critical surface tensions were the same (19-24). An agreement was also found in the work of El-Shimi and Goddard (1974) and Liao and Zatz (1979).

1.3 SURFACE FREE ENERGY

Surface free energy is classically defined as half the work or energy required to separate to infinity unit area of two adjacent atomic planes in a vacuum (Andrews and King, 1978). In practice, most measurements are carried out in the presence of a fluid environment ie gas, vapour, liquid; therefore the concern in this study is the interfacial energy rather than in vacuo surface energy. However, the term surface free energy is commonly applied and in these studies are used instead of the interfacial energy to identify the energy between solid or liquid and vapour phase.

Surface free energy (γ_S or γ_L) arises from various intermolecular forces resulting in an attraction amongst the adjacent molecules. The London dispersion force is predominant in every intermolecular attraction, which is explained in detail in the second part, and the others are due to the nature of the material such as the hydrogen bond and the metallic bond. Therefore surface free energy is composed of two parts ie. dispersion forces and polar forces (Fowkes, 1962, 1964).

$$\gamma_S = \gamma_S^d + \gamma_S^p \qquad \ldots 1.28$$

$$\gamma_L = \gamma_L^d + \gamma_L^p \qquad \ldots 1.29$$

1.3.1 SURFACE FREE ENERGY DETERMINATION

Unlike liquids, solid surface free energy cannot be measured directly due to the immobility of the molecules, the heterogeneity of the surface caused by the different crystal faces, impurities, and surface roughnesses (Zografi,1968). An approach to obtaining the surface energy is by means of contact angle measurements. The starting point is Young's equation:

$$\gamma_L \cos\theta + \Pi_e = \gamma_s - \gamma_{sL} \quad ..1.30$$

where Π_e is the change in surface free energy per square centimeter due to any adsorption of vapour from the liquid to the solid surface.

Π_e is assumed to be zero since from theoretical and experimental evidence, the adsorption of high energy material cannot reduce the surface free energy of a low energy material. The liquid has the higher energy than the solid when a contact angle is formed (Young's equation), therefore, Π_e is assumed to be zero.

From equation 1.30 , γ_L and cos θ can be measured, γ_s and γ_{sL} are unknown. Fowkes (1964) has derived a model to estimate the interfacial forces from a knowledge of the surface free energies of the two phases, which is shown in Fig. 1.4. The interface is composed of two adjacent interfacial regions so the

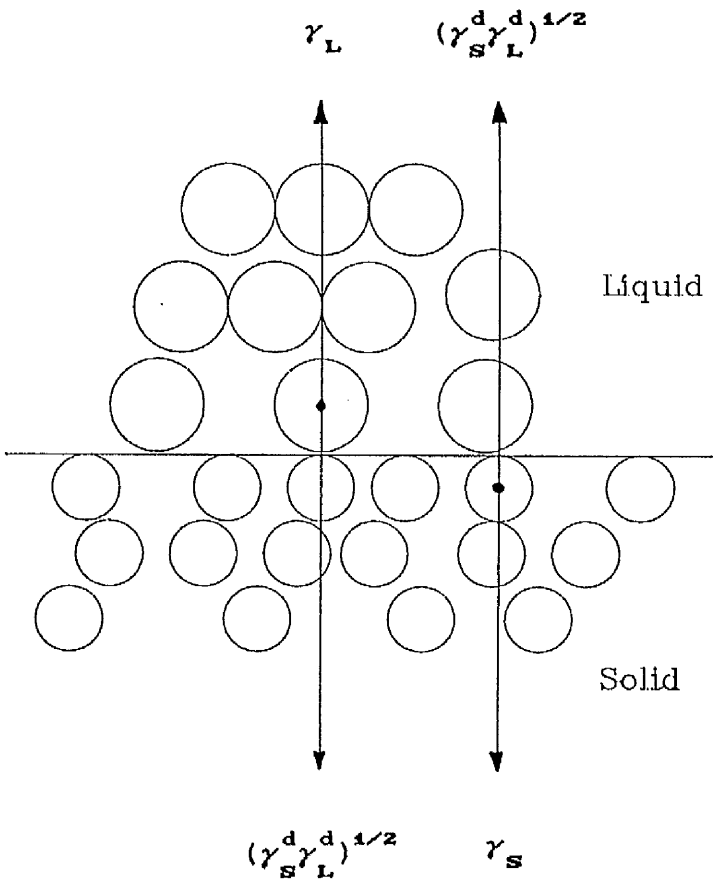

FIG. 1.4 FOWKES' MODEL TO ESTIMATE THE INTERFACIAL FORCES BETWEEN TWO DIFFERENT SURFACE ENERGIES.

interfacial tension must be the sum of the tensions in each of these regions. The interfacial region of the solid phase arises from the difference of the surface free energy of solid attracted to the bulk phase and the London dispersion interaction force attracted to the liquid phase since both forces are in a different direction. A similar reaction exists in the interfacial region of the liquid. Therefore the interfacial tensions in these two layers are:

$$\gamma_{sL} = \gamma_s + \gamma_L - 2\varphi^d \qquad \ldots 1.31$$

where φ^d is London dispersion interaction force.

The equation is only applicable to hydrophobic materials whereas the interaction from polar forces should be included for hydrophilic materials. Therefore the equation should be derived as :

$$\gamma_{sL} = \gamma_s + \gamma_L - 2\varphi^d - 2\varphi^p \qquad \ldots 1.32$$

where φ^p is non dispersion interaction force.

Fowkes (1964) suggested that the geometric mean of the surface free energy components should predict the magnitude of these interaction forces. Therefore equation 1.32 will be:

$$\gamma_{sL} = \gamma_s + \gamma_L - 2(\gamma_s^d \gamma_L^d)^{1/2} - 2(\gamma_s^p \gamma_L^p)^{1/2} \qquad \ldots 1.33$$

Wu (1971) suggested the use of a harmonic mean gave more reliable results for a system containing two relatively polar polymers. Equation 1.32 becomes

$$\gamma_{sL} = \gamma_s + \gamma_L - \frac{4(\gamma_s^d \gamma_L^d)}{\gamma_s^d + \gamma_L^d} - \frac{4(\gamma_s^p \gamma_L^p)}{\gamma_s^p + \gamma_L^p} \quad \ldots 1.34$$

A combination of equation 1.34 with Young's equation gives

$$\gamma_L(1+\cos\theta) = \frac{4(\gamma_s^d \gamma_L^d)}{\gamma_s^d + \gamma_L^d} + \frac{4(\gamma_s^p \gamma_L^p)}{\gamma_s^p + \gamma_L^p} \quad \ldots 1.35$$

Equation 1.35 can be rearrange to give equation 1.36

$$(b+c-a)\gamma_s^d \gamma_s^p + c(b-a)\gamma_s^d + b(c-a)\gamma_s^p + abc = 0 \quad \ldots 1.36$$

where $a = \gamma_L (1+\cos\theta)/4$

$b = \gamma_L^d$

$c = \gamma_L^p$

From a knowledge of contact angles, the two unknowns in the equation can be found by using two liquids of known surface dispersion and polar forces.

The components of the liquid forces are estimated by means of contact angle measurements on a solid having only dispersion forces, such as paraffin ($\gamma_s^d = \gamma_s = 25.5$ mN/m)and applying the combination of Fowkes'and Young's equations.

$$\gamma_L(\cos\theta+1) = 2(\gamma_s^d \gamma_L^d)^{1/2} \quad ...1.37$$

1.3.2 COMPARISON BETWEEN CRITICAL SURFACE TENSION AND SURFACE FREE ENERGY

Girifalco and Good (1957) proposed the equation for the interpretation of interfacial forces:

$$\gamma_{sL} = \gamma_s + \gamma_L - 2\varphi(\gamma_s \gamma_L)^{1/2} \quad ...1.38$$

where φ is the interaction parameter which depends on the molecular parameter: the dipole moments, the polarizabilities, the ionization energies and the molar volumes. The combination of Girifalco and Good and Young's equation is given by:

$$\gamma_s = \frac{\gamma_L(1+\cos\theta)^2}{4\varphi^2} \quad ...1.39$$

At the critical surface tension, $\cos\theta = 1$ then the critical surface tension is equal to surface free energy when φ is unity.

Girifalco and Good found that φ can deviate from 0.5 to more than 1 when the ratio of dispersion to polar forces of the phases in contact are dissimilar. The lower φ was found when the predominant forces between the interfaces were of different types eg. London vs. metallic forces while values of ϕ high than 1 are found for specific interactions. The work of Wu (1971) is also in agreement with that of Girifalco and Good. At the critical surface tension Wu's equation (1.35) becomes:

$$\gamma_c = \frac{2(\gamma_s^d \gamma_L^d)}{\gamma_s^d + \gamma_L^d} + \frac{2(\gamma_s^p \gamma_L^p)}{\gamma_s^p + \gamma_L^p} \quad \ldots 1.40$$

From equation 1.40 surface free energy is equal to the critical surface tension when the dispersion forces of the liquid and solid are equivalent and the polar forces of liquid and solid are equivalent.

1.3.3 PROBLEMS OF SURFACE FREE ENERGY DETERMINATIONS

A basic assumption for the estimation of the surface free energy is that the Π_e value is considered to be negligible. In fact Π_e becomes significant in the case of hydrophilic materials and high surface energy solids and when the molecules of the liquid are small enough to penetrate through the solid surface. These solids will adsorb a liquid layer and reduce the surface free energy.

$$\Pi_e = \gamma_s - \gamma_{sv} \quad \ldots 1.41$$

Busscher et al.(1983) found that surface free energies without taking Π_e into account were the surface free energies determined on the adsorbed liquid layer , whereas the surface free energy considering the value of Π_e is a measurement on the base solid surface (Fig. 1.5). They found that both approaches actually yield the same results when an appropriate interpretation is applied.

Another assumption is that no highly specific interactions and orientation of molecules occurs at the solid-liquid interface. If this assumption is correct, the surface free energy and its components measured using different liquid pairs will be identical. Good (1964) found that the orientation effect leads to a changed interfacial entropy, hence a greater interfacial tension is obtained. This orientation effect also exists at the liquid-vapour interface resulting in an increased γ_{Lv}. The entropy effect will be negligible when both terms increase by the same magnitude. The other type of interaction is called Lewis-acid-base interaction which may result in the orientation of molecules (Ratner and Hoffman, 1981). This interaction tends to happen in liquids having high hydrogen bonding tendencies such as water, glycerol and formamide.

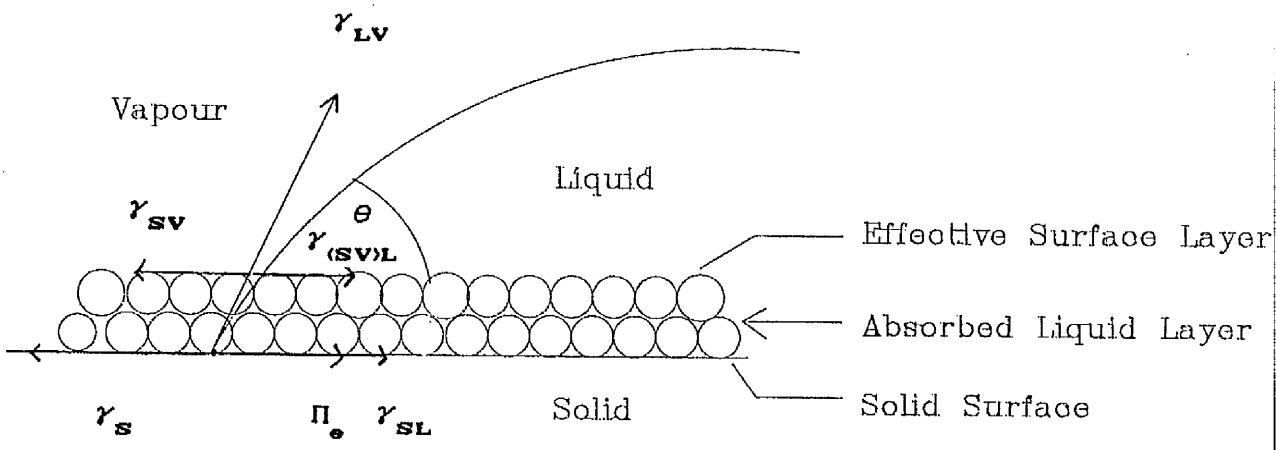

FIG. 1.5 INTERFACIAL FREE ENERGIES IN A SOLID-LIQUID-VAPOUR SYSTEM, SHOWING THE EFFECTS OF SPREADING PRESSURE ON THE INTERFACIAL FREE ENERGIES.

The other problem of surface energy measurements is the reproducibility of the method of measuring contact angles. A change of contact angle results in a change of surface free energy. The hysteresis effect causes the Young's angle not to be an equilibrium angle and thus Young's equation is not applicable. The result obtained is highly dependent on the accuracy and reproducibility of the contact angle measurement. This will be especially so when powder systems are being investigated.

The understanding of many pharmaceutical processes which involve solid surface reactions would benefit from a knowledge of solid surface free energies. Such processes include tabletting, disintegration and dissolution of solid dosage forms and adsorption. The approach to determining the surface free energies of solids by means of contact angle measurements is well established for solids which can be prepared with smooth flat surfaces (Fowkes, 1964; Dann,1970a,b). The objective of this part of the work is to establish a method to elucidate the surface free energy of a solid which is in powder form. A comparison is made between contact angles measured on flat surfaces and powders using the h-ϵ, tilting plate and penetration rate methods. A comparison is also made between contact angles measured using the liquid penetration method on powders and tablets since they are the most commonly used dosage form. The surface free energies and their components are calculated from a knowledge of contact angles measured using appropriate liquids with known surface energies. The work has been carried out on polymer materials which are available in smooth sheets and powder forms which can be compressed into compacts.

CHAPTER 2

MATERIALS AND METHODS

1. MATERIALS

Three polymers were used for static contact angle studies in both sheet and powder form. These are polytetrafluorethylene (PTFE), polymethylmethacrylate (PMMA) and polyhexamethylene adipamide (Nylon 66). The comparison of static and dynamic angles was studied using a vinyl chloride vinyl acetate copolymer (Corvic 47/488). A list of the solid materials studied, their suppliers and their characteristics is given in table 2.1.

The test liquids for static contact angle measurements are shown in table 2.2. These liquids were chosen to obtain a range of different surface tensions.

Table 2.3 shows the test liquids, their suppliers and their characteristics for dynamic contact angle studies. The liquid used were separated into two groups. The organic solvents were chosen to act as wetting liquids and the other group were non-wetting liquids chosen to form finite contact angles.

TABLE 2.1

THE POLYMERS USED IN THIS STUDY

Materials	Suppliers	Characteristics
Polytetrafluoro-ethylene	BDH Chemicals Ltd. England	fine particle size <5 μm.
	Amari plastics Co.,U.K.	solid sheet form
Polymethyl methacrylate	BDH Chemical Ltd. England	low M.W., used as received
	Amari plastic Co.,U.K.	solid sheet form
Nylon 66	BDH Chemicals Ltd. England	bead form, ground to give a smaller particle size
	Amari plastic Co.,U.K.	rod form
Corvic	I.C.I. U.K.	sieved to give a 180-250 μm size fraction

TABLE 2.2

THE LIQUIDS USED FOR STATIC CONTACT ANGLE MEASUREMENTS

Materials	Suppliers	Characteristics
Water	-	double distilled
Glycerol	BDH Chemicals Ltd. England	used as received
Formamide	BDH Chemicals Ltd. England	used as received
Polyglycol E-200	The Dow Chemical Co. Ltd. U.K.	used as received
Polyglycol 15-200	The Dow Chemical Co.Ltd. U.K.	used as received
Polyglycol P-1200	The Dow Chemical Co. Ltd. U.K.	used as received

TABLE 2.3

THE TEST LIQUIDS USED FOR DYNAMIC ANGLE MEASUREMENTS

Materials	Suppliers	Characteristics
Wetting liquids		
1. Methanol	Fisons PLC. Loughborough, England	analytical reagent
2. Ethanol	Fisons PLC. Loughborough, England	laboratory reagent
3. Propanol-2	Fisons PLC Loughborough, England	laboratory reagent
4. Cyclohexane	Fisons PLC Loughborough, England	laboratory reagent
Non-wetting		
1. Water	-	double distilled
2. Formamide	BDH Chemicals Ltd. England	used as received
3. Polyglycol E-200	The Dow Chemical Co. Ltd., U.K.	used as received

2 METHODS

2.1 CONTACT ANGLE MEASUREMENTS

Contact angle measurements were carried out on PTFE, PMMA and Nylon 66 available in both powder and solid sheet form by the h-ϵ and tilting plate methods to determine the validity of these measurements. A comparison of dynamic angles determined by the liquid penetration method and static angles determined by the h-ϵ method was studied using Corvic 47/488 powder.

2.1.1 h-ϵ

The method is based on the measurement of the maximum drop height of a liquid drop formed on a saturated compact or a smooth solid sheet. Contact angles on solid sheets of PMMA, PTFE and Nylon 66 can be measured directly, but in powder form a pressure is required to form a smooth compact. The device used consists of a stainless steel punch, a punch guide, a 5.1 cm. diameter die and a base plate as shown in Fig 2.1. The powders of PMMA, PTFE, Nylon 66 and Corvic 47/488 were distributed evenly in the die in order to get a constant porosity throughout the compact. Pressures of 14.4, 48.0, 57.6 and 62.4 MN/m^2 for PTFE, PMMA, Nylon 66 and Corvic respectively were applied by means of a hydraulic press (model p16 Beckman Instruments Inc. Fullerton, Calif, U.S.A.). After the

application of the required pressure, the punch, the punch guide and the die were removed, leaving the compact in the base plate. Pre-heating of PMMA and Nylon 66 powder were required prior to compaction to aid in the formation of the compact. The heating period and temperature were restricted by the powder used and care must be taken to avoid a depolymerized process. The heating temperatures were 100° and 120° for PMMA and Nylon respectively; both were heated for 30 mins. The compact was weighed and the thickness of the compact was measured, using a dial guage (Baty guage), allowing the calculation of the porosity of the cake ie.:

$$\epsilon = 1 - \frac{\rho_B}{\rho_g} \qquad \ldots 2.1$$

where ρ_B is equivalent to weight of compact/Πr^2 T (T is tablet thickness and r is tablet radius). Prior to the measurement , presaturation of the compact was achieved by dropping the test liquid from a reservoir through a needle onto the prepared cake which was on a horizontal level table as shown in Fig. 2.2. The liquid was slowly added to avoid entrapping air until the compact was saturated and a finite angle was formed. Further liquid drops were added until a maximum height was obtained. Beyond this point, additional drops resulted only in an increased drop diameter. The maximum height was then measured using a cathetometer (type 6368, Griffin and George Ltd.). The angle was calculated by the application of equation 1.10 or 1.11 . At least five readings were taken for each liquid.

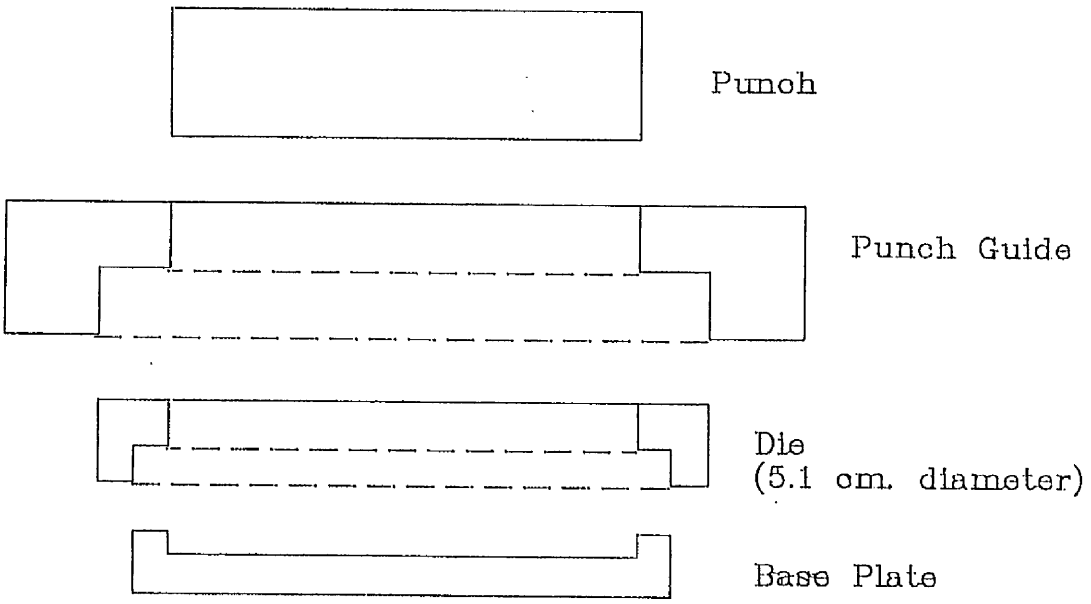

FIG. 2.1 SET USED FOR THE PREPARATION OF COMPACTS FOR THE h-ε METHOD

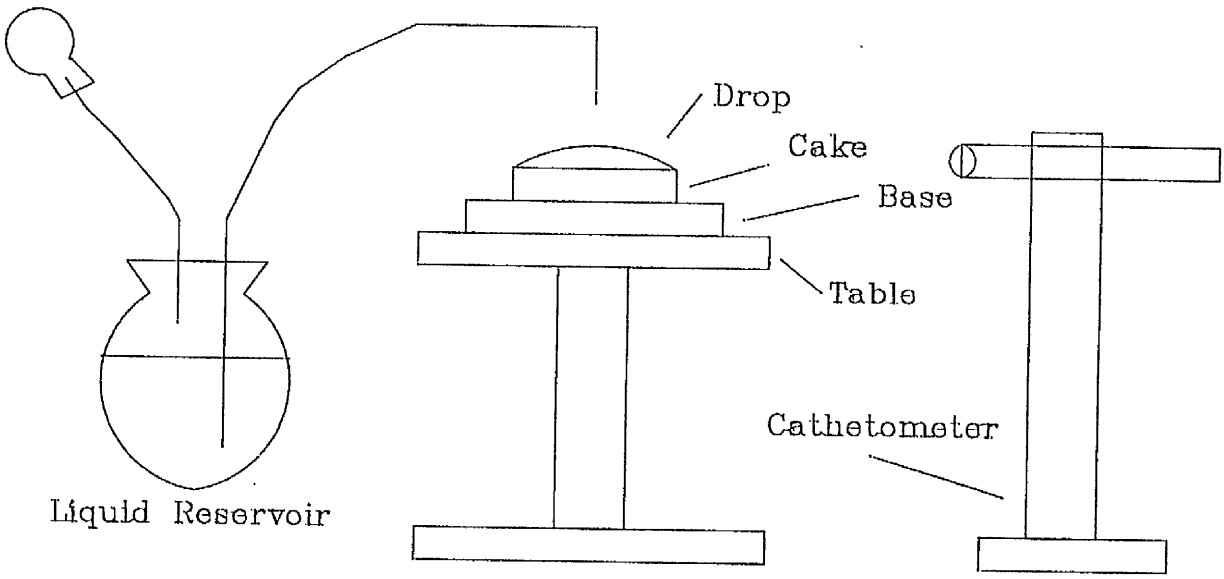

FIG. 2.2 THE h-ε METHOD APPARATUS

2.1.2 TILTING PLATE METHOD

Pieces of PMMA, PTFE and Nylon 66 sheet measuring 5x2.5 cm. were connected to a protractor scale on a microscope by a metal clip and immersed in a small glass container of test liquid. The sheet was slowly rotated until the menicus as viewed through the microscope disappeared. The angle formed between the sheet and the horizontal level of liquid at this point is the contact angle. The contact angle was obtained by approaching the reading from both sides. Prior to use the plates were carefully cleaned with detergent, thoroughly rinsed and dried in a hot air oven.

2.1.3 PENETRATION METHOD

One of the problems of the penetration method for determining contact angles is the achievement of a horizontal level of penetrating liquid to allow accurate measurement of the distance moved by the liquid. This can be overcome by measuring the volume penetrated (Mohammad and Fell, 1982 and Nagami et al.,1969) or the weight (van Kamp et al. 1986b). The method of Van Kamp was adopted for this study. The test sample was connected to a reservoir of the test liquid on an electronic balance as shown in Fig.2.3. The test was carried out on 5 gm. samples of Corvic powder packed to give a constant porosity in glass tubes terminating in a porosity-1 glass filter, and on 1.27 cm. diameter flat-faced Corvic tablets prepared at 224 MN/m^2 on

an instrumented single punch tablet machine (Manesty, Liverpool). The weight loss of liquid from the container with time was recorded after the glass filter had been saturated to get the actual value of penetrated liquid. Graphs of the square of weight loss of liquid against time were constructed. At least four reliable gradients from the plots were accepted for each liquid and the Washburn equation was applied.

2.2 SURFACE TENSION MEASUREMENT

Measurement of liquid surface tension was carried out by the drop volume method at 23° C using an Agla micrometer syringe (Burroughs Wellcome and Co.London) and applying the correction factors of Harkins and Brown (1919). The following equation was applied:

$$\gamma = \frac{\rho g V C}{r} \qquad \ldots 2.2$$

where V is the liquid volume, C is the correction factor and r is the tip radius.

The dispersion force and polar force contributions to the surface tension was measured using the contact angle ($h-\epsilon$) of the liquid formed on a paraffin compact which has only dispersion forces, 25.5 mN/m ,and the equation 1.37 was applied.

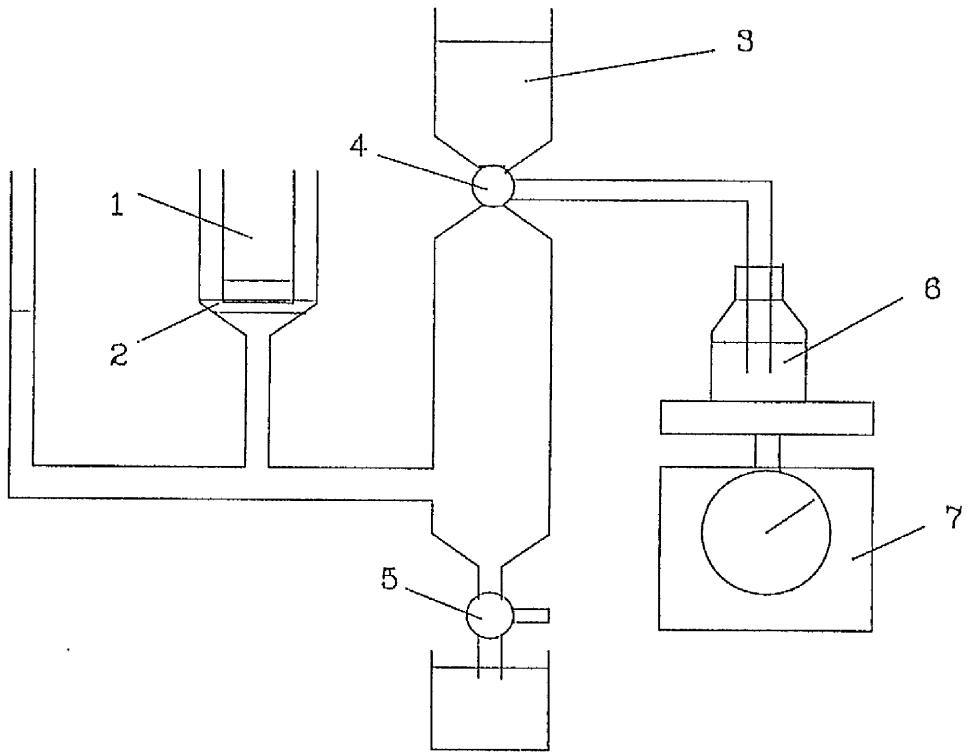

FIG. 2.3 THE LIQUID PENETRATION METHOD APPARATUS

1. A GLASS FILTER TUBE CONTAINS TEST SAMPLE
2. GLASS FILTER
3. RESERVOIR
4. THREE WAY STOPCLOCK
5. TWO WAY STOPCLOCK
6. CONTAINER
7. ELECTRONIC MICROBALANCE

2.3 SOLID DENSITY

The measurements were carried out using an Air Comparison Pycnometer (model 930 Beckman Instruments Inc. Fullerton, Calif, U.S.A.). The method is based on air displacement, the true volume of a known weight of test powder being measured. Hence, the density of the powders can be calculated.

2.4 LIQUID DENSITY

Liquid density was measured using a digital densitometer (DMA 02 C Anton Parr) at 25°C. The method is based on the change of natural frequency of a hollow oscillator when filled with different gases or liquids. The different mass and thus the density, of the liquid or gas changes the natural frequency which is measured in terms of the period t (since t= 1/f where f is the frequency). The relationship between the difference of the densities of the sample undertest and a reference sample can be obtained by

$$d_1 - d_2 = \frac{1}{A}\left(t_1^2 - t_2^2 \right) \qquad \ldots 2.3$$

where d_1, d_2 is the density of sample 1,2 ,t is the period change, suffix 1,2 are the test sample and the reference sample respectively, A is the apparatus constant. A was determined by measuring the period of two samples of known density. Water and air were used in this study, hence A is calculated by the application of equation 2.4. The t of the test liquid was measured and the density was calculated by treating water as a reference sample.

2.5 SCANNING ELECTRON MICROSCOPY

Photomicrographs of Corvic tablets and powder were obtained to investigate the effect of compaction pressure on surface characteristics. The test specimens were mounted on circular aluminum stubs using colloidal silver (Polaron Equipment Ltd.,England) and left overnight to ensure the silver solvent evaporated before the coating procedure took place. The test specimens were coated with gold, using a direct current sputter technique under vacuum. The total coating period was 2.5 mins. divided into 0.5 min periods to allow a thin layer of coating to be deposited at each stage. The coating process was operated at 25 Kvolts. Scanning was carried out using a Cambridge Stereoscan (model S4-10 Cambridge, Scientific Instruments Ltd, England) with a beam specimen angle between 0-45 degree and photomicrographs were taken at magnifications of 200 x.

CHAPTER 3

RESULTS AND DISCUSSION

3.1 THE VALIDITY OF CONTACT ANGLE MEASUREMENTS

Polymers were chosen for this study since they are an ideal material, available in both powder and smooth solid form. These materials are able to form compacts and the contact angles can be measured using a wide range of liquids without problems of solubility.

Table3.1 gives the properties of the test liquids. The contact angles against paraffin increase in accordance with the increase of surface tension. These values and the application of equation 1.37 enable the calculation of the components of surface tension shown in the table 3.1. A comparison of contact angles on powders and solid sheet was made. Table 3.2 gives the contact angle values on PTFE, PMMA and Nylon 66, available in powder and sheet form. In all cases there is good agreement between the different methods and materials in sheet and powder form. The results are also in agreement with the work of Kossen and Heertjes (1965).

The appropriate equation. must be chosen for the calculation of the angle around 90°. Equation 1.10 is applied when the liquid penetrates into the compact and Equation 1.11 is applied when the liquid does not penetrate. The result will be meaningless if the wrong equation is used.

TABLE 3.1

PROPERTIES OF TEST LIQUIDS

Liquids	Density (g/cm³)	θ° against paraffin	γ (mN/m)	γ^{d} (mN/m)	γ^{P} (mN/m)
Water	0.997	112	72.8	20.7	52.1
Glycerol	1.258	97	66.7	34.0	32.7
Formamide	1.133	91*	58.2*	32.1	26.1
PolyglycolE-200	1.121	73	43.0	30.0	13.0
Polyglycol15-200	1.062	62	36.0	27.5	8.5
PolyglycolP-1200	1.001	57	31.2	23.0	8.2

* Data from Dann (1970a)

TABLE 3.2

CONTACT ANGLE (DEGREES) ON PTFE, PMMA, NYLON 66

Liquids	PTFE			PMMA			NYLON 66		
	sheet		powder	sheet		powder	sheet		powder
	h-ε	tilt	h-ε	h-ε	tilt	h-ε	h-ε	tilt	h-ε
Water	107	104	112	75	75	75	70	68	—
Glycerol	105	101	102	67	67	66	63	61	63
Formamide	—	—	—	—	—	—	53	52	56
POLYGLYCOL E-200	80	79	78	41	42	41	—	—	—
POLYGLYCOL 15-200	78	77	77	34	35	34	31	28	—
POLYGLYCOL P-1200	64	64	65	0	0	0	—	—	—

One problem in using the h-ϵ method is that a fairly low angle ($<30^{\circ}$) can not be measured accurately due to the small drop height. Polyglycol p-1200 spreads completely on PMMA sheet and compacts and the drop height of Polyglycol 15-200 on Nylon compacts is too small to be able to detect.

Table 3.3 gives the effect of porosity on the contact angle of water on PMMA compacts. The contact angles were independent of the porosity. This result is in agreement with Kossen and Heertjes (1965), Efentakis (1979), Mohammad (1983) and Lerk et al. (1976) on pharmaceuticals and polymers. It implies that this technique is not affected by the applied pressure once a smooth compact is formed.

The solid surface free energy and the components were calculated using equation 1.36 taken from Wu (1971). The results, calculated from all the liquid pairs are given in tables 3.4, 3.5, 3.6. Since the values of γ_s^p ,γ_s^d , and γ_s should yield positive numerical values in order to have physical meaning, the liquid pairs which produced negative values are discarded. For PMMA (table 3.4) the calculated values from the different methods, forms and liquid pairs are in very good agreement except the components of the last three pairs. A similar agreement is obtained for Nylon 66 (table 3.5), except for the components of the pair glycerol and formamide. However, similar agreement is not found for PTFE (table 3.6). Although the total surface energy values for the different methods, forms and liquid pairs are acceptably close, the individual components of the energy vary widely.

TABLE 3.3

THE EFFECT OF POROSITY ON THE CONTACT ANGLES OF WATER ON PMMA COMPACTS

Porosity	Contact angles(degrees)
0.371	76
0.115	73
0.072	75

TABLE 3.4

SURFACE FREE ENERGY VALUES FOR PMMA (mN/m)

Liquid pair	Sheet(h-ε)			Sheet(tilt)			Powder(h-ε)		
	γ_s^d	γ_s^p	γ_s	γ_s^d	γ_s^p	γ_s	γ_s^d	γ_s^p	γ_s
Water-glycerol	16.7	18.7	35.4	17.8	18.1	35.8	17.9	18.1	35.9
Water-E-200	18.3	17.8	36.2	17.7	18.1	35.8	18.2	17.9	36.1
Water-15-200	17.3	18.4	35.7	17.2	18.4	35.6	17.3	18.3	35.7
Water-P-1200	17.5	18.3	35.7	17.5	18.2	35.7	17.5	18.3	35.7
Glycerol-E-200	19.1	16.3	35.4	17.7	18.1	35.8	18.4	17.6	35.9
Glycerol-15-200	17.5	17.9	35.3	17.1	18.8	35.9	17.2	18.7	36.0
Glycerol-P-1200	17.7	17.7	35.3	17.4	18.4	35.9	17.4	18.6	35.9
E-200-15-200	16.2	23.6	39.8	16.6	20.9	37.5	16.3	22.8	39.1
E-200-P-1200	16.2	23.6	39.8	17.1	19.7	36.8	16.4	22.7	39.1
15-200-P-1200	16.2	23.7	39.9	15.1	30.4	45.5	16.2	23.3	39.5

TABLE 3.5

SURFACE FREE ENERGY VALUES FOR NYLON 66 (mN/m)

liquid pair	Sheet(h-ε)			Sheet(tilt)			Powder(h-ε)		
	γ_s^d	γ_s^p	γ_s	γ_s^d	γ_s^p	γ_s	γ_s^d	γ_s^p	γ_s
Water-glycerol	18.0	20.5	38.5	17.7	22.3	40.0			
Water-15-200	17.5	20.8	38.3	17.8	22.2	40.0			
Glycerol-15-200	17.4	21.2	38.6	17.9	22.1	40.0			
Water-Formamide	19.2	19.8	39.0	17.8	22.3	40.0			
Glycer.-Forma.	25.0	14.3	39.3	18.1	21.8	39.9	13.9	25.6	39.5
Form.-15-200	17.0	22.8	39.8	17.9	22.1	40.0			

TABLE 3.6

SURFACE FREE ENERGY VALUES FOR PTFE (mN/m)

Liquid pair	Sheet(h-ε)			Sheet(tilt)			Powder(h-ε)		
	γ_s^d	γ_s^p	γ_s	γ_s^d	γ_s^p	γ_s	γ_s^d	γ_s^p	γ_s
Water-glycerol	5.4	10.2	15.6	6.1	11.1	17.2	16.7	2.0	18.7
Water-E-200	12.4	5.6	18.0	10.6	7.9	18.5	20.2	1.0	21.2
Water-15-200	9.4	7.2	16.6	8.6	9.1	17.7	12.3	3.7	16.0
Water-P-1200	11.7	5.9	17.6	10.0	8.2	18.2	14.8	2.7	17.5
Glycerol-E-200	-	-	-	16.0	2.8	18.8	-	-	-
Glycerol-15-200	11.1	4.6	15.7	9.3	7.5	16.8	10.4	6.1	16.5
Glycerol-P-1200	-	-	-	11.8	5.4	17.2	12.7	4.4	17.1
E-200-15-200	6.4	17.1	23.5	6.6	16.9	23.4	6.5	18.7	25.2
E-200-P-1200	10.1	8.4	18.5	9.0	10.4	19.4	7.8	14.3	22.1

The difference between these materials can be attributed to the precision of the measurements and the sensitivity of the equation 1.36 to changing values of contact angles. Contact angles can be measured, using the techniques of this study, to ± 3°. The calculated change of the components and the total energy from the original values are shown in table 3.7 for the worst case when one contact angle of the liquid pairs is increased by 3° and the other reduced by 3°. It can be seen that the higher energy surfaces ie.PMMA, Nylon are much less sensitive to change than that for the low energy surface ie. PTFE. The total surface energy is changed to a lesser extent than the components in all materials. The sensitivity to change is less when the liquid pairs form widely different contact angles.

The values of surface free energy and its components are thus subject to the chosen liquid pairs used for the measurement which is in agreement with the work of Kaelble (1970). A good pair should give large differences in contact angles to get the least possible change of surface energy due to the reproducibility of the measurement. As can be seen from table 3.4, the last three pairs of liquids and the pair of formamide and glycerol from table 3.5 give the greatest variation of the components from the other liquid pairs and these have the closest contact angles. Estimates of the individual components of the surface energies of higher energy surfaces are reasonable but those of low energy surfaces may be subject to considerable error.

TABLE 3.7

CHANGES IN SURFACE ENERGY VALUES CAUSED BY AN ASSUMED 3° CHANGE IN CONTACT ANGLE (mN/m)

Liquid pairs	Percentage change from experimental value								
	PMMA			Nylon 66			PTFE		
	γ_s^d	γ_s^p	γ_s	γ_s^d	γ_s^p	γ_s	γ_s^d	γ_s^p	γ_s
Water-PEG P-1200	4	12	4	-	-	-	31	45	5
Water-PEG 15-200	10	11	1	3	7	2	25	150	8
Water-Glycerol	46	26	8	33	20	7	154	62	13

Interestingly, contact angles of water on Nylon 66 compacts could not be measured as the compact disintegrated into particles when the liquid drops were formed on the compact. Nylon is composed of a large number of amide groups which could have a high interaction with the water molecules. Matsunaga (1977) found that the polar interfacial interaction between Nylon and water molecule is very high, 47 mN/m, compared to PMMA, 27 mN/m and PTFE , 0 mN/m. The polar force was estimated from a knowledge of the polymer composition. On the assumption of spherical monomer units and the sum of the interaction between functional groups and water molecules at the surface, the polar interfacial force was obtained and was in agreement with measured values.

3.2 THE CRITICAL SURFACE TENSION

The critical surface tensions (γ_c) of the polymers were obtained from plots of γ_L against $\cos\theta$ (fig 3.1, 3.2, 3.3). The values are listed in table 3.8. The results are significantly different from the literature values which may be due to the series of liquids used, as mentioned previously. The critical surface tension of PTFE is negative which is meaningless. Long extrapolations are required in the studied liquids. Zisman's plot method is applicable when a homologous series of liquids, with mainly dispersion forces, is used. Therefore, the plot of dispersion force against cos θ is shown in Fig. 3.4. A straight line was not obtained. Plots of 1/square of surface tension against cos θ suggested by Dann (1970) are shown in Figs. 3.5-3.7 and results are in table 3.8 in the bracket. The results are also different from the literature except PTFE. Therefore the use of the critical surface tension

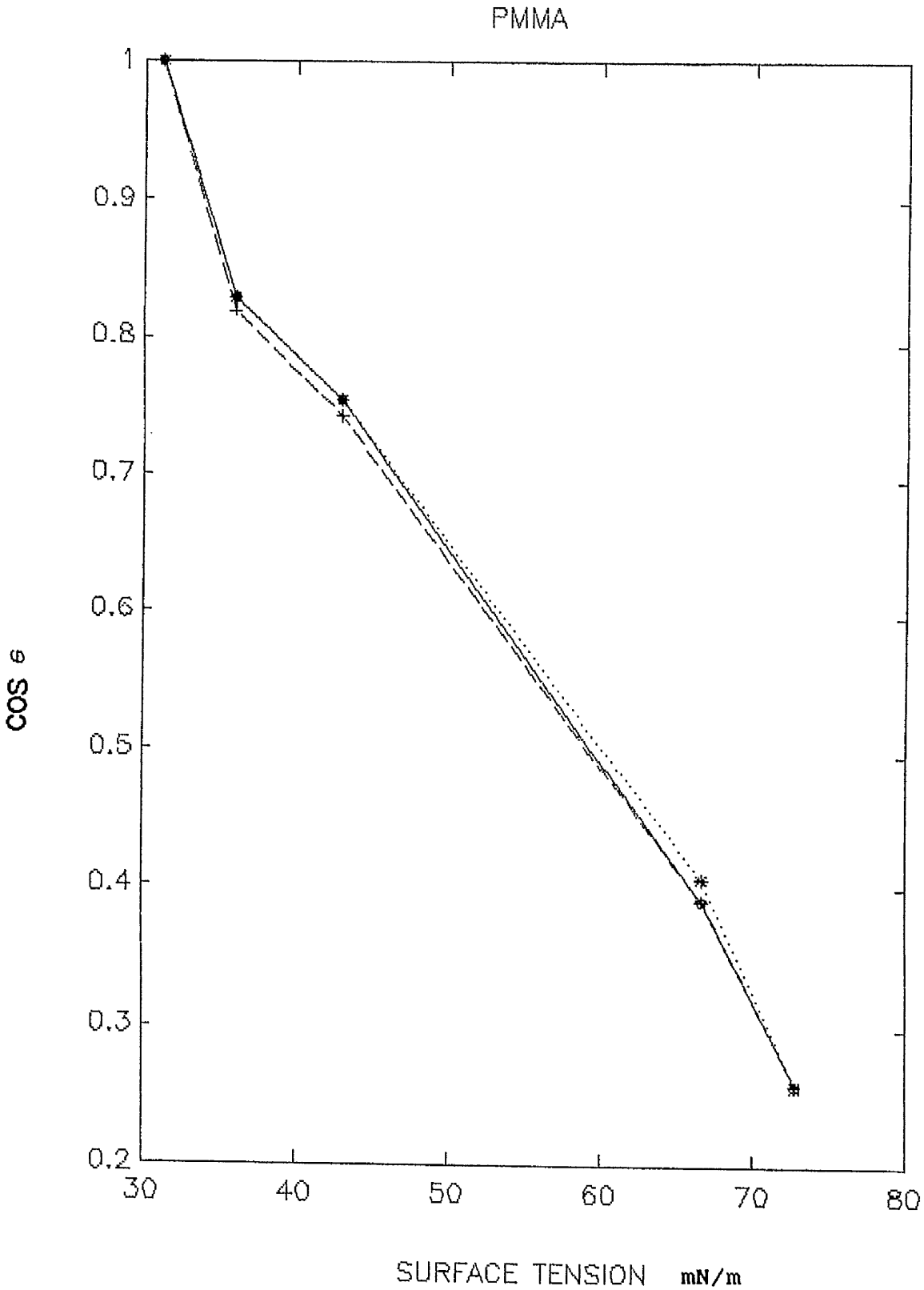

FIG. 3.1 THE RELATIONSHIP BETWEEN COSINE OF THE CONTACT ANGLE OF PMMA AND SURFACE TENSION OF TEST LIQUIDS

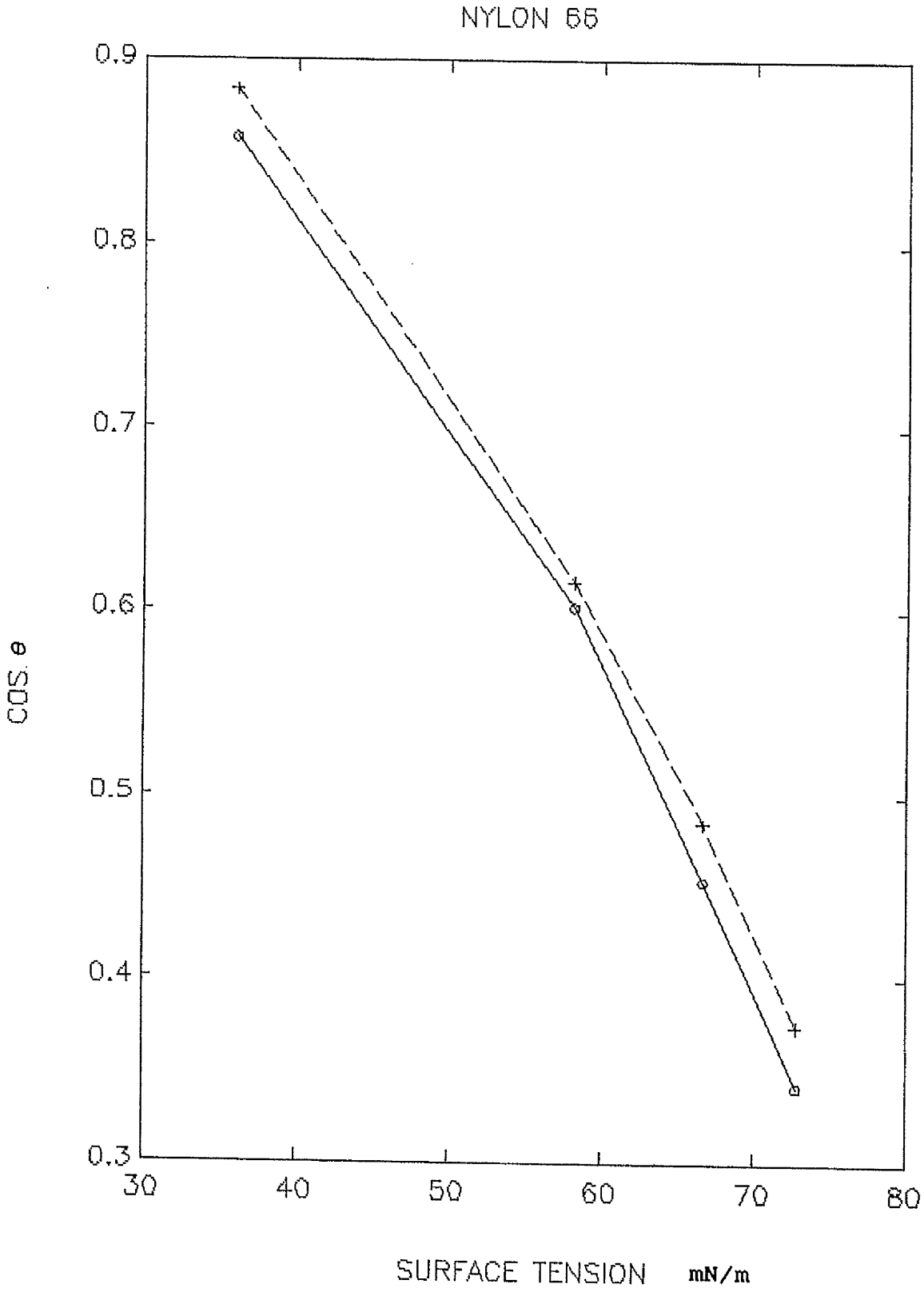

FIG. 3.2 THE RELATIONSHIP BETWEEN COSINE OF THE CONTACT ANGLE OF NYLON 66 AND SURFACE TENSION OF TEST LIQUIDS

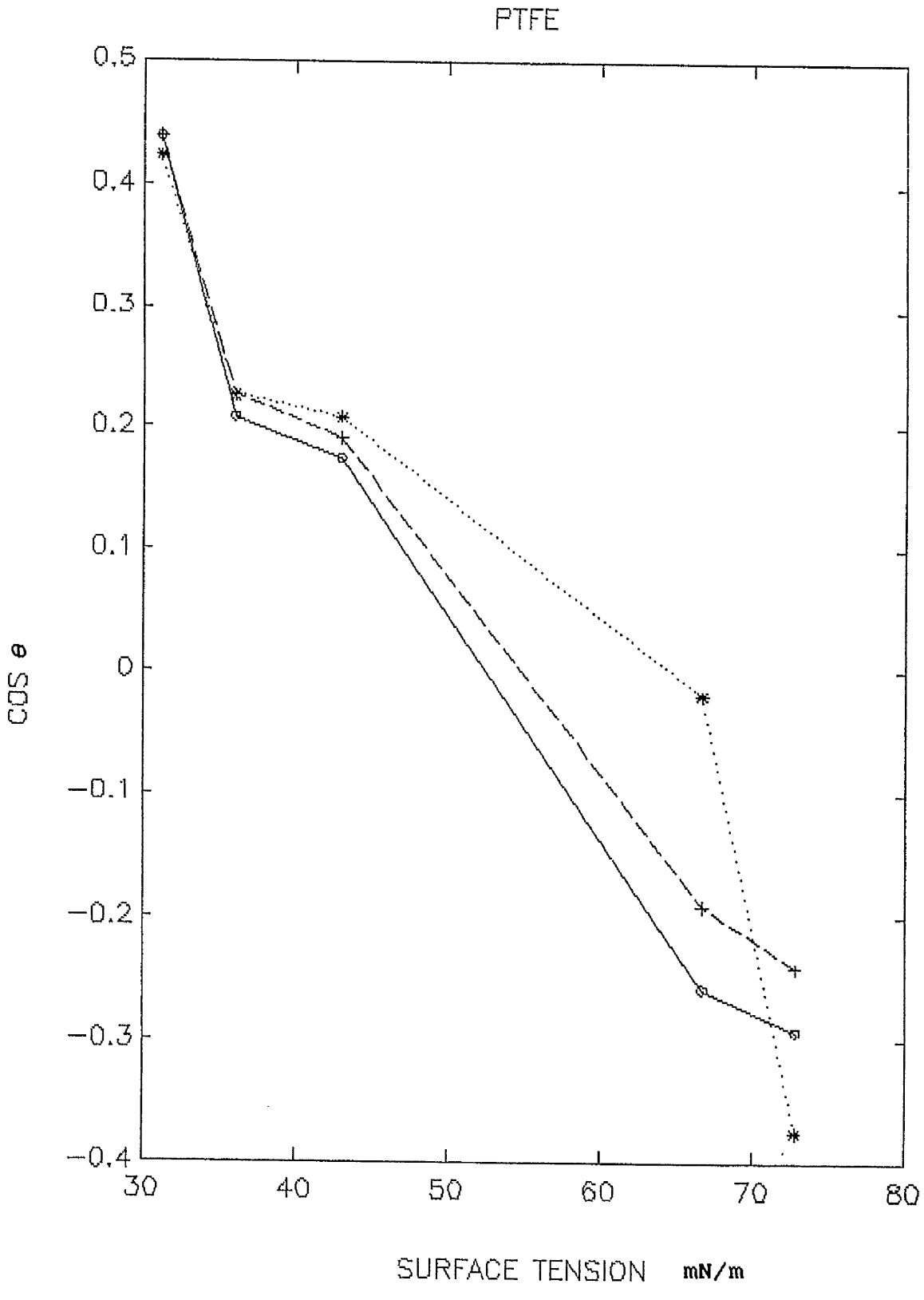

FIG. 3.3 THE RELATIONSHIP BETWEEN COSINE OF THE CONTACT ANGLE OF PTFE AND SURFACE TENSION OF TEST LIQUIDS.

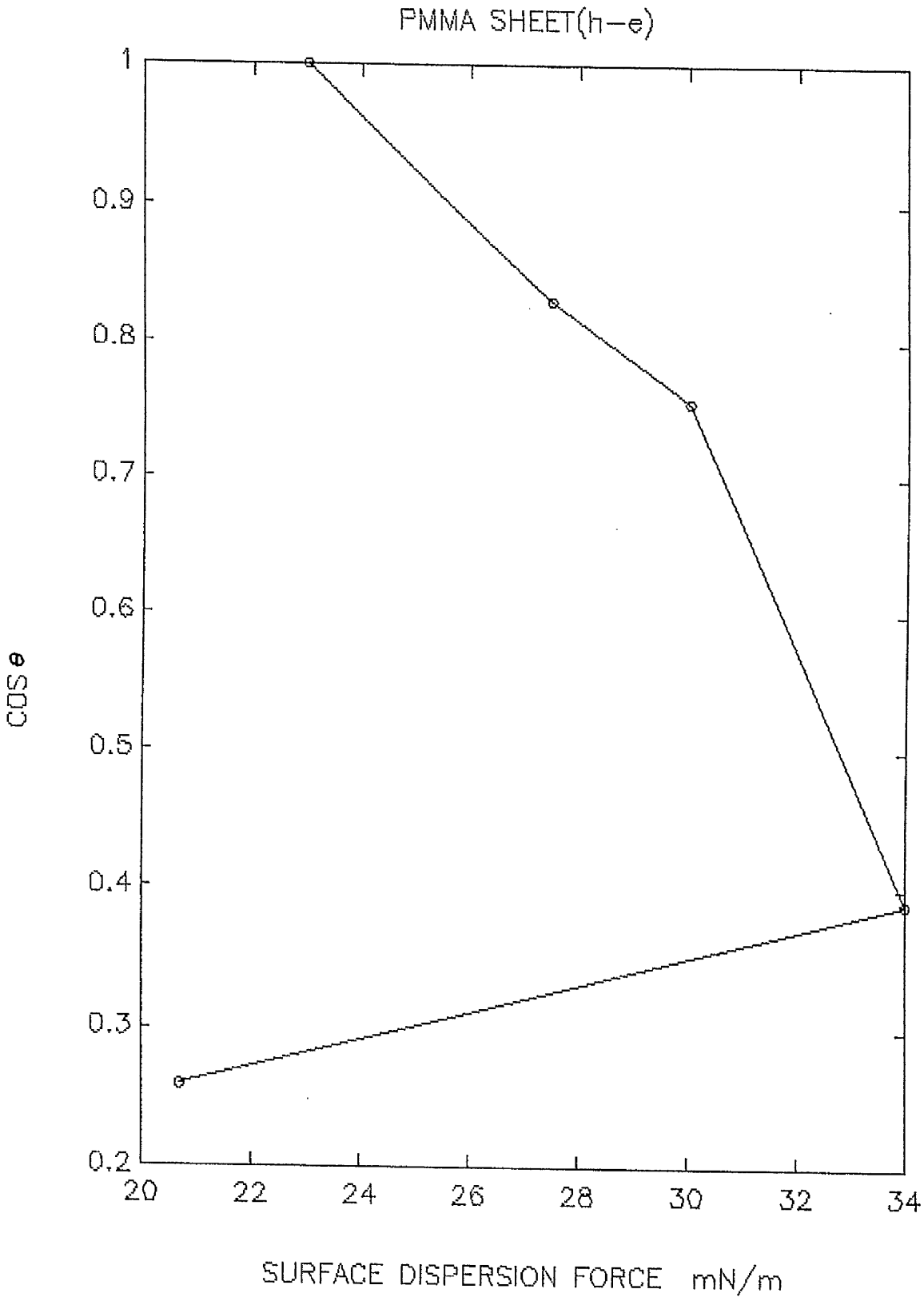

FIG. 3.4 THE RELATIONSHIP BETWEEN COSINE OF THE CONTACT ANGLE OF PMMA AND DISPERSION FORCE OF TEST LIQUIDS

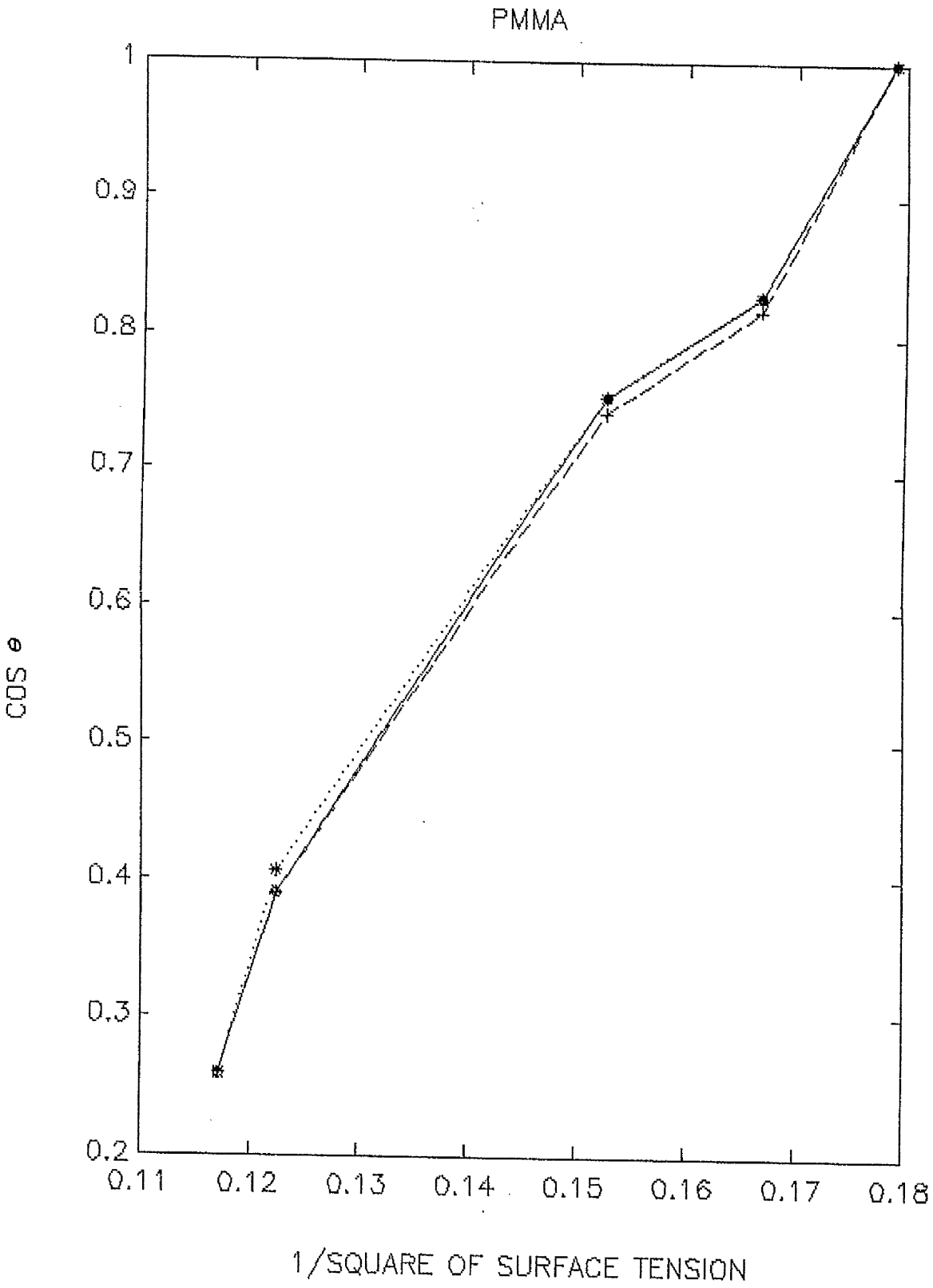

FIG. 3.5 THE RELATIONSHIP BETWEEN COSINE OF THE CONTACT ANGLE OF PMMA AND 1/SQUARE OF SURFACE TENSION OF TEST LIQUIDS

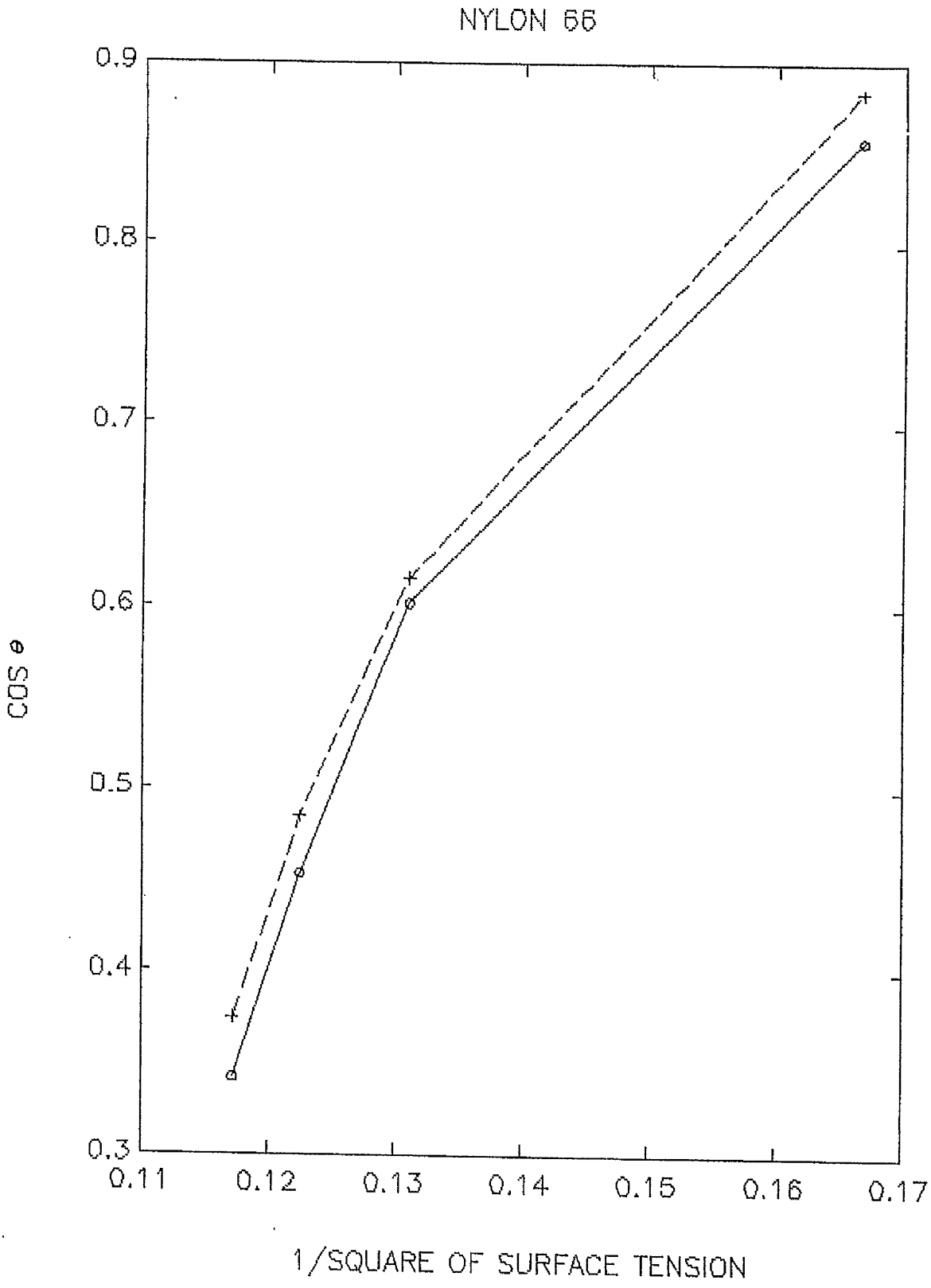

FIG. 3.6 THE RELATIONSHIP BETWEEN COSINE OF THE CONTACT ANGLE OF NYLON 66 AND 1/SQUARE OF SURFACE TENSION OF TEST LIQUIDS

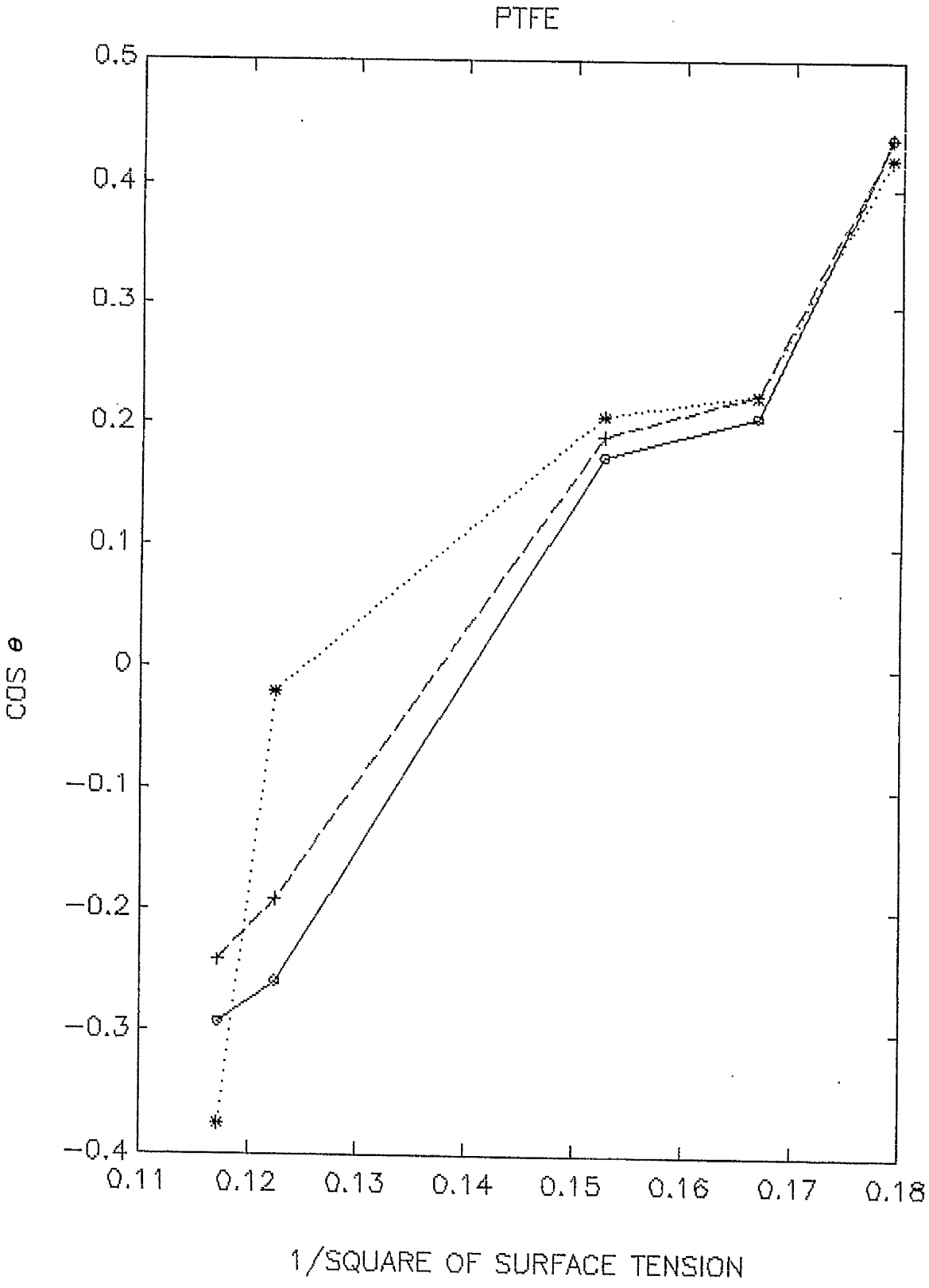

FIG. 3.7 **THE RELATIONSHIP BETWEEN COSINE OF THE CONTACT ANGLE OF PTFE AND 1/SQUARE OF SURFACE TENSION OF TEST LIQUIDS**

TABLE 3.8

CRITICAL SURFACE TENSION OF PMMA, PTFE, NYLON 66 (mN/m)

Solids	γ_c^*	Sheet		Powder
		h-ε	Tilt	h-ε
PMMA	39.0	28.6 (31.3)	28.0 (31.1)	28.5 (31.3)
PTFE	18.5	-9.9 (19.0)	-6.7 (18.3)	-9.3 (18.1)
Nylon 66	46.0	31.0 (31.1)	30.0 (31.9)	-

* Data from Zisman (1963)

as an empirical term to interprete in pharmaceutical processes becomes restricted to the liquid used.

3.3 LIQUID PENETRATION STUDIES

Table 3.9 gives the relevant properties of the liquids used in the penetration studies. Plots of the square of weight uptake against time gave straight lines in accordance with the Washburn equation. An example is shown in Fig 3.8.

3.3.1 CHOICE OF PERFECTLY WETTING LIQUIDS

The use of equation 1.19 to estimate the contact angle requires data from a perfectly wetting liquid. Studebaker and Snow (1955) used the criterion that if any two liquids yielded a value of 1 for cos θ from equation 1.19, they were more likely to be perfectly wetting than partially wetting to the same extent. Buckton (1985) and Buckton and Newton (1985) in their studies on penetration into barbiturate powders were not able to obtain a perfectly wetting liquid. The liquid which gave the highest cos θ value was assumed to be the best wetting liquid. In common with this work, no perfectly wetting liquid could be found, using the criterion of Studebaker and Snow (1955). Therefore in this study the best wetting liquid was used which gave the highest value of the capillary radius when cos $\theta = 1$ was substituted into equation 1.14. The calculated results for the capillary radius of corvic powders and tablets are shown in table 3.10 where it can be seen that propanol-2 is the best wetting liquid. All contact angle results were calculated using this liquid as the standard.

The correct choice of a perfectly wetting liquid is critical. Table 3.11 shows the calculated values of the contact angles using different liquids as the "Standard". Different "perfectly wetting liquids" give different contact angles for formamide and polyglycol E-200 whereas for water only slight changes of contact angles are obtained. For the powder, the angle of formamide using propanol as the best wetting liquid is 80° which changes to 62° using methanol as the best wetting liquid whereas the water angle is slighly changed from 87° to 82° . Similar responses are obtained in tablets. In contrast, Buckton and Newton (1985) found that the choice of perfectly wetting liquid was not too critical when an extrapolation technique was used for contact angle of water on barbiturates.

3.3.2 COMPARISON OF CONTACT ANGLES OF POWDERS AND TABLETS

Table 3.12 gives the contact angles values determined from penetration into powder beds and tablets. The gradients of plots of the square of weight of liquid uptake against time and their correlation coeffecients are also given. There is a good agreement between the two penetration studies.

The agreement between powders and tablets indicates that at the studied pressure, the surface characteristic of the powders has not been changed which can be seen from the scanning electron microscopic pictures before and after compaction (Fig.3.9). Similar agreement was obtained by Fukuoka et.al (1981). They found that the penetration rate (function of cos θ and capillary radius) of Magnesium oxide, Magnesium carbonate, crystalline cellulose, Magnesium silicate and lactose in powders was always higher than tablets. The higher rate was attributed to the higher capillary radius while the contact angle remained constant which was due to the low pressure applied which did not crush the particles. However, Buckton and Newton (1986) found that the contact angles on Barbiturate powders were higher than tablets. The discrepancy was thought to be due to deformation of the uppermost surface. After a certain pressure a further increase did not alter the contact angle. Hence the contact angle on a tablet was not representative for the powder in this study.

The coefficient of variation for the tablets was always found to be higher than in powders due to the small size of tablets. This is in agreement with the work of Fukuoka et al. (1981).

Therefore, precautions must be taken in interpretating results from penetration studies. A comparison of contact angles between powders and tablets should be made for each powder prior to any further studies.

TABLE 3.9

PROPERTIES OF TEST LIQUIDS

Liquids	η* ($mNm^{-2}s$)	γ_{LV} (mN/m)	γ_L^d (mN/m)	γ_L^p (mN/m)
Water	1.00	72.8	20.7	52.1
Formamide	3.30	58.2	32.1	26.1
E-200	58.10	43.0	30.0	13.0
Methanol	0.59	22.6*	15.4	7.2
Ethanol	1.22	22.1*	17.8	4.3
Cyclohexane	1.02	27.8*	26.9	0.9
Propanol	2.40	20.8*	16.2	4.6

* Data from handbook of Chemistry and Physics

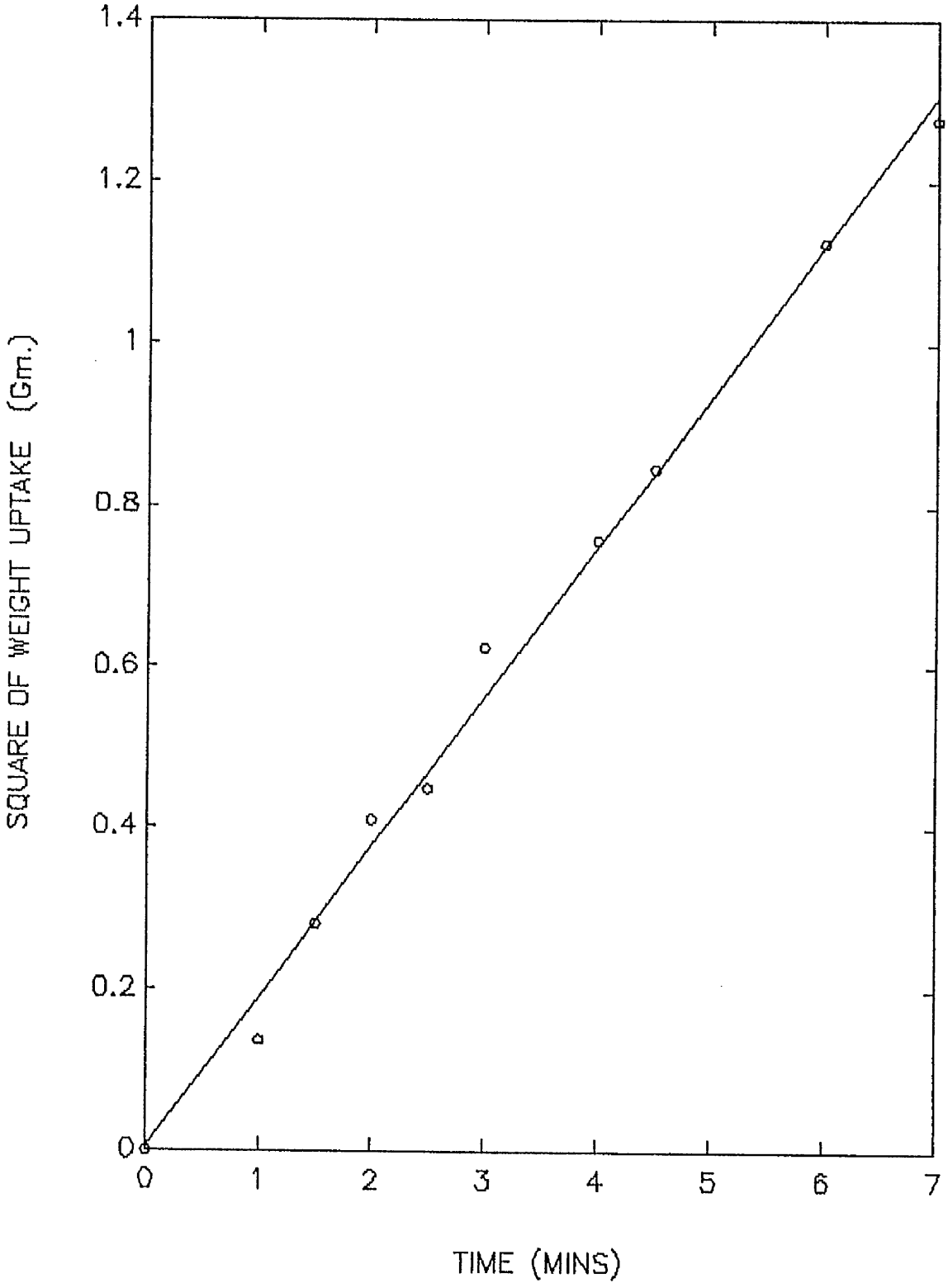

FIG. 3.8 THE RELATIONSHIP BETWEEN THE SQUARE OF WEIGHT UPTAKE OF PROPANOL AND TIME

TABLE 3.10

CALCULATED VALUES OF CAPILLARY RADII USING DIFFERENT LIQUIDS TREATED AS " PERFECTLY WETTING "

Liquid	Capillary radius (cm)	
	Powder	Tablet
Water	.002000	.000075
Formamide	.007520	.002030
Polyglycol E-200	-	.000100
Methanol	.016090	.011100
Ethanol	.021000	.012030
Cyclohexane	.022500	-
Propanol-2	.043400	.033580

TABLE 3.11

CONTACT ANGLES (DEGREES) OF CORVIC CALCULATED USING DIFFERENT LIQUIDS AS " PERFECTLY WETTING "

Non wetting Liquid	Perfectly wetting liquid							
	Powder (θ)				Tablet (θ)			
	MeOH	ETOH	Prop	Cyclo	MeOH	ETOH	Prop	Cyclo
Water	82.7	84.4	87.2	84.8	89.9	89.6	89.9	-
Formamide	62.2	69.0	80.0	70.5	79.5	80.3	86.5	-
E-200	-	-	-	-	58.0	68.4	79.8	-

TABLE 3.12

CONTACT ANGLES (DEGREES) ON CORVIC POWDER DETERMINED BY LIQUID PENETRATION INTO POWDER BEDS AND COMPACTS

Liquids	Powder			Tablet		
	gradient	θ	R^2	gradient	θ	R^2
Water	0.07415	87.2	.9100	0.00275	89.9	.9743
Formamide	0.06627	80.0	.9610	0.01793	86.5	.9383
E-200	-	-	-	0.00219	80.0	.9170
Methanol	0.3075	68.3	.9868	0.2133	70.6	.9773
Ethanol	0.1898	61.2	.9886	0.109	69.0	.9511
cyclohexane	0.3066	58.8	.9920	-	-	-
Propanol-2	0.1882	0	.9903	0.1455	0	.9340

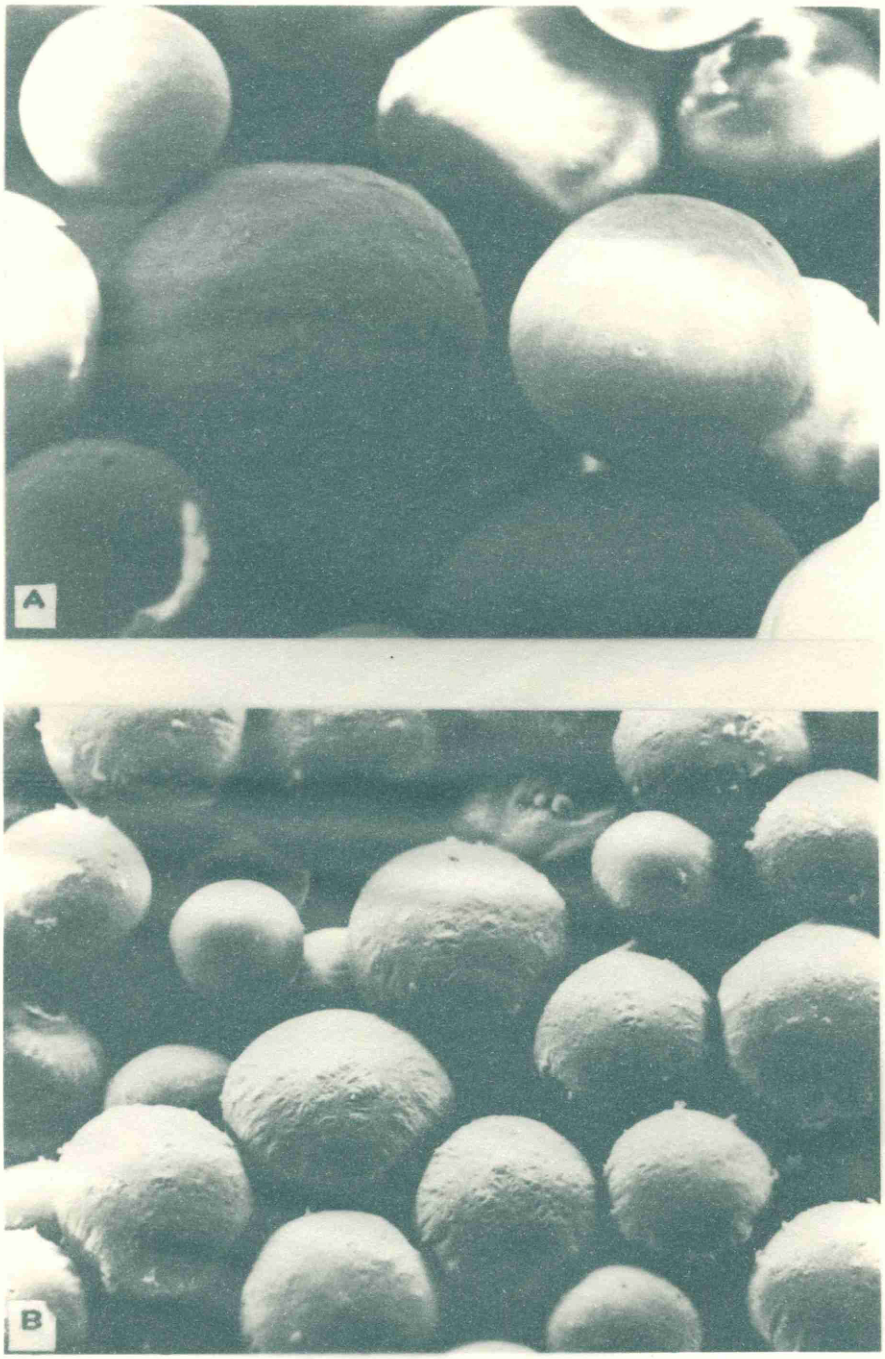

FIG. 3.9 SCANNING ELECTRON MICROGRAPHS OF CORVIC POWDER BEFORE (A) AND AFTER COMPACTION (B) AT MAGNIFICATIONS OF 200 X

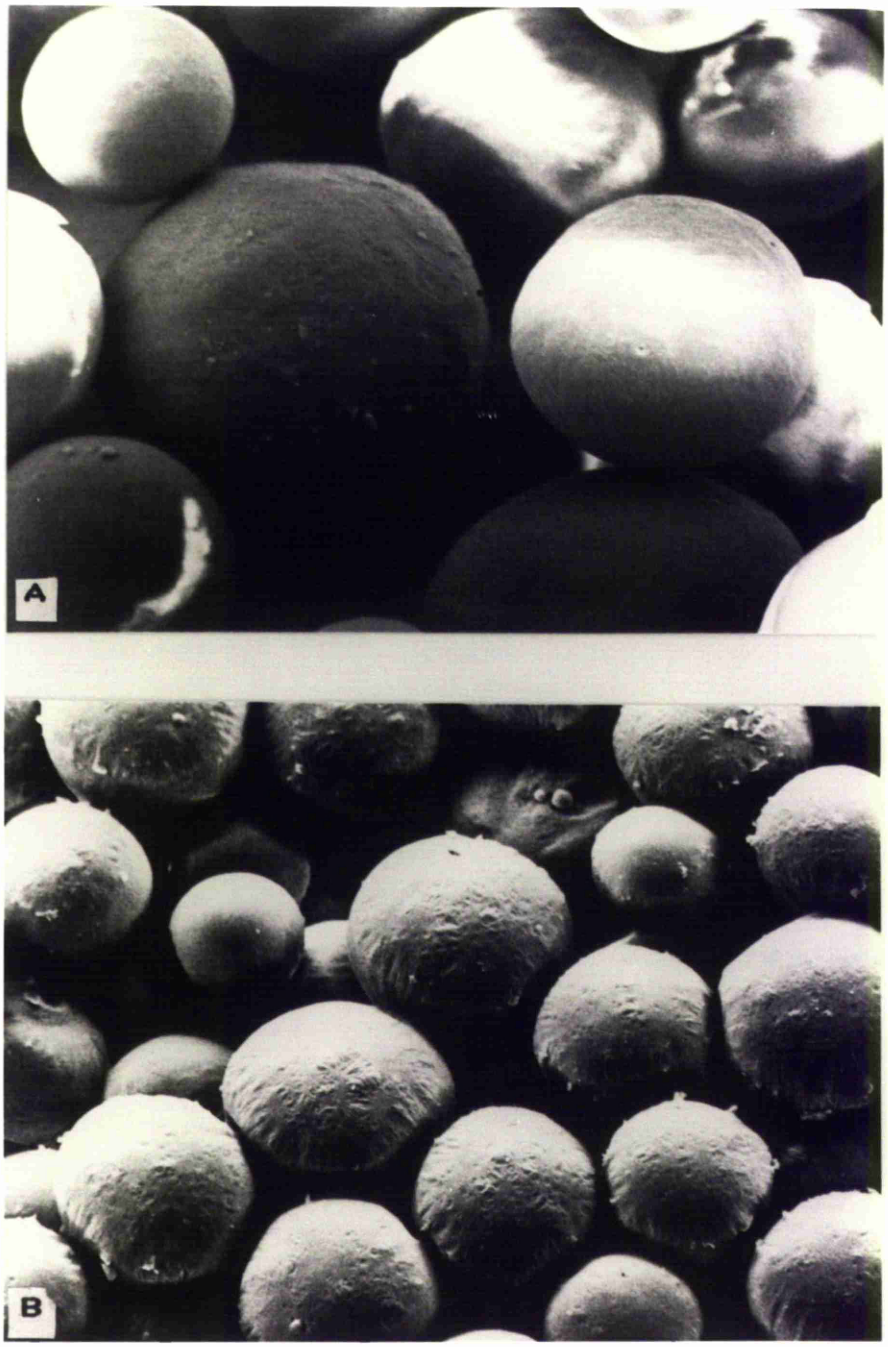
A
B

3.3.3 STATIC AND DYNAMIC CONTACT ANGLES

A comparison of the static angles on Corvic tablets determined by the h-ϵ method and the dynamic angles from liquid penetration studies is shown in table 3.13. Higher values were always obtained from the liquid penetration method. Methanol, ethanol and cyclohexane exhibit effectively zero angles when the h-ϵ method was applied, yet high angles were observed in the liquid penetration technique. Similar agreement was found in the work of Hansford et al. (1980). The contact angle of griseofulvin powder beds determined by the liquid penetration was higher than griseofulvin compacts determined by the h-ϵ method and also in agreement with the work of Mohammad and Fell (1982) on mixtures of Corvic and Polyethylmethacrylate.

The significant difference is certainly not due to powder being compressed since results discussed previously give good agreement between powders and tablets using the same method. The disagreement may result from the dynamic nature of the penetration method. If the velocity of the driving force is higher than the natural recovery velocity, so that the molecules do not have sufficient time to recover from the displacement causing disorientation of the molecules, the normal surface tension at the interface is exceeded. Consequently, a higher contact angle will be formed in accordance with Young's equation.

Table 3.14 gives the surface energies of the powders as calculated from the various liquid pairs, using the Wu equation (1971). The surface energy calculated from the dynamic angle is lower than from the static angle. The total surface energy is in very good agreement regarding liquid pairs chosen, whereas their components are variable depending on the liquid pair chosen (Luangtana-anan and Fell,1987) and as discussed in section 3.1.

TABLE 3.13

CONTACT ANGLES ON CORVIC TABLETS DETERMINED BY LIQUID PENETRATION AND THE $h-\varepsilon$ METHOD

Liquid	Contact angle (degrees)	
	Liquid penetration	$h-\varepsilon$
Water	89.9	71.2
Formamide	86.5	60.3
PEG E-200	79.9	36.9
Methanol	70.6	0
Ethanol	69.0	0
Cyclohexane	-	0
Propanol-2	0	0

TABLE 3.14

SURFACE ENERGIES OF CORVIC AND THEIR COMPONENTS (mN/m) CALCULATED USING VARIOUS LIQUID PAIRS

Liquid-liquid	Liquid penetration						h-ε		
	Powder			Tablet					
	γ_s^p	γ_s^d	γ_s	γ_s^p	γ_s^d	γ_s	γ_s^p	γ_s^d	γ_s
Water-formamide	17.7	8.2	25.9	19.7	4.8	24.5	22.7	13.7	36.4
Water-E-200	-	-	-	18.2	6.1	24.3	19.6	18.7	38.3
Water-methanol	24.9	2.5	27.4	-	-	-	27.3	8.8	36.1
Water-etanol	19.6	6.3	25.9	19.3	5.1	24.4	23.5	12.7	36.2
Water-cyclohexane	12.9	15.2	28.1	-	-	-	-	-	-
Water-propanol	14.7	12.1	26.7	13.1	12.4	25.5	25.0	11.0	36.0
Formamide-ethanol	21.8	6.2	28.0	19.0	5.1	24.1	24.8	12.6	37.4
Formamide-cyclohex.	9.1	15.2	24.3	-	-	-	10.7	25.4	36.1
Formamide-propanol	11.4	12.8	24.2	6.9	14.5	21.4	28.9	10.7	39.6
Formamide-E-200	-	-	-	15.9	6.7	22.6	12.3	23.0	35.3
E-200-ethanol	-	-	-	24.0	4.9	28.0	-	-	-
E-200-cyclohexane	-	-	-	-	-	-	9.8	25.0	35.2

CHAPTER 4

CONCLUSIONS

A comparison of surface free energy determinations has been made among different polymeric materials, that is PTFE, PMMA, Nylon 66 and Corvic. Contact angle measurements are widely used to establish surface free energy values. A good agreement was observed between the angles obtained in both methods ie. tilting plate method and the h-ϵ method and for both powders and smooth solid surfaces. This agreement indicates that these methods are applicable to the measurement of powders and that pressure does not change the surface characteristics of the materials used. Therefore the surface free energy values determined by the h-ϵ method can be a reflective value for the powders.

To calculate the surface free energy of a solid at least two liquids with known surface free energies are used. The choice of liquid pairs is critical for the determination of individual components of the surface energy of the solid. Liquid pairs with widely differing surface tension are a better choice to give reliable results. Surface free energy determinations are less sensitive to the accuracy of contact angle measurements for higher energy solids.

Contact angles obtained from the h-ϵ and tilting plate methods are static angles. The determination of contact angles on powders can be performed by the h-ϵ method. However, the liquid penetration technique is the only method available to determine the contact angle of a powder without compression.

Good agreement is obtained between powders and tablets using this method. This agreement, again, supports the previous study that the pressure does not change the surface characteristics of a solid and the contact angle. Hence, the surface free energy after compaction can be a representative value for the powder.

The angle determined by penetration is much higher than the static angle which is possibly due to the kinetic effect. The surface free energy of powders and tablets are in very good agreement for every liquid pair studied, but the components varied widely. The surface energy determined by this method is lower than that from static angles. Since there are a lot of problems in dealing with the kinetic method and the energy changes according to the velocity, hence, surface free energy obtained by the static study seems to be a better representative value of the solid surface energy.

Athough these studies were carried out on polymer materials, the results establish the validity of determining surface energies of pharmaceuticals in powder form and indicate the precautions that must be taken in interpreting results.

PART 2

CHAPTER 1

INTRODUCTION

1.1 MECHANISMS OF COMPACTION

In the compaction of dry powders, two distinctive processes are of interest (Seelig and Wulff, 1946):

a). consolidation of the particles

b). bonding mechanisms

A) CONSOLIDATION OF PARTICLES

In this process particles rearrange or deform as shown in Fig.1.1 (Cooper and Eaton ,1962). Initially particles will primarily slide past one another to fill in the holes which are the same size as the particles. Slight modifications to the particles may occur by fragmentation and plastic flow. At the end of this step a loose powder bed is formed. This rearrangement of the particles will occur depending on the particle size, shape, the die diameter and also the flowability of the powder. Further rearrangement is associated with a filling of voids that are substantially smaller than the original particles. For this to occur plastic flow and/or fragmentation is required.

Many studies have been carried out to evaluate which of the two mechanisms is the predominant one in the consolidation of specific materials. Nystrom and Karehill (1986), Alderborn et al. (1985,1987) and Duberg and Nystrom (1985) used surface area measurements determined either by gas adsorption or permeametry to indicate the degree of fragmentation, since fragmentation will lead to an increase in surface area.

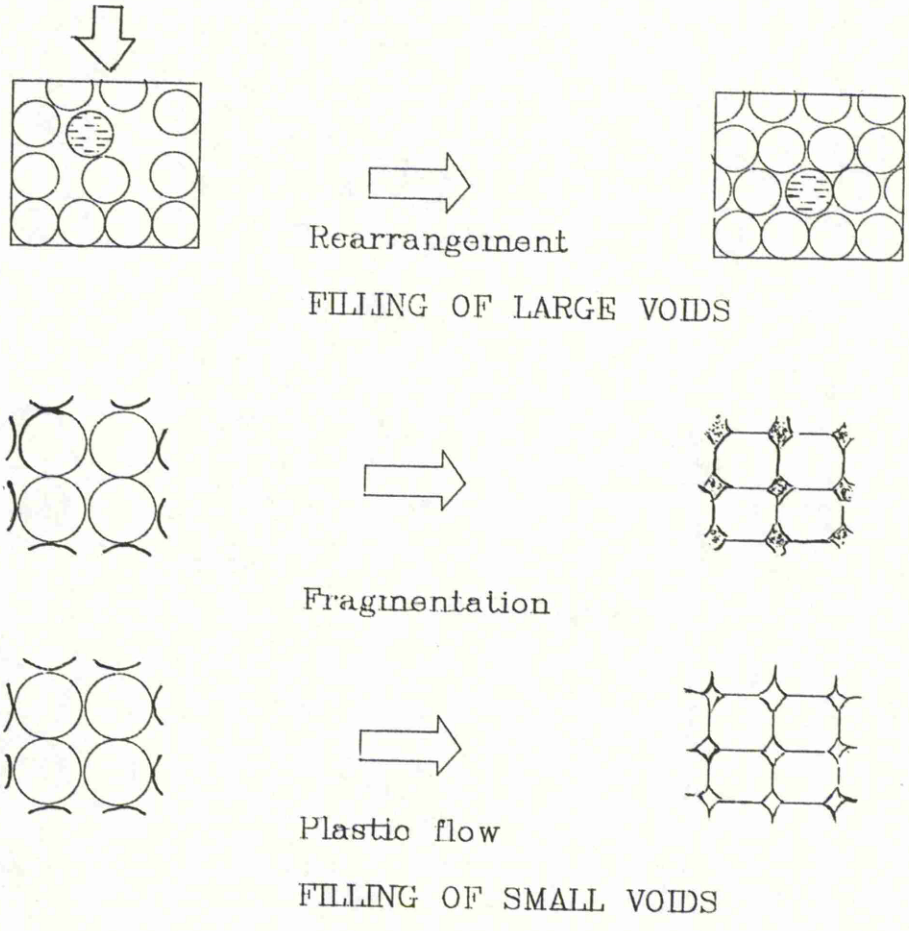

FIG. 1.1 **DIAGRAM OF DIFFERENT METHOS OF PARTICLE CONSOLIDATION**

The isotropy ratio is another parameter providing information on fragmentation (Nystrom, 1981; Alderborn and Nystrom, 1982a, 1984; Duberg and Nystrom, 1982, 1985). It is the ratio between the axial tensile strength and the radial tensile strength of a coherent compact. Duberg and Nystrom (1985) found that a high ratio occurred in fragmenting systems such as lactose and Emcompress whereas the low values are in powders which undergo plastic deformation such as sodium chloride, sodium bicarbonate and Avicel PH 105. They also found that the addition of Avicel as a second material changed the isotropy ratio for fragmenting particles but had no effect on materials exhibiting plastic flow.

The response of the additional material also indicates the consolidation mechanism. de Boer et al.(1978) found that magnesium stearate decreased the strength of materials consolidating by plastic flow whereas the strength of tablets of materials which fragmented remained constant. This is in agreement with the work of Vromans et al. (1988). However, they showed that the susceptibility of a material to magnesium stearate lubrication did not neccessarily reflect the degree of fragmentation propensity. In fact it depended on a number of factors including particle sizes, flowability and mechanism of consolidation. Nystrom et al (1982) studied the effect of various binder particle size on the mechanical strength of tablets. They found that addition of the binder to sodium chloride, which deformed by plastic flow, was most affected by particle size variation of the binder whereas with lactose, the effect was very small. Scanning electron microscopy is also widely used to confirm the consolidation process (de Boer et al.,1978).

Cole et al. (1975) studied stress relaxation behaviour and concluded that sodium chloride and potassium choride which deform by plastic flow exhibited a high stress relaxation while fragmenting materials such as lactose and potassium citrate gave lower values. An increased tensile strength dependent on an increasing time of compaction was found in materials which exhibit plastic flow and showing a considerable stress relaxation (David and Augsburger, 1977).

Porosity measurements are commonly used to characterize consolidation mechanisms (Heckel, 1961; Cooper and Eaton, 1962; Hersey et.al,1972; de Boer et.al, 1978; Chowhan and Chow, 1980; Sheikh-Salem and Fell, 1981; Duberg and Nystrom 1982, 1985; Humbert Drotz, 1983a; and Alderborn et al.,1987). Plotting the relationship between porosity and pressure as suggested by Heckel (1961) has been used to distinguish between materials which consolidate by fragmentation plastic flow (Hersey and Rees, 1971)

Although there are many parameters used to determine the fragmentation propensity, none of them give quantitative values. In addition, some powders lie between both mechanisms. The consolidation mechanism depends on the nature of the material, speed of compaction and particle size (Sheikh-Salem and Fell, 1981, 1982).

B) THE BONDING MECHANISMS

The consolidation process results in particles being brought closer together so that they can interact and hence form bonds. Five different bonding mechanisms have been proposed as below: (Rumpf, 1962)

1). SOLID BRIDGES

They arise from a melting of material at the interparticulate contact points causing the particles to fuse and form solid bridges. Melting is brought about from either external heat applied during a sintering process or from the process of compression. Travers and Merriman (1970) found a temperature cycle occurred during the compression process, the temperature rising during compaction and falling when the pressure was removed.

York and Pilpel (1973) suggested that the heat generated by friction during compression was sufficient to cause the melting of particles at the contact points resulting in an increased tensile strength. This effect was applicable to low melting point powders. Danjo and Otsuka (1988) found that an increase in storage temperature led to a higher tensile strength which was brought about by melting at interparticulate contact points. Hanus and King (1968) suggested that changes in temperature during compression were related to the speed of compression and the applied pressure.

2). MECHANICAL INTERLOCKING

The mechanism is due to the interlocking of irregularly shaped particles during compaction and is more likely to be of consequence for plastically deforming materials than brittle ones.

3) ADHESIVE AND COHESIVE BONDING FORCES

These forces arise when viscous binders are involved and liquids in this stage are defined as immobile liquids. Strength of agglomerates arise from cohesive force between particles themselves and adhesive forces between particles and the binders. The strength of bonds depend on the amount and quality of binding agents.

4) INTERFACIAL FORCE AND CAPILLARY PRESSURE AT FREELY MOVABLE LIQUID SURFACES

The force depends on the amount of liquid in the system. At low liquid levels a ring shape at the point of contact is formed. This stage is the called pendular state as shown in Fig.1.2. The cohesive forces between two particles depends on the surface tension of this liquid bridge, the curvature and the diameter of the particles. The strength of this stage increases with decreasing moisture content, as the curvature increases. The tensile strength of a moist powder in the pendular state can be calculated by (Capes, 1980) :

$$\sigma = -\frac{9}{4}\,\frac{1-\epsilon}{\epsilon}\,\frac{\gamma}{d} \qquad \ldots 1.1$$

where σ is tensile strength, ϵ is porosity of agglomerate and d is particle diameter.

As the amount of liquid increases beyond the point of ring coalescence the funicular state is reached with its continuous net work of liquid interspersed with air. The capillary state prevails when all the pores become filled with liquid. At this stage the force is due to the pressure deficiency and can be expressed by Laplace equation. The tensile strength is given by:

$$\sigma = 6 \frac{1-\epsilon}{\xi} \frac{\gamma}{d} \qquad \ldots 1.2$$

The strength of the capillary state is about three times that of the pendular state and the funicular state is between both states.

5) ATTRACTIVE FORCES

These forces are due to the coulombic forces between charged species as well as covalent bonds, hydrogen bonds and Van der Waals forces.

In the compaction process, the steps described do not necessarily follow each other in sequence, but an overlap may occur and some stages may be absent. The bonding mechanisms described are general for powders and are not all necessarily involved in tabletting. Solid bridges can be formed during granulation and compression steps . Mechanical interlocking is generally regarded as being of little significance. Adhesive and cohesive forces may be applicable when binders are involved.

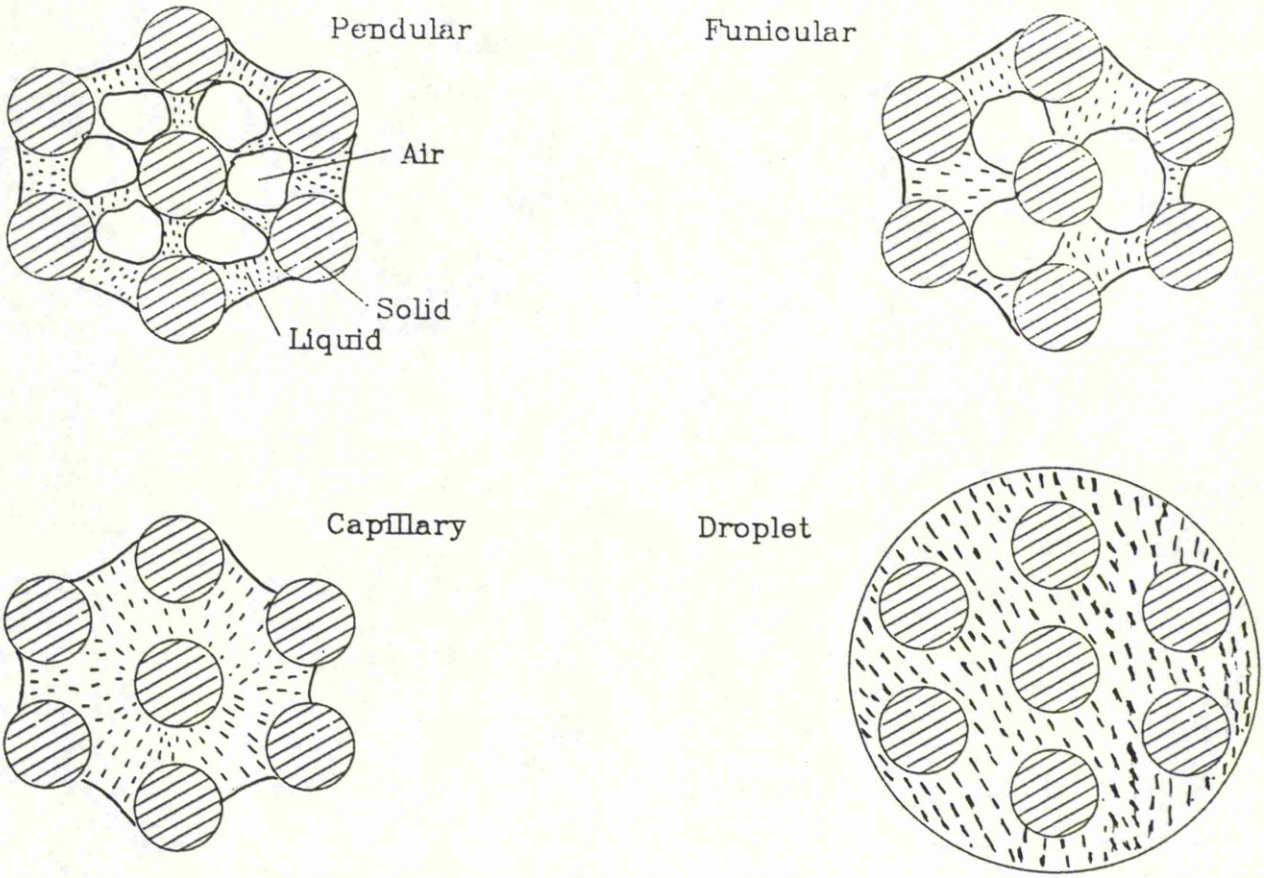

FIG. 1.2 DIAGRAM OF DIFFERENT STAGES OF INTERFACIAL FORCE BETWEEN FREELY MOVABLE LIQUIDS

Interfacial forces will apply in the wet granulation stages. Finally, attractive forces will always contribute to the strength of tablets and, of these, Van der Waals will occur for all materials especially, when the direct compression is involved . Therefore, they will be described in detail in the next section.

1.2 VAN DER WAALS FORCES

Van der Waals forces are always present as part of the several intermolecular forces. The force between two molecules is a short-range force whereas the force between macroscopic bodies is a long-range force and is of interest in tabletting. The force varies with distance, it can be effective from a large distance, greater than 10 nm., down to interatomic spacing, 0.2 nm. (Israelachvili,1985).

1.2.1 TYPES OF VAN DER WAALS ATTRACTIVE FORCES

1. Induction or Debye forces

These forces arise from an electric field produced by one permanent dipole molecule acting on a second dipole. This field will induce a dipole in the second molecule resulting in the polarizability of the second molecule and therefore there is a similar phenomena from the second molecule acting on the first molecule occurs. This effect results in the attraction.

2. Orientation or Keesom forces

They arise from the interaction of two permanent dipoles exerting electrostatic forces which mutally orientate each other and contribute to the polarizability and attractive effect.

3 Dispersion or London forces

Forces arise from fluctuations in electron charge distribution around atoms or molecules. These deformable electron clouds in adjoining molecules distort one another, resulting in an instantaneous dipole. This instantaneous dipole happens in the direction of the charge fluctuating with the frequency of the charge fluctuations. The instantaneous dipole generates an electric field that polarizes any nearby neutral atom, inducing a dipole moment in it. The resulting interaction between the two dipoles gives rise to an instantaneous attractive force between the two atoms.

These three types of forces contribute to the total Van der Waals force. All the molecules can display the dispersion component of attraction since they all are polarizable. Therefore dispersion forces are always present in every type of molecule and give the major contribution to the Van der Waals force whereas the first two forces require a dipole moment which depend on the properties of the molecules.

Van der waals potential energy (ΔF) depends on the geometry of macroscopic bodies (Israelachivilli, 1985). Two flat plate surfaces are commonly used as a model to derive the energy. It can be expressed by: (Hamaker, 1937)

$$\Delta F = -\frac{A}{12\pi d_0^2} \qquad \ldots 1.3$$

where A is the Hamaker constant and d_0 is the distance of separation (0.2 nm.). The negative sign indicates an attraction when the Hamaker constant is positive.

1.2.2 HAMAKER CONSTANT

The Hamaker constant (A) can be derived by two approaches.

1) The microscopic approach

This is based on a summation of interaction energy between macroscopic bodies over all pairs of atoms and molecules. The Hamaker constant, A, of two bodies of material is given by:

For identical bodies

$$A_{11} = \pi^2 q_1^2 \beta_{11} \qquad \ldots 1.4$$

For dissimilar bodies

$$A_{12} = \pi^2 q_1 q_2 \beta_{12} \qquad \ldots 1.5$$

where q is the number of atoms per unit volume, β is the Van der Waals constant and subscript 1,2 define the different materials. Since the dispersion component is the dominant contributor to the attraction, β can be expressed by only the dispersion force as below:

$$\beta_{11} = \frac{3}{4}\alpha^2 h\upsilon_{11} \quad \ldots 1.6$$

$$\beta_{12} = \frac{3}{4}\alpha_1\alpha_2 h\upsilon_{12} \quad \ldots 1.7$$

where α is the polarizability of the atom, related to the refractive index; h is Plank's constant and υ is the frequency of electron in the ground state.

The technique has some defects due to simplifying the addition of molecular interactions and limiting the number of pairs of atoms or molecules used in the calculation of the A value. The effect of neighbouring atoms on the arbitrary atoms is not taken into account. The molecules nearer the surface screen the interactions of molecules buried more deeply in the material. If there is a heterogeneous effect this will lead to difficulty in interpreting their polarization. The equation is only applicable in vacuum or air but not in liquid media. The equation is derived from an assumption that interaction bodies must not undergo distortions in shape and size due to the interactions and only one electron is involved in the fluctuations, whereas electrons in all the orbitals may contribute to the Van der Waals forces (Mahanty and Ninham, 1976 and Tabor, 1982).

2) The macroscopic approach

The theory is based entirely on measurable bulk properties rather than molecular parameters. Lifshitz (1957) has developed the theory in a very general form, treating bodies and intervening media in terms of dielectric constants and a quantum

theory is applied. The screening effects are built into the solution. The work of Krupp (1967), Visser (1972), Israelachvili (1973,1985) studied the Hamaker constant on the basis of this theory.

The Hamaker constant between two different bodies acting through an intervening medium 3, A_{132} , is given by

$$A_{132} = \frac{3\overline{h\omega}_{132}}{4\sqrt{2}\pi} \qquad \ldots 1.8$$

where $\overline{h\omega}_{132}$ is the Lifshitz-Van der Waals constant, which is expressed by:

$$\overline{h\omega}_{132} = h \int_0^\infty \frac{\Sigma_1(i\beta) - \Sigma_3(i\beta)}{\Sigma_1(i\beta) + \Sigma_3(i\beta)} \frac{\Sigma_2(i\beta) - \Sigma_3(i\beta)}{\Sigma_2(i\beta) + \Sigma_3(i\beta)} d(\beta)$$

where $\Sigma(i\beta)$ is the dielectric constant of material 1 along the imaginary frequency axis $i\beta$. According to Krupp (1967) the Lifshitz constant between two different bodies is given by:

$$\overline{h\omega}_{12} = (\overline{h\omega}_{11}\overline{h\omega}_{22})^{1/2} \qquad \ldots 1.9$$

According to equations 1.8 and 1.9 the Van der Waals force between any two bodies in vacuum is always attractive. The force between two identical bodies in a medium is also attractive (A positive) while that between different bodies can be attractive or repulsive (equation 1.8). The force will be repulsive when the dielectric constant of a medium lies between that of the two bodies ($\Sigma_1 < \Sigma_3 < \Sigma_2$ or $\Sigma_1 > \Sigma_3 > \Sigma_2$).

1.2.3 VAN DER WAALS ENERGY AND SURFACE ENERGY

Regarding the difficulty with the complexity of the macroscopic and microscopic theory, several treatments have been developed to simplify and extend its findings. Surface free energy terms have been introduced since they are determined from the forces between molecules and surfaces. Van der Waals energy is the reversible work required to separate two parallel plates from a distance d to infinity. This energy is equal to the work to produce two new unit surfaces. The change of free energy for identical surfaces is:

$$\Delta F_{ii} = -2\gamma_{iv} \qquad \ldots 1.10$$

and for dissimilar surfaces is:

$$\Delta F_{ij} = \gamma_{ij} - \gamma_{iv} - \gamma_{jv} \qquad \ldots 1.11$$

where i and j are two different surfaces, v is the vapour phase. Combining equation 1.3 and 1.10 give:

$$A = 24\pi d_0^2 \gamma \qquad \ldots 1.12$$

In other words, surface energy is equal to half of the Van der Waals energy needed to separate two surfaces from contact to infinity. Hiemenz (1986) suggested that equation 1.12

is apt to work best for a nonpolar materials. However, for a material with interactions other than London forces, it may be better to use the dispersion component of surface energy rather than the total energy. The following equation is used in which its numerical coefficient is only about one-seventh of that in equation 1.12

$$A = \frac{4\pi}{1.2} \gamma^{d} d_0^2 \qquad \ldots 1.13$$

1.2.4 VAN DER WAALS FORCES IN INTERVENING MEDIA

If two particles are brought close together, dispersion medium must be displaced to the position originally occupied by the interaction bodies which is shown in Fig. 1.3 (Shaw, 1986). The change in the potential energy is given by:

for dissimilar particles

$$F_{132} = F_{33} + F_{12} - F_{13} - F_{23} \qquad \ldots 1.14$$

for identical particles

$$F_{131} = F_{33} + F_{11} - 2F_{13} \qquad \ldots 1.15$$

Substituting equations 1.10 and 1.11 into equations 1.14 and 1.15 yield:

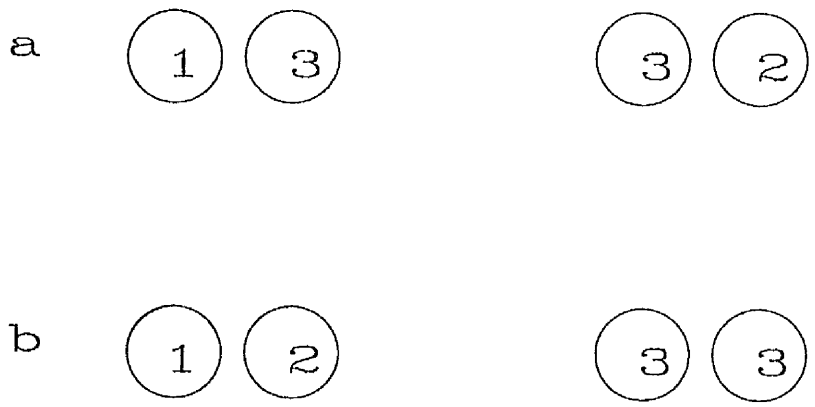

FIG. 1.3 THE INTERACTION BETWEEN TWO PARTICLES 1 AND 2 IN AN INTERVENING MEDIA 3

a) WHEN THE PARTICLES ARE FAR APART

b) WHEN PARTICLE 2 IS BROUGHT CLOSE TO PARTICLE 1

$$F_{132} = \gamma_{12} - \gamma_{13} - \gamma_{23} \quad \ldots 1.16$$

$$F_{131} = -2\gamma_{13} \quad \ldots 1.17$$

Therefore equation 1.3 can be rewritten in terms of surface energy.

$$A_{132} = -12\pi d_0^2 (\gamma_{12} - \gamma_{13} - \gamma_{23}) \quad \ldots 1.18$$

$$A_{131} = 24\pi d_0^2 \gamma_{13} \quad \ldots 1.19$$

Fowkes (1964) derived the interfacial force from the interaction between the surface of both layers

$$\gamma_{13} = \gamma_1 + \gamma_3 - 2(\gamma_1^d \gamma_3^d)^{1/2} \quad \ldots 1.20$$

Wu (1971) took into account polar interactions between solid and liquid phases, therefore equation 1.20 should be:

$$\gamma_{13} = \gamma_1 + \gamma_3 - 2(\gamma_1^d \gamma_3^d)^{1/2} - 2(\gamma_1^p \gamma_3^p)^{1/2} \quad \ldots 1.21$$

Neumann et al. (1979, 1982), Van Oss et al. (1980, 1983) determined the Hamaker constant of various polymers embedded in a melt of Napthalene, using surface energy measurements.

1.2.5 COMBINING RULE

Each of the terms from equation 1.14 and 1.15 can be expressed by the Hamaker constant (Heimenz 1986; Shaw 1986) since they depend in the same way on the size and distance parameters.

$$A_{132} = A_{33} + A_{12} - A_{13} - A_{23} \quad \ldots 1.22$$

$$A_{131} = A_{33} + A_{11} - 2A_{13} \quad \ldots 1.23$$

Berthelot's rule derives A in terms of the geometric means of the individual media

$$A_{13} = (A_{11}A_{33})^{1/2} \quad \ldots 1.24$$

Therefore equations 1.22 and 1.23 can be rewritten as follows:

$$A_{132} = (\sqrt{A_{11}} - \sqrt{A_{33}})(\sqrt{A_{22}} - \sqrt{A_{33}}) \quad \ldots 1.25$$

$$A_{131} = (\sqrt{A_{11}} - \sqrt{A_{33}})^2 \quad \ldots 1.26$$

The right hand side of equations 1.25 and 1.26 can be expressed in terms of surface energy

$$A_{132} = 24\pi d_0^2 (\gamma_{11}^{1/2} - \gamma_{33}^{1/2}) (\gamma_{22}^{1/2} - \gamma_{33}^{1/2}) \quad \ldots 1.27$$

$$A_{131} = 24\pi d_o(\gamma_1^{1/2} - \gamma_3^{1/2})^2 \quad \ldots 1.28$$

The difference between the Hamaker constant from equation 1.18 and 1.19 and from equation 1.27 and 1.28 is due to the application of Berthelot's rule. Girifalco and Good (1957) suggested the interaction parameter φ should be included in equation 1.24.

$$A_{13} = \varphi(A_{11}A_{33})^{1/2} \quad \ldots 1.29$$

where φ is the interaction parameter $= \dfrac{\gamma_1 + \gamma_2 - \gamma_{12}}{2(\gamma_1\gamma_2)^{1/2}}$

Visser (1972) defined C as a correction factor for the transmission of a foree through a third medium. Equations 1.22 and 1.23 should be amended:

$$A_{132} = C(A_{33} + A_{12} - A_{13} - A_{23}) \quad \ldots 1.30$$

$$A_{131} = C(A_{33} + A_{11} - 2A_{13}) \quad \ldots 1.31$$

The comparison between Hamaker constants derived from the microscopic and macroscropic approaches was made and the difference was by a factor of C which is in the range between 1.6-1.8 (Visser, 1972).

1.2.6 EFFECTIVE DISTANCE

The London dispersion equations (equation 1.6 and 1.7) are valid when the distances of separation are associated with the corresponding wavelength (frequency) which causes an instantaneous dipole. The non-retarded forces which contribute to the Van der Waals force are exhibited when the wavelength is equal to, or larger than, the distance of separation. Tabor (1982) and Jaycock and Parfitt (1981) found that at a distance below 30 nm. the non retardation effect applied. Beyond this point, the wavelength is lower than the distance of separation resulting in too rapid fluctuations to enable the field to reach a neighbouring atom without much change in electron configuration. The system will tend to ignore the faster fluctuations and will pick out those which are slow enough to give good correlation.

Another region (below 0.2 nm.) in which the Van der Waals energy can give misleading results is in the case of atomic contact. The distance must be fairly long compared with the atomic diameter to produce a dipole attributed to the Van der Waals force according to equation 1.6 and 1.7. The minimum effective distance was found to be 0.2 nm. (Israelachvili, 1985; Tabor, 1982). A value of 0.182 nm. was found for a number of polymers (Neumann et al., 1979). Van Oss and Good (1984) studied the equilibrium distance between two bodies immersed in a liquid. The distance in air or in an intervening liquid are in the same order of magnitude (d_0 = 0.182 - 0.2 nm.).

1.3 THE STRENGTH OF TABLETS

The mechanical strength of compressed tablets has been described by various terms such as fracture resistance (Endicott et al, 1961 and David and Augsburger, 1974), tensile strength (Nelson,1956; Fell and Newton, 1968; 1970a,b; Ridgway, 1970 and Newton et al.1971) crushing strength (Brook and Marshall, 1968;). Among these terms, tensile strength is the most useful in indicating the strength of compacts.

1.3.1 DETERMINATION OF TENSILE STRENGTH

Various methods have been utilized in the evaluation of tablet strength. Most of these methods have not taken into account the mode of fracture which will alter the measured stength. However, tensile strength is based on the state of fracture and independent of tablet dimensions and provides a measurement of the inherent strength of the compacted material.

Tensile strength tests can be divided into two groups, axial or radial, according to the plane of fracture. The diametral compression test (radial tensile strength) is most commonly used for tablets and was first studied on concrete (Carneiro et.al, 1953; Mitchell, 1961; Rudnick et al. 1963).

The radial tensile strength is measured when the material, in the form of a right circular cylinder, is compressed diametrically between two flat platens. Maximum tensile stresses are developed across the loaded diameter and are proportional to the applied load. Under proper conditions these stresses cause the cylinder to fracture along the diametral plane. The magnitude of these stresses, then , can be calculated by:

$$\sigma = \frac{2P}{\pi dT} \qquad \ldots 1.32$$

where σ is the maximum tensile stress, P is the applied load, d is the specimen diameter, and T is thickness of the specimen.

1.3.2 CRITERIA OF FAILURE

Equation 1.32 will be applicable on the condition that fracture must be initiated by tensile stresses acting across the loaded diameter. However, the other stresses might interfere and prevent the initiation of failure in normal tension (Rudnick et al.1963). The value of the compressive and shear stresses exhibit a minimum at the centre of the loaded diameter, and a maximum at the loading point. In practice, the ideal line loading of normal tension will never happen. The stress will distribute evenly over an actual contact area in a parabolic pattern. To minimize the effect of other stresses the width of the contact area should be 1/10 of the specimen diameter to yield a constant tensile stress over most of the loaded diameter except the region near the contact point. To ensure failure in tension

a narrow pad of soft material can be used between the specimen and the loading platen for some materials in which the shear and compressive stresses are of high magnitudes. The type, thickness and size of the pad will effect the result of the test. (Rudnick et.al.1963; Fell and Newton,1970b; Addinall and Hackett, 1964).

1.3.3 MODE OF FAILURE

Different stresses cause fracture in different patterns as shown in Fig. 1.4.

Fig. 1.4a is the failure in tension, the specimen is broken in halves. along the loaded diameter.

Fig. 1.4b is the triple cleft failure which is caused by an initial fracture in tension, followed by secondary fracture in each half under remaining load. Valid tensile strength data can be obtained from materials fracturing in this manner.

Fig. 1.4c is the failure caused by compressive and shear stress. This failure may cause an irregular fracture pattern when there is a secondary failure.

1.3.4 FACTORS INFLUENCING THE TENSILE STRENGTH VALUES

Fracture occurs when the applied stress reaches a critical value to initiate a crack. The failure plane produced depends on physical properties of materials and test conditions.

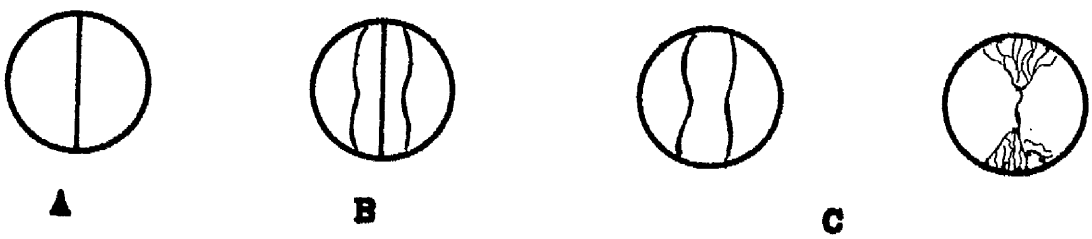

FIG. 1.4 MODE OF FAILURE

a) TENSION

b) TRIPLE CLEFT

c) COMPRESSIVE AND SHEAR STRESS

Rudnick (1963) found that there was no absolute value of tensile strength of each material. The strength values obtained under any set of conditions were regarded as "true values" for that test condition. The following factors influence the tensile strength values:

1 PARTICLE SIZE

A larger particle size is expected to exhibit the lower strength. Fell and Newton (1968) found that the tensile strength of lactose compacts increased with a decrease in particle size. Skeikh-Salem and Fell (1982) reported that compaction speed was an important factor in determining the effect of particle size on the tensile strength of sodium chloride and lactose compacts. At the lower compaction speed the largest particle size of sodium chloride gave the highest tensile strength because the particles have sufficient time to flow and attain greater bonding whereas at the higher speed different trends were observed. For lactose, the intermediate particle size exhibit the highest tensile strength. Therefore, the effect of particle size is a characteristic of material itself.

2 THE TEST CONDITIONS

Padding affects the tensile strength by giving a uniform distribution of applied load along a specimen length and reducing compressive and shear stresses. A higher strength was found when a pad was used (Fell and Newton, 1970b; Addinall and Heckett, 1964). The test environment also affects the results. Stockdale (1951) showed that the strength of glass was reduced to some extent in a water environment.

1.3.5 OTHER METHODS OF THE STRENGTH MEASUREMENT

1) THE AXIAL TENSILE STRENGTH

This is the force required to break a tablet in the axial plane. Fig. 1.5 shows the axial tensile strength testing machine adapted by Nystrom et al. (1977). The tablet is fixed between a pair of adapters using an adhesive which had no effect on the tablet. The force is applied to the adapter until the tablet is broken in the axial direction. Tensile strength is calculated from:

$$\sigma_z = \frac{4P_z}{\pi d^2} \qquad \ldots 1.33$$

where σ_z is the axial tensile strength, P_z is the breaking force

The axial tensile strength is widely used in predicting the capping tendency since the force to break the tablet is parallel to the internal stress causing the capping (Nystrom 1977, 1978). Work has also been carried out on the ratio of axial tensile strength to radial tensile strength (isotropy ratio) to predict the fragmentation propensity and to study consolidation mechanism (Nystrom, 1981, Alderborn and Nystrom, 1982a, 1984 and Duberg and Nystrom, 1982,1985).

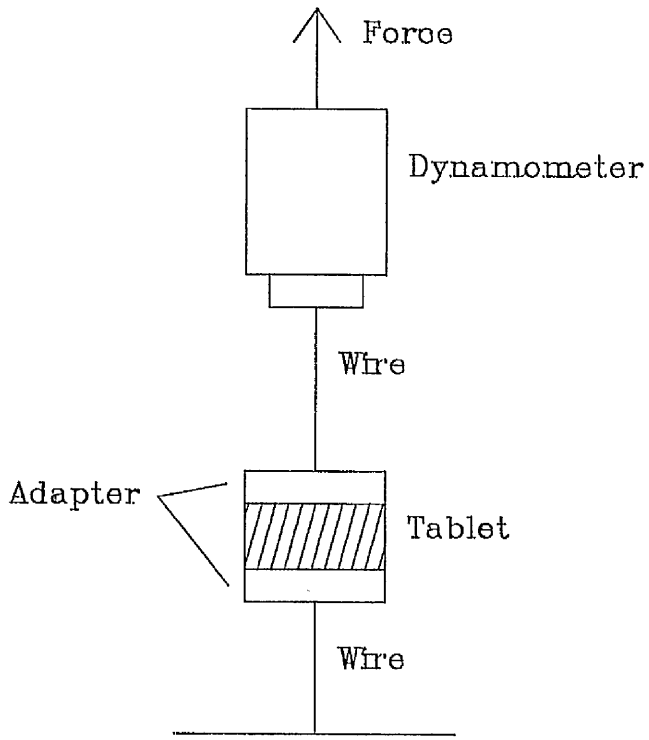

FIG. 1.5 AXIAL TENSILE STRENGTH APPARATUS

2) CRUSHING STRENGTH

This is the simplest method and is commonly used commercially for the testing of tablets. A compressional force is applied diametrically to a tablet until it breaks. Many testers such as Monsanto, Pfizer, Strong-Cobb, Heberlein and Erweka are available for this test. In the last two testers, the force is applied by an electric motor, whereas the others are by hand. These testers give a variation in results due to the inaccuracy in instrument scale values, zero errors and varying methods of applying the load (Brook and Marshall, 1968). Because test conditions to ensure tensile failure are not usually applied, further variation in results will be due to different modes of failure.

3) FLEXURE OR FRACTURE RESISTANCE TEST

The test was used by Endicott and Lowenthal (1961) and David and Augsburger (1974). The tablet is supported at two extreme ends of one of its flat faces and a knife edge applied at the opposite face (Fig. 1.6). The applied load P on the knife edge at the centre of tablet causes tensile stresses and compression stresses until fracture occurs, splitting the tablet in tension. The tensile strength is calculated by :

$$\sigma = \frac{3Pb}{4dT^2} \qquad \ldots 1.34$$

where b is the fulcrum distance

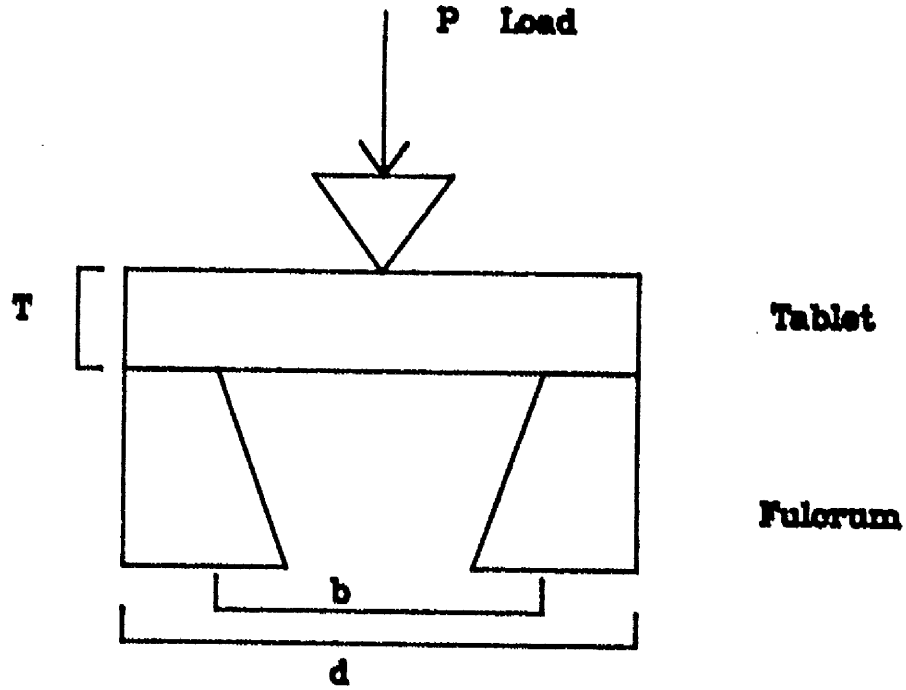

FIG. 1.6 FRACTURE RESISTANCE TEST

The force required in this method is less than that used in the diametral tensile strength test. Therefore, it is suitable for very strong tablets. The distance between the fulcrum can be adjusted to get a measurable fracture force.

1.4 AIMS AND OBJECTIVES

In the compaction of powders, a major contribution to bond formation is molecular interaction ie. Van der Waals forces. An approach to estimating the magnitude of these forces in a simple way from a knowledge of surface free energy was investigated since the latter term can be achieved from contact angle measurements.

The objective of the work reported in this chapter is to determine possible relationships between calculated strength in terms of Hamaker constants and experimentally measured tensile strength. As the Lifshitz theory allows calculation of Hamaker constants in liquid media of different dielectric constants , tablet strengths are also measured in these media.

These relationships will be examined initially using polymers and extended to pharmaceutical materials and mixtures. As the subsequent disintegration of compacts in liquid media is an important process, correlations between this and bonding mechanisms and strength will be studied.

CHAPTER 2

MATERIALS AND METHODS

1 MATERIALS

The materials chosen were those that could be readily characterised by contact angle measurements and would give minimal problems due to solubility. They were polytetrafluoroethylene (PTFE), polymethylmethacrylate (PMMA), polyvinylchloride (PVC), polyethylene(PET), polyethylmethacrylate (PEM), vinyl choride vinyl acetate copolymer (Corvic 47/488), Emcompress, magnesium carbonate, and methylcellulose. The materials studied, suppliers and characteristics are given in table 2.1.

A series of alcohols was chosen for the test liquids as they gave a wide range of dielectric constants but their surface tensions were of the same magnitude. The characteristics of these test liquids are given in table 2.2.

TABLE 2.1

SOLID MATERIALS, THEIR SUPPLIERS AND THEIR CHARACTERISTICS

Materials	Suppliers	Characteristics
PTFE	BDH Chemicals Ltd. England	sieved to give a 180-500 μm size fraction
PVC	BDH Chemicals Ltd. England	high M.W. sieved to give a 180-250 μm. size fraction
Corvic	I.C.I. England	sieved to give a 90 - 125 μm size fraction
PET	BDH Chemicals Ltd. England	unfractionated chromatographic analysis grade
PMMA	BDH Chemicals Ltd. England	high M.W., sieved to give a 180-250 μm. size fraction

PEM	Cole polymers Croydon, England	sieved to give a 90 - 125 μm. size fraction
Emcompress	Cambrian Chemicals Croydon, England	sieved to give a 180 - 250 μm. size fraction
Magnesium carbonate	BDH Chemicals England	sieved to give a 180 - 250 μm. size fraction
Methyl cellulose	BDH Chemicals Ltd. England	sieved to give a 180 -250 μm. size fraction

TABLE 2.2

TEST LIQUIDS, THEIR SUPPLIERS AND CHARACTERISTICS

Liquids	Suppliers	Characteristics
Methanol	Fisons Loughborough U.K.	Analytical reagent
Ethanol	Fisons Loughborough U.K.	Laboratory reagent
Propanol-2	Fisons Loughborough U.K.	Laboratory reagent
Butanol-1	Fisons Loughborough U.K.	Laboratory reagent
Hexanol-1	Fisons Loughborough U.K.	Laboratory reagent
Octanol-1	BDH Chemicals Ltd U.K.	Laboratory reagent
2 methyl-2-butanol reagent	BDH Chemicals Ltd. U.K.	Laboratory reagent

2 METHODS

2.1 BOND STRENGTH OF PURE MATERIALS

2.1.1 PREPARATION OF TABLETS

Two processes were used for the preparation of tablets:

a) Compression

b) Fusion

1.27 cm. diameter flat faced tablets were prepared by direct compression using a single punch tablet machine (F3 Manesty, Liverpool) from PTFE, PVC, Corvic, Emcompress, magnesium carbonate and methyl cellulose. The upper punch of the machine was instrumented using strain gauges in order to detect the force applied to the powder. The output of the strain gauges was recorded on a U.V. recorder (SE 3006 North Feltham Trading Estate, Middlesex, U.K.). Different weights of powder were used and pressures applied to give acceptable tablets (table 2.3). The speed of compression was about 300 cm/min.

Tablet prepared by fusion method were from PET, PMMA and Corvic. A brass mould enabling the preparation of ten flat faced 1.27 cm. diameter tablet was used. Different weights of powders, temperatures and periods of heating were applied and are shown in table 2.4.

TABLE 2.3

COMPRESSED MATERIALS, WEIGHTS, APPLIED PRESSURES AND METHODS OF PREPARATION

Materials	Weight (mg.)	Pressure (MN/m²)	Method
PTFE	530	135.5	compressed continously
PVC	530	135.5	compressed continously
Corvic	530	226	compressed continously
Emcompress	570	226	compressed individually
Magnesium-carbonate	570	226	compressed individually
Methyl cellulose	565	108.4	compressed individually

TABLE 2.4

TABLETS PREPARED BY FUSION, WEIGHTS TEMPERATURE AND HEATING PERIODS

Materials	Weight (mg.)	Temp. (°C)	Time (min.)
Polyethylene	300	90	30
PMMA	450	150	45
Corvic	550	105	30

The tablet dimensions of all these compacts were determined using a dial gauge (Baty Gauge).

2.1.2 DIAMETRAL COMPRESSION TEST

The tensile strength of the tablets was determined following the procedure of Fell and Newton (1968). The test specimens were studied in air and in different liquid media. Specimens in liquid media were obtained by immersion of the compacts in the appropriate liquid for periods of time sufficient to ensure complete saturation. The time periods were determined experimentally from observation of broken compacts and varied from 5 mins to 2 hours.

These wet and dry test compacts, then were placed between the two flat plattens of an Instron instrument (Instron Ltd., floor model, High Wycombe, Bucks, England). The load was applied to the tablet diametrically at a crosshead speed of 0.1 cm/min. The system is shown in Fig.2.1. The maximum load at failure was obtained from the chart recording of applied load and crosshead movement. The tensile strength was calculated by the application of equation 1.32. The tablet were visualized after breaking to ensure their saturation and to check that failure occurred in normal tension. Only results from tablets breaking clearly in tension were accepted (Fell and Newton, 1970a,b). The mean tensile strength of at least five tablets was calculated.

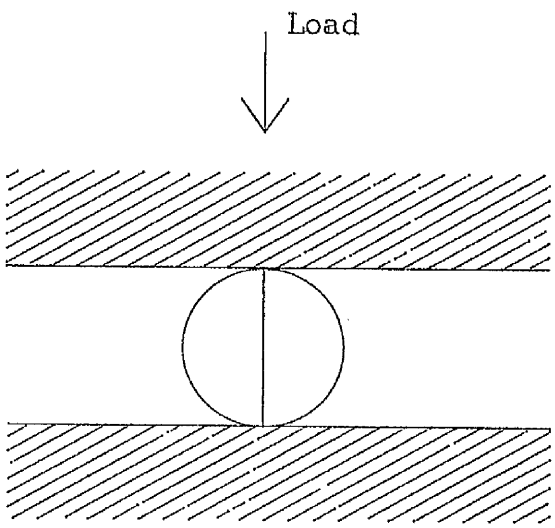

Figure 2.1 Diametral Compression Test

2.1.3 SURFACE FREE ENERGY OF TEST COMPACTS

The surface free energies were studied by contact angle measurements as described in part 1. The surface free energies of PMMA, PTFE and Corvic were obtained from the first part of work of in which the contact angles were measured by the h-ϵ method. A direct measurement was used for all the rest of compacts.

The dispersion and polar forces of the series of alcohols were determined from contact angles formed on a paraffin compact as explained in part 1 section 2.2.

2.1.3.1 DIRECT CONTACT ANGLE MEASUREMENT

A contact angle is obtained directly by constructing a tangent line to the point of contact of a drop of liquid on a test solid compact. Fig 2.2 shows this apparatus used which consists of a microscope with an eye piece protractor, a specimen holder and lamp mounted on an optical bench. A small drop of liquid is added from an agla syringe through a needle onto a tablet. The angle is detected through the eye piece and the reading is taken from the microscope scale. The advantage of this method is that the result is obtained quickly, requiring only a small amount of solvent and powder.

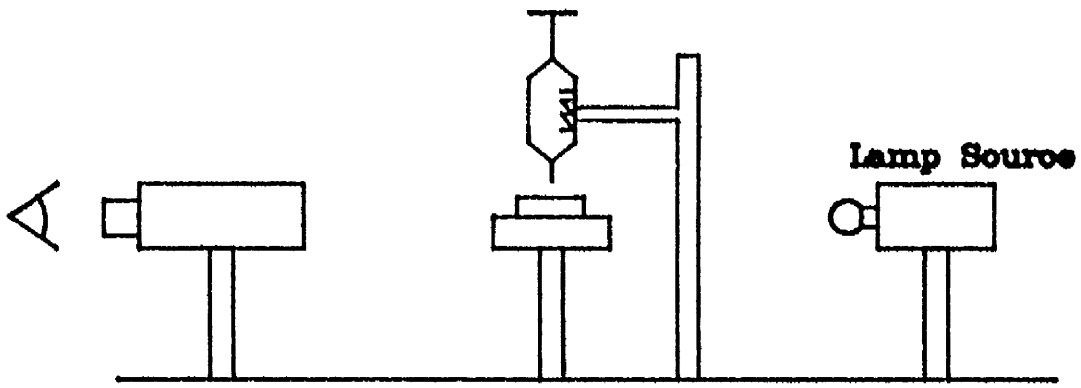

FIG. 2.2 DIAGRAM OF APPARATUS USED TO MESURE THE CONTACT ANGLE OF A COMPRESSED TABLET DIRECTLY

2.2 BOND STRENGTH OF MIXTURES

Three different types of mixture were used for this study. They were mixtures of PVC and PTFE, of magnesium carbonate and Emcompress and of PEM and Corvic. The mixtures of PVC and PTFE were determined for their tensile strength changes in a series of alcohols and in air while mixtures of magnesium carbonate and Emcompress were detected only in air. The last mixtures were used to assess the effect of pressure and mixture composition on tensile strngth.

2.2.1 PREPARATION OF MIXTURES

Mixtures of PVC and PTFE were prepared in the following ratios 0:100, 10:90, 25:75, 50:50, 75:25, 100:0 %v/v., magnesium carbonate and Emcompress at 100:0, 75:25, 50:50, 25:75, 0:100 %v/v. and PEM and Corvic at 100:0, 80:20, 50:50, 20:80, 0:100 %w/w. Mixing was carried out using a Turbula mixer (Willy A, Bachofen Maschinenfabrik, Basel) at the speed of 90 r.pm. for 10 mins.

2.2.2 PREPARATION OF TABLETS

Tablets of PVC and PTFE mixtures and of magnesium carbonate and Emcompress mixtures were prepared using a single punch tablet machine as described above, whereas of PEM and Corvic mixtures was compressed using an Instron instrument

(Instron Ltd. High Wycombe, Bucks, England) fitted with a 5000 kg. capacity load cell. Table 2.5 shows weights of the mixtures and applied pressures.

Fig. 2.3 shows the Instron instrument adapted to take a conventional punch and die system. The lower punch stands on the load cell while the upper one fits in a holder which screws directly into the crosshead. The die is supported on a special holder which prevents the transmission of die wall friction to the load cell. Prior to the compaction process, calibration of the Instron load cell was achieved by using known weight on the load cell. The mixtures were carefully filled in the 1.27 cm. diameter die, pre-lubricated with 1% suspension of magnesium stearate in carbon tetrachloride. The powder was compressed at a crosshead speed of 0.2 cm/min. The crosshead was reversed automatically at the same speed when the applied load reached the required pressure which was recorded on the chart recorder. The tablet then was carefully removed from the die by the aid of the lower punch. The dimensions and the weight of all the test compacts were measured.

2.2.3 DIAMETRAL COMPRESSION TEST

All the compacts were subjected to the tensile strength test as described previously. The mixtures of PVC and PTFE were saturated in a series of alcohols for two hours prior to the tensile strength test. The breaking speed was 0.1 cm/min. The mean strength of at least five tablets was calculated.

TABLE 2.5

MIXTURES OF TEST MATERIALS, WEIGHTS AND APPLIED PRESSURES

Mixtures	Weight (mg.)	Pressure $(MN/m)^2$
PVC:PTFE	530	135.5
0:100		
10:90		
25:75		
50:50		
75:25		
100:0		
Mag.:Emcom	570	226
100:0		
75:25		
50:50		
25:75		
0:100		
PEM:Corvic	500	77.4, 116.1, 154.8, 193.5
100:0		
80:20		
50:50		
20:80		
0:100		

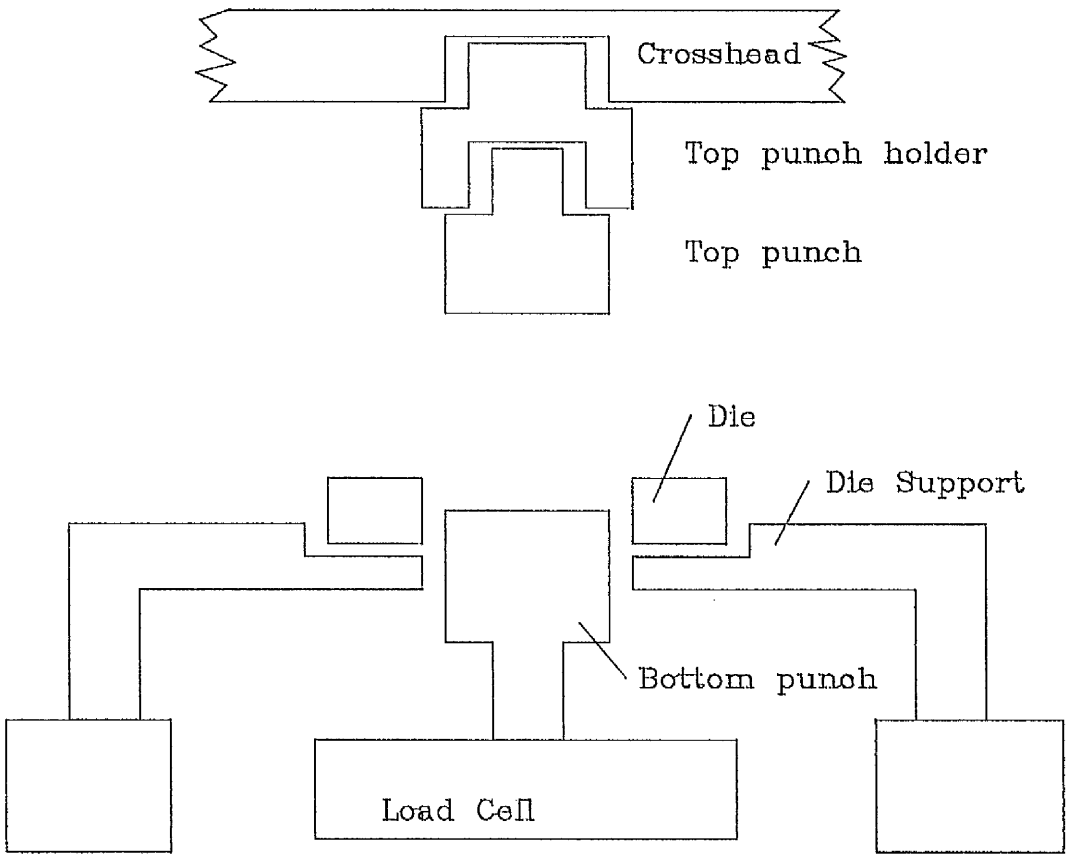

FIG. 2.3 PUNCH AND DIE SYSTEM FITTED TO THE INSTRON INSTRUMENT

2.3 SCANNING ELECTRON MICROSCOPY

Photomicrographs of tablet surfaces of the following mixtures were taken; 100:0, 25:75 and 0:100 of magnesium carbonate and Emcompress. The studies were also carried out on the tablet surfaces and the broken surfaces of 100% and 75% PTFE tablets and further investigations on powders of PVC and PTFE. The method of this study is described in part 1 section 2.4.

2.4 DISINTEGRATION TEST

The disintegration test was carried out using the method described in the BP 1981. The instrument consists of 6 glass tubes closed at the lower end by 2.0 mm. aperture steel mesh. The test was carried out on PVC,PTFE,and Corvic tablets. The media used was methanol, ethanol, hexanol and 2-methyl-2 butanol. Six tablets from each powder were chosen, placing one in each tube, adding a cylindrical plastic disc on top of each compact to ensure sinking of the tablets. The tubes were raised and lowered in the disintegration media at a constant frequency so that at the highest position, the mesh still remained below the surface of disintegrating media. The average disintegration time of six tablets was recorded.

CHAPTER 3

RESULTS AND DISCUSSION

3.1 BONDING MECHANISMS OF PURE MATERIALS

The properties of the series of alcohols with varying dielectric constants from 32.7 to 5.82 are shown in table 3.1. The surface tension measured by the drop volume method unless otherwise indicated and their surface dispersion and polar forces calculated from contact angle measurements on paraffin compacts are also given. Table 3.2 gives the surface free energies and their components of the test compacts, determined by h-ϵ or direct method. The tablet dimensions are shown in table 3.3.

The tensile strengths and Hamaker constant values (A) in different liquids and air of PVC, Corvic and PTFE, calculated according to equation 1.19 and 1.12 are shown in table 3.4 and those of Emcompress, magnesium carbonate and methyl cellulose in table 3.5. The Hamaker constants of all the materials change with a change in dielectric constant. The change can be divided into two groups: hydrophilic and hydrophobic powders. For hydrophilic powders ie. all the powders except PTFE, according to their proportion of polar forces to total energies, (table 3.2) the Hamaker constants increase as the dielectric constants decrease. The Hamaker constants for materials separated by an intervening media were calculated based on the magnitude of the interfacial forces (equation 1.19). In other words the A value depends on the balance between the total energy of solid and liquid phases and the degree of interaction

TABLE 3.1

PROPERTIES OF TEST LIQUIDS

Liquids	x dielectric constants	θ on paraffin	surface-tension(mN/m)		
			γ_s^d	γ_s^p	γ_s
Methanol	32.7	35.1	18.2	5.5	*23.7
Ethanol	24.5	29.5	19.3	4.4	*23.7
Propanol	19.9	16.9	19.5	3.5	*23.0
Butanol	16.1	21.0	22.2	2.4	24.6
Hexanol	13.3	25.2	22.8	2.5	25.3
Octanol	10.3	27.0	26.6	0.9	27.5
2methyl-2-butanol	5.8	19.4	22.9	1.7	24.6

x data from Handbook of Chemistry and Physics

* data from Ohm and Lippold (1985)

TABLE 3.2

SURFACE FREE ENERGIES AND THEIR DISPERSION AND POLAR FORCES

Solids	γ_s^p	γ_s^d	γ_s
P.T.F.E.	2.0	16.0	18.0
P.V.C.	26.0	20.0	46.0
CORVIC	24.0	12.0	36.0
PMMA	17.7	18.2	35.9
POLYETHYLENE	1.1	32.1	33.2
PEM x	10.0	30.0	40.0
EMCOMPRESS	49.3	1.3	50.6
MAGNESIUM CARBONATE	42.5	14.7	57.2
METHYL CELLULOSE	31.8	18.1	49.9

x Data from Mohamad 1983

TABLE 3.3

DIMENSIONS OF TABLETS

Solids	density g/cm³	weight gm.	diameter cm.	thickness cm.	porosity
PTFE	2.3882	0.533	1.2688	0.2024	0.1286
PVC	1.6540	0.534	1.2795	0.3856	0.3497
CORVIC	1.3629	0.846	1.2810	0.5790	0.1685
PMMA	1.1500	0.450	1.2632	0.4540	0.3166
POLYETHYLENE	0.9363	0.300	1.2432	0.4020	0.3513
CORVIC (fusion)	1.3629	0.550	1.2672	0.6150	0.4831
EMCOMPRESS	2.3500	0.570	1.2786	0.2352	0.2683
MAGNESIUM CARBONATE	2.1777	0.570	1.2852	0.3074	0.3410
METHYL CELLULOSE	1.3395	0.565	1.2784	0.4090	0.1964

TABLE 3.4

TENSILE STRENGTH, $\sigma \times 10^5$ N/m^2 AND HAMAKER CONSTANT, $A \times 10^{-20}$ N.m FOR PTFE, PVC AND CORVIC

Dielectric constant	PTFE		PVC		Corvic	
	σ	A	σ	A	σ	A
32.7	5.62	0.23	0	1.91	0	1.79
24.5	5.03	0.16	0	2.25	0.02	2.18
19.9	4.67	0.10	0.98	2.60	0.25	2.52
13.3	4.78	0.16	5.49	3.12	1.10	3.18
5.8	4.46	0.16	9.71	3.60	2.32	3.64
Air	6.66	4.50	12.07	11.49	4.19	8.9

TABLE 3.5

TENSILE STRENGTH, $\sigma \times 10^{5}$ N/m^{2} AND HAMAKER CONSTANT, $A \times 10^{-20}$ N.m FOR EMCOMPRESS, MAGNESIUM CARBONATE AND METHYL CELLULOSE

Dielectric constants	Emcompress		Mg. carbonate		Methyl cellulose	
	σ	A	σ	A	σ	A
32.7	7.16	2.07	18.24	1.19	0	2.71
24.5	7.79	2.43	21.83	1.43	0	3.14
19.9	-	-	-	-	0	3.55
16.1	8.14	3.33	22.27	2.06	-	-
13.3	8.28	3.29	23.11	2.02	0.09	4.19
5.8	10.11	3.79	25.49	2.41	0.12	4.74
AIR	8.54	12.09	23.64	11.02	4.37	12.46

of the dispersion and polar forces between the liquid and solid phases (Wu's equation). The changes in tensile strength according to the changes in dielectric constant are in agreement with the A values. The higher dielectric constant gives the lower tensile strengths which is in agreement with the work of Fraser (1973). The tensile strength of PVC and Corvic in methanol could not be tested as all the compacts disintegrated into particles. The relationships between the changes in Hamaker constant and tensile strength to the changes in dielectric constant are shown in Figs.3.1-3.5. Both curves show similar trends. This indicates that these compacts are formed by Van der Waals forces and the magnitude of the bonds can be estimated by the Hamaker constant value.

For hydrophobic powders ie.PTFE, however, the opposite effects were observed. The higher is the dielectric constant, the higher the tensile strength and Hamaker constant. The only forces operating in this system are dispersion forces, therefore the magnitude of these forces are calculated according to Fowkes' equation. In other words, the A value depends on the degree of interaction of the dispersion forces between the solid and liquid phases. Since methanol has the lowest dispersion force value it gives the lowest degree of interaction, hence, the highest tensile strength and also the highest Hamaker constant. Fig. 3.6 shows the relationships between the tensile strengths, Hamaker constants and the dielectric constants. As with the hydrophilic powders, there is a relationship between the tensile strength and the Hamaker constant.

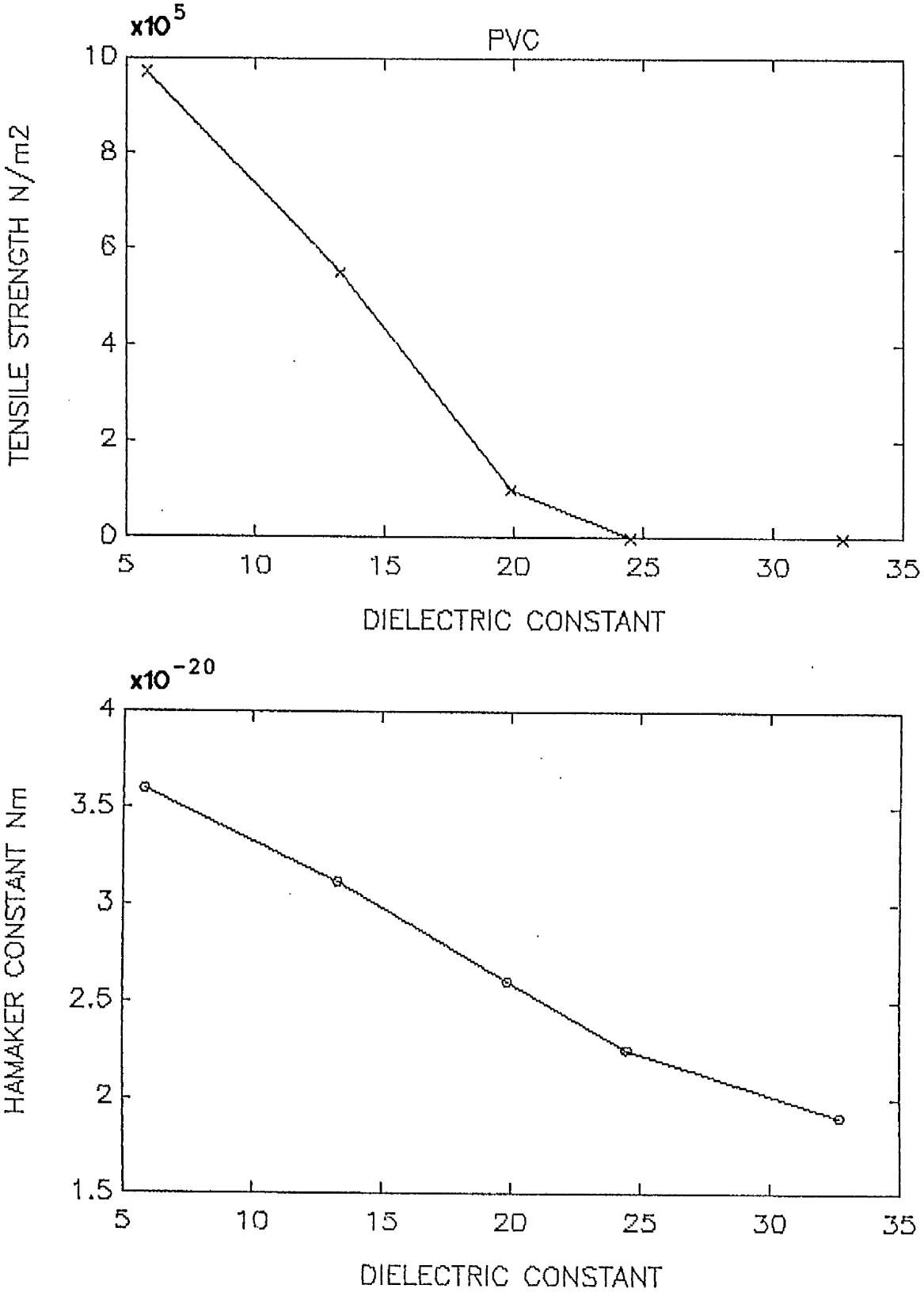

FIG. 3.1 RELATIONSHIPS BETWEEN CHANGES IN TENSILE STRENGTH AND HAMAKER CONSTANT TO CHANGES IN DIELECTRIC CONSTANT FOR PVC

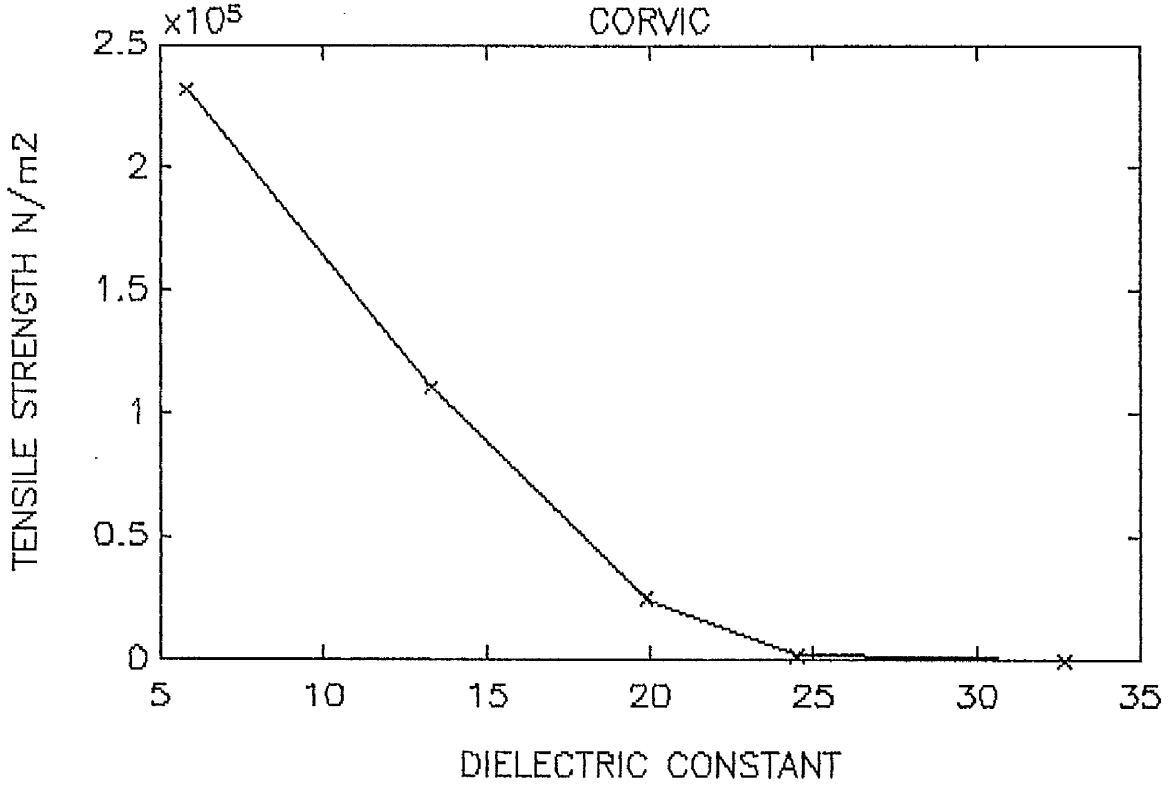

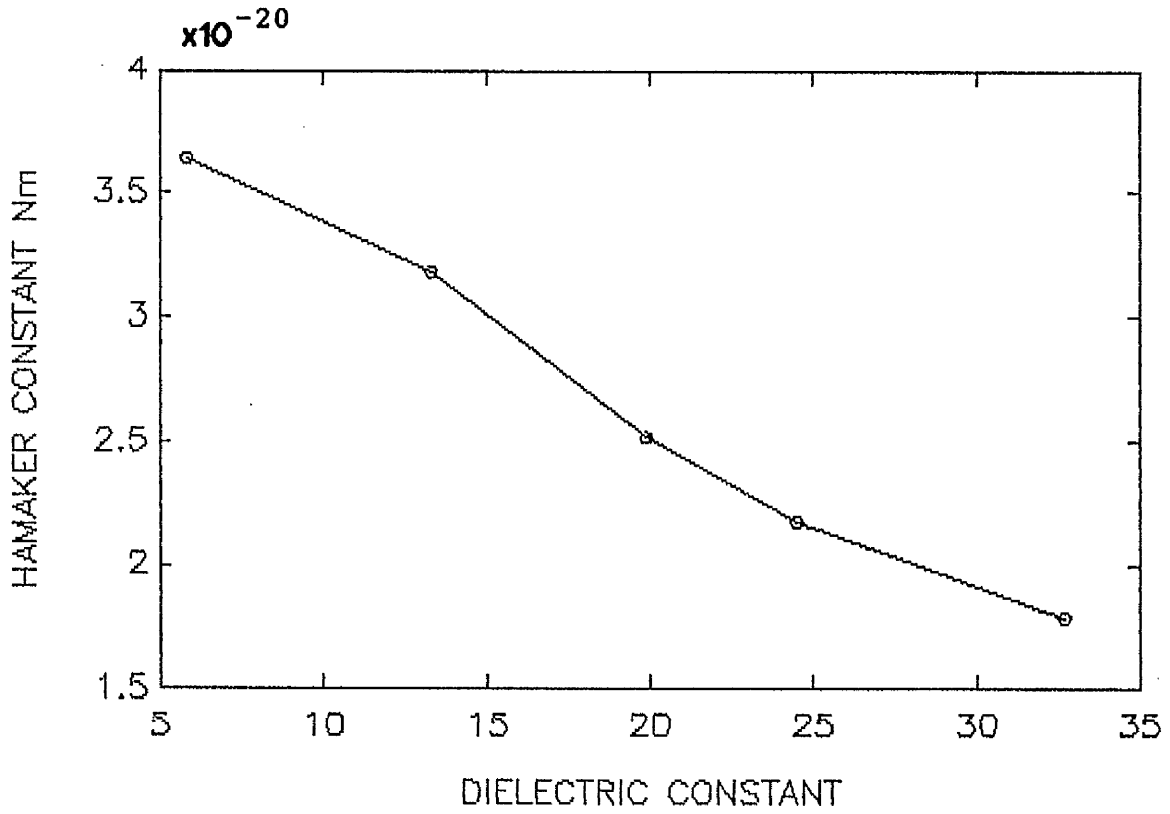

FIG. 3.2 **RELATIONSHIPS BETWEEN CHANGES IN TENSILE STRENGTH AND HAMAKER CONSTANT TO CHANGES IN DIELECTRIC CONSTANT FOR CORVIC**

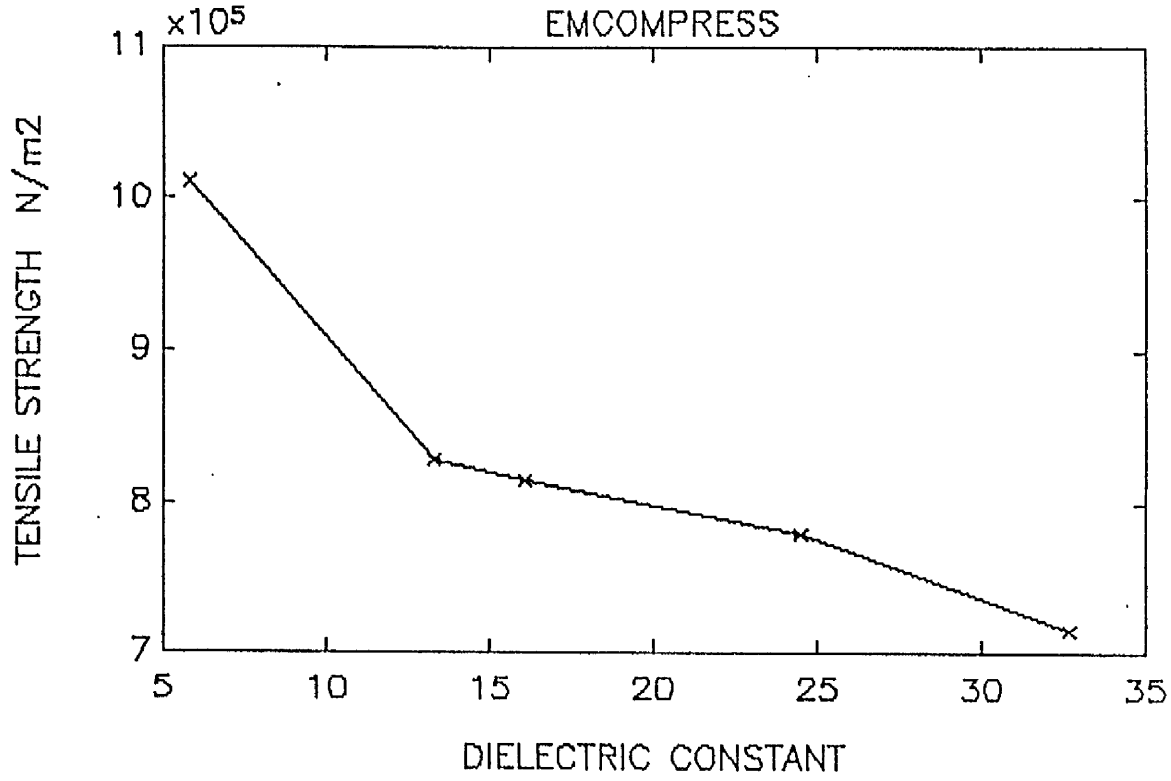

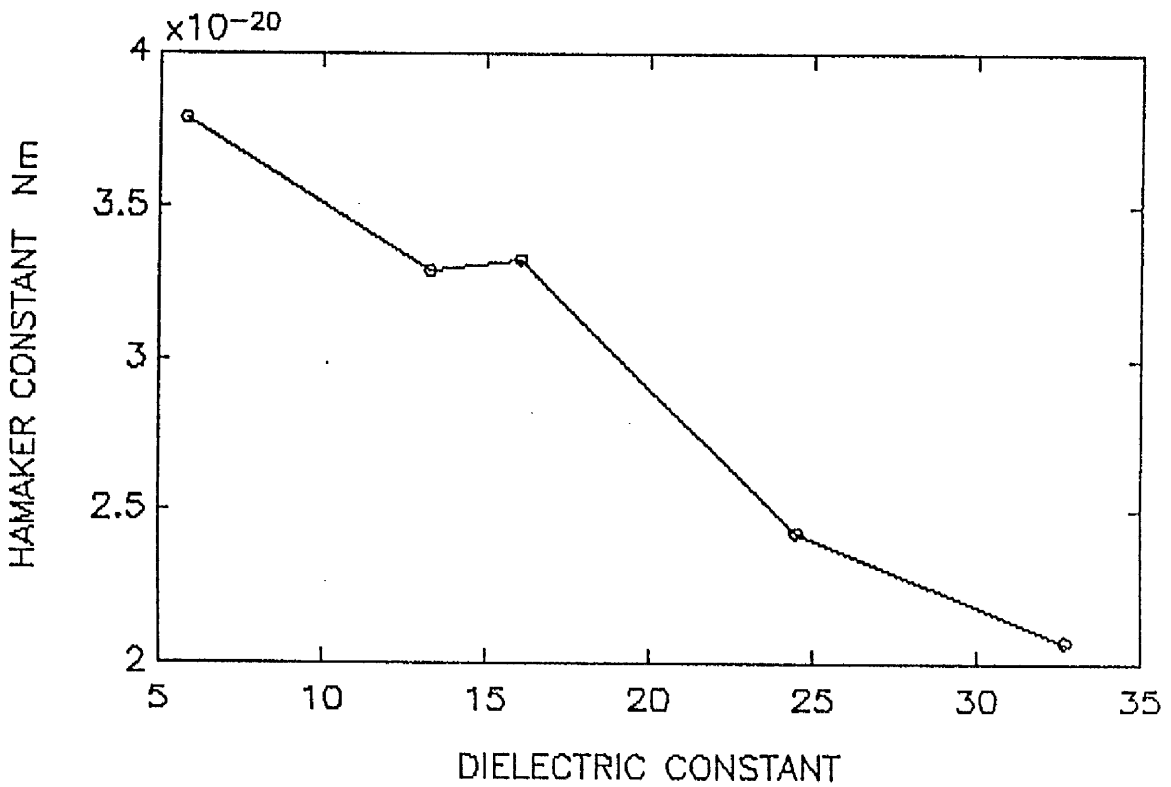

FIG. 3.3 RELATIONSHIPS BETWEEN CHANGES IN TENSILE STRENGTH AND HAMAKER CONSTANT TO CHANGES IN DIELECTRIC CONSTANT FOR EMCOMPRESS

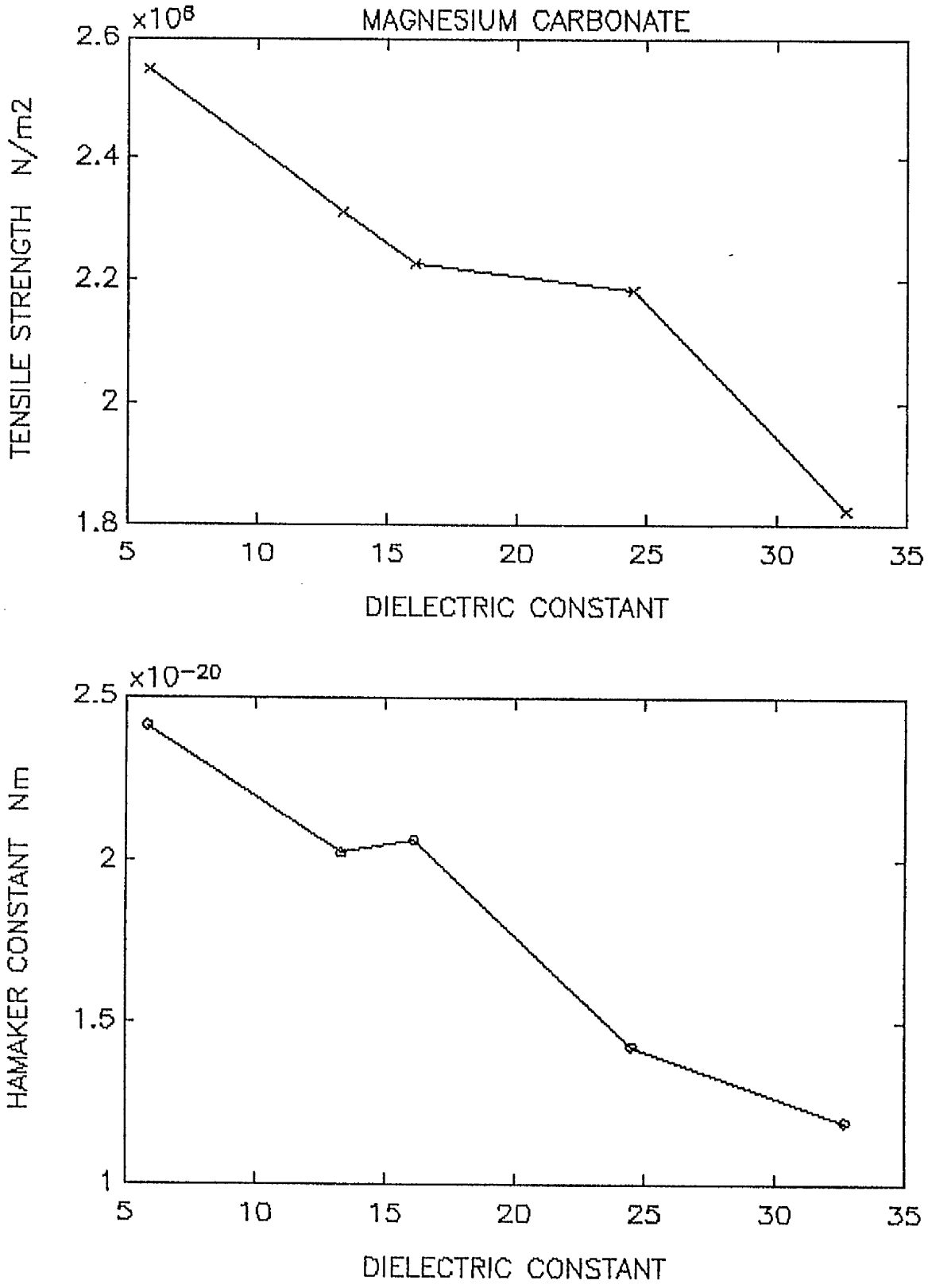

FIG. 3.4 RELATIONSHIPS BETWEEN CHANGES IN TENSILE STRENGTH AND HAMAKER CONSTANT TO CHANGES IN DIELECTRIC CONSTANT FOR MAGNESIUM CARBONATE

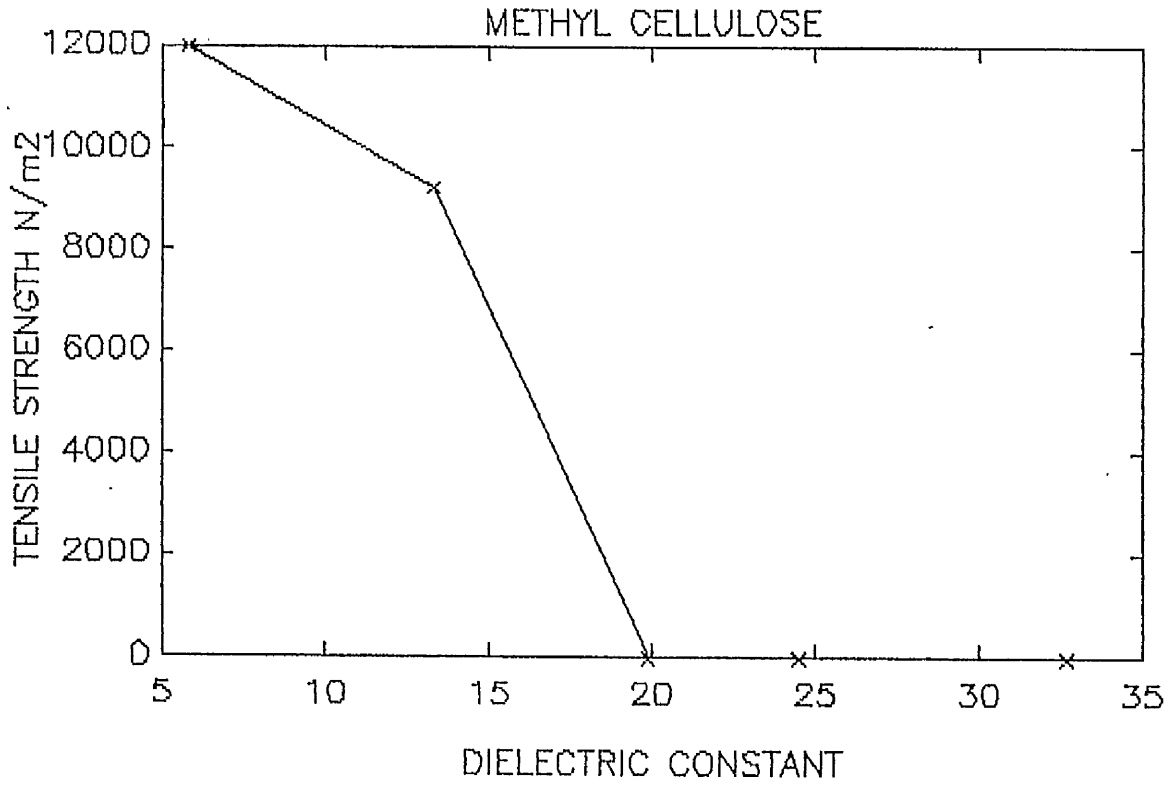

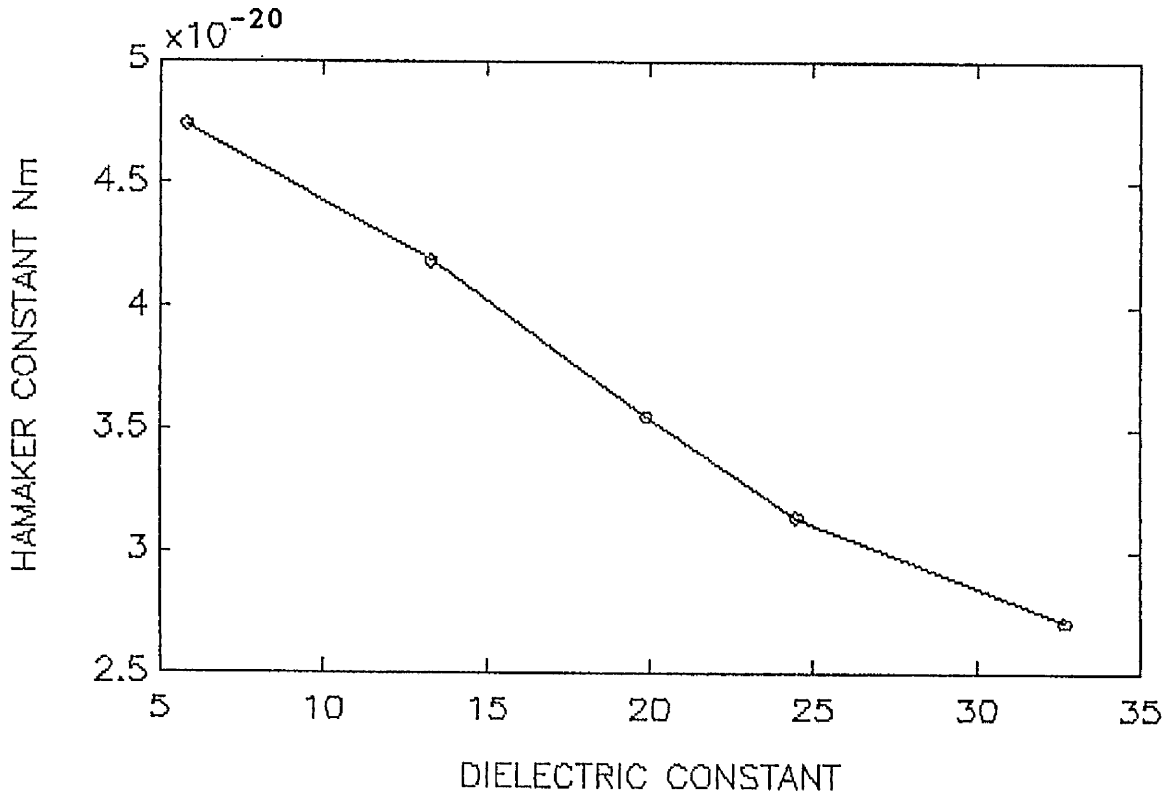

FIG. 3.5 RELATIONSHIPS BETWEEN CHANGES IN TENSILE STRENGTH AND HAMAKER CONSTANT TO CHANGES IN DIELECTRIC CONSTANT FOR METHYL CELLULOSE

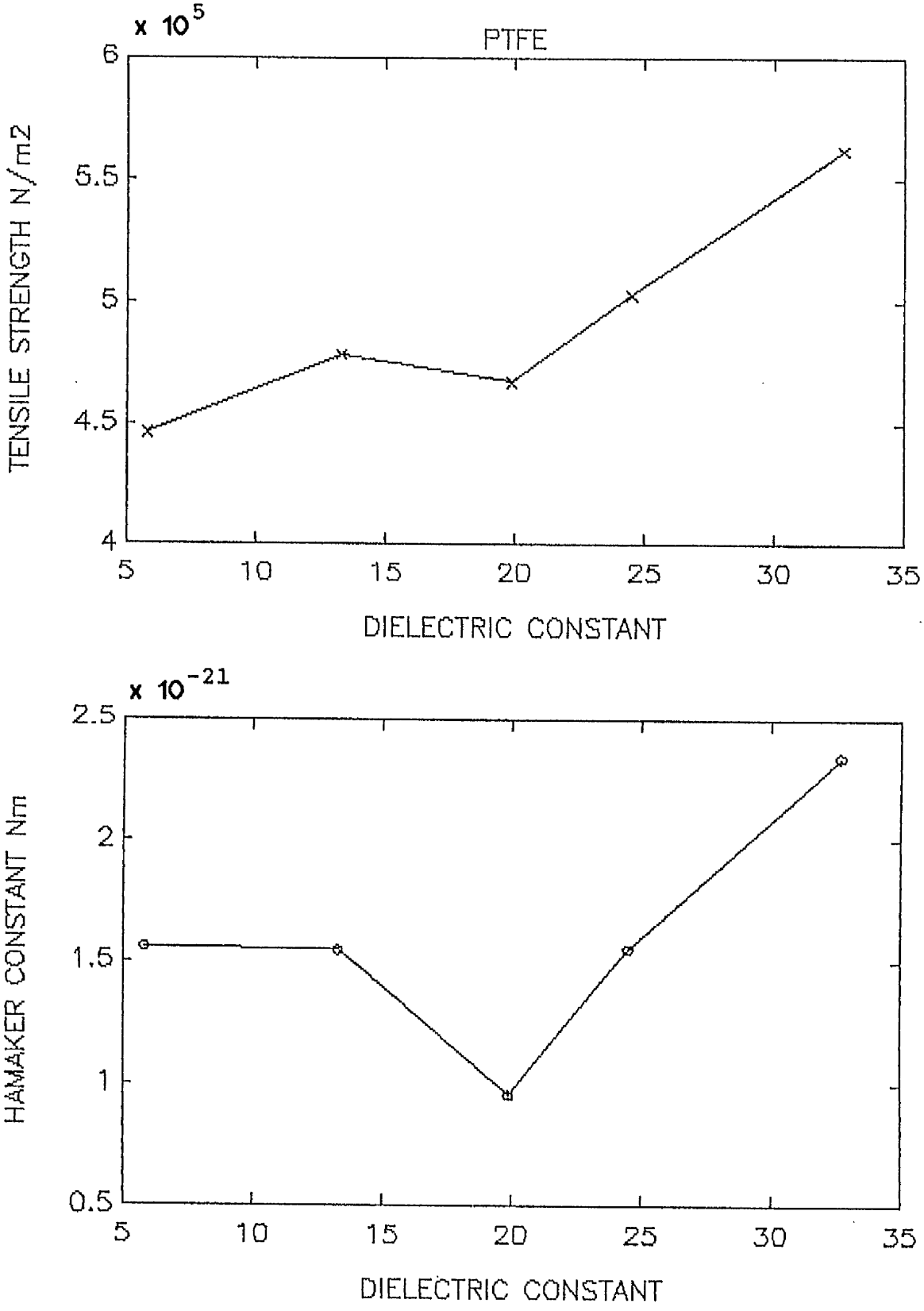

FIG. 3.6 RELATIONSHIPS BETWEEN CHANGES IN TENSILE STRENGTH AND HAMAKER CONSTANT TO CHANGES IN DIELECTRIC CONSTANT FOR PTFE

The tests explained so far were applied to tablets bonded by Van der Waals attractive forces whereas tablets bonded by the other mechanisms were not expected to respond to the change of dielectric constant. However PMMA, Corvic, and PET tablet prepared by a fusion method gave similar results to the previous group, prepared by direct compression (table 3.6). Bonds in these tablets were expected to be formed by melting and subsequent cooling leading to solid bridges. The results can be divided into two groups ie. the hydrophobic (PET) and the hydrophilic groups (PMMA and Corvic). Plots of tensile strengths and Hamaker constants against dielectric constants are shown in figs. 3.7-3.9. Similar trends are seen for both curves. This result implies that the strength of compacts prepared by fusion is due in part to Van der Waals forces.

Table 3.7 gives the tensile strength of PTFE compacts formed by direct compression both with and without heating the powders before compression. Higher tensile strengths were found after heating. Plots between tensile strengths and dielectric constants of both groups give the same trends as the change in Hamaker constants with dielectric constants (Fig. 3.10). The results indicate that an increased strength is due to increasing solid bridge formation by the fusion process and Van der Waals forces are present in both groups. These results are supportive of the previous results, showing the existence of Van der Waals forces in compacts formed by the fusion method.

TABLE 3.6

TENSILE STRENGTH, $\sigma \times 10^{5}$ N/m^{2} AND HAMAKER CONSTANT, $A \times 10^{-20}$ N.m FOR POLYEHYLENE, PMMA AND CORVIC PREPARED BY FUSION METHOD

	Hydrophobic				Hydrophilic	
Dielectric constants	Polyethylene		PMMA		Corvic	
	σ	A	σ	A	σ	A
32.7	7.48	0.91	3.75	0.87	0.34	1.79
16.1	4.12	0.29	8.19	1.81	1.47	3.18
10.3	3.25	0.07	10.75	2.80	1.91	4.55
Air	6.83	1.44	19.77	10.84	2.20	10.8

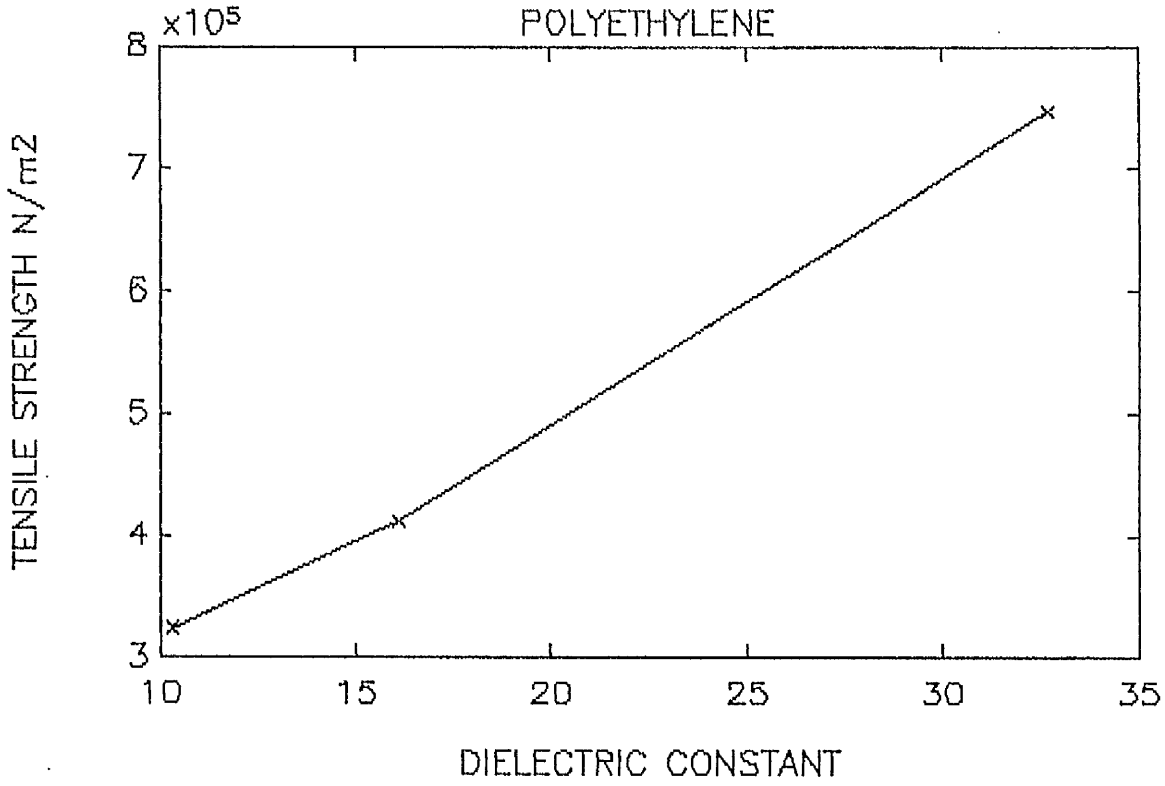

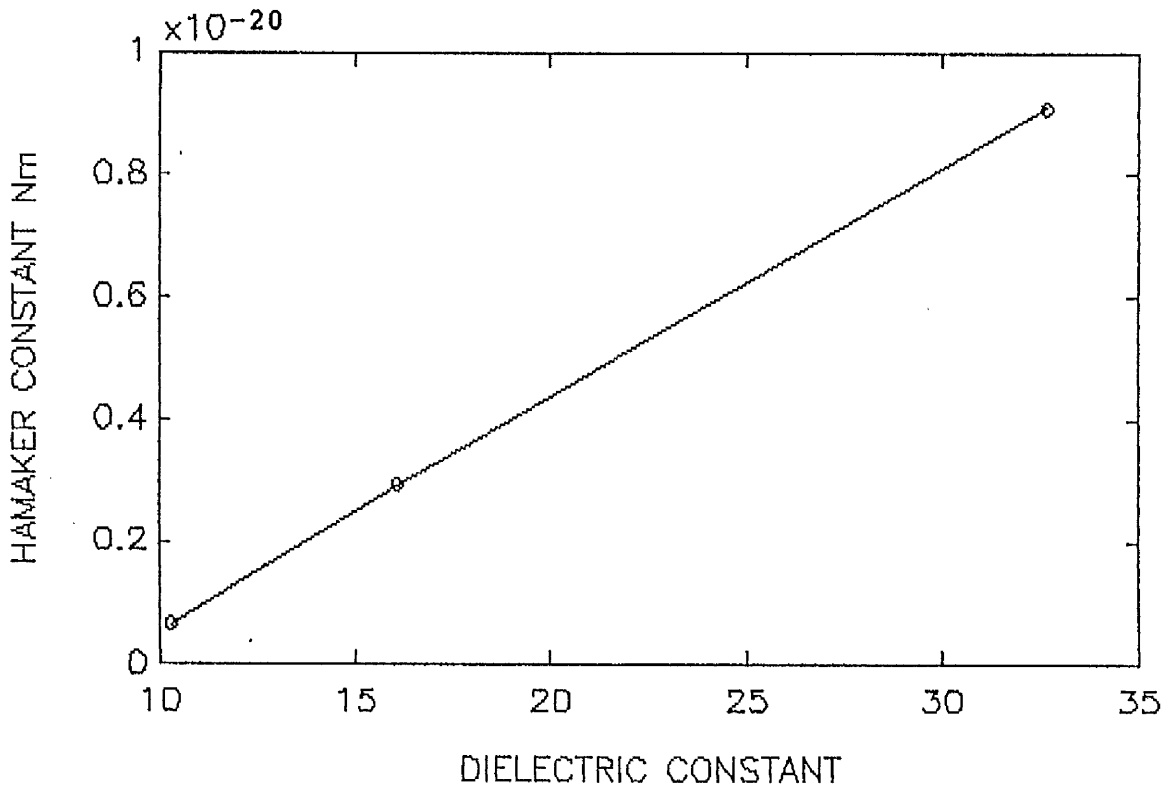

FIG. 3.7 RELATIONSHIPS BETWEEN CHANGES IN TENSILE STRENGTH AND HAMAKER CONSTANT TO CHANGES IN DIELECTRIC CONSTANT FOR PET

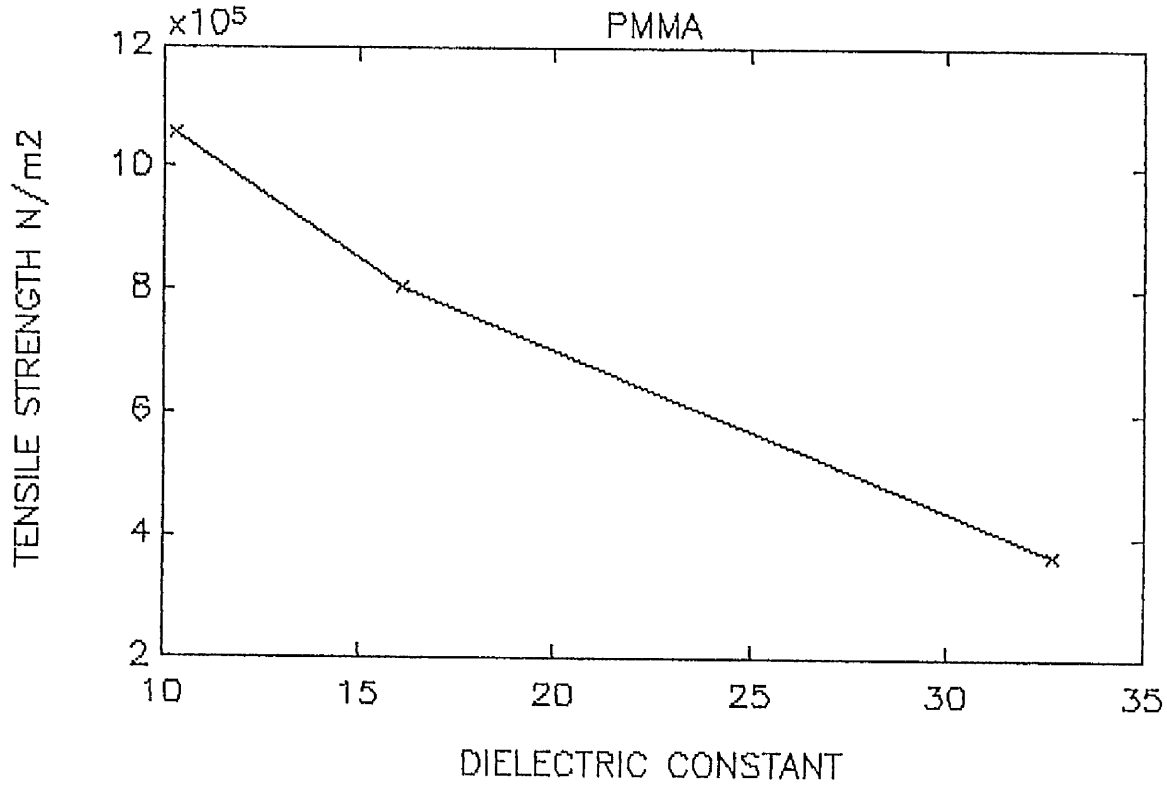

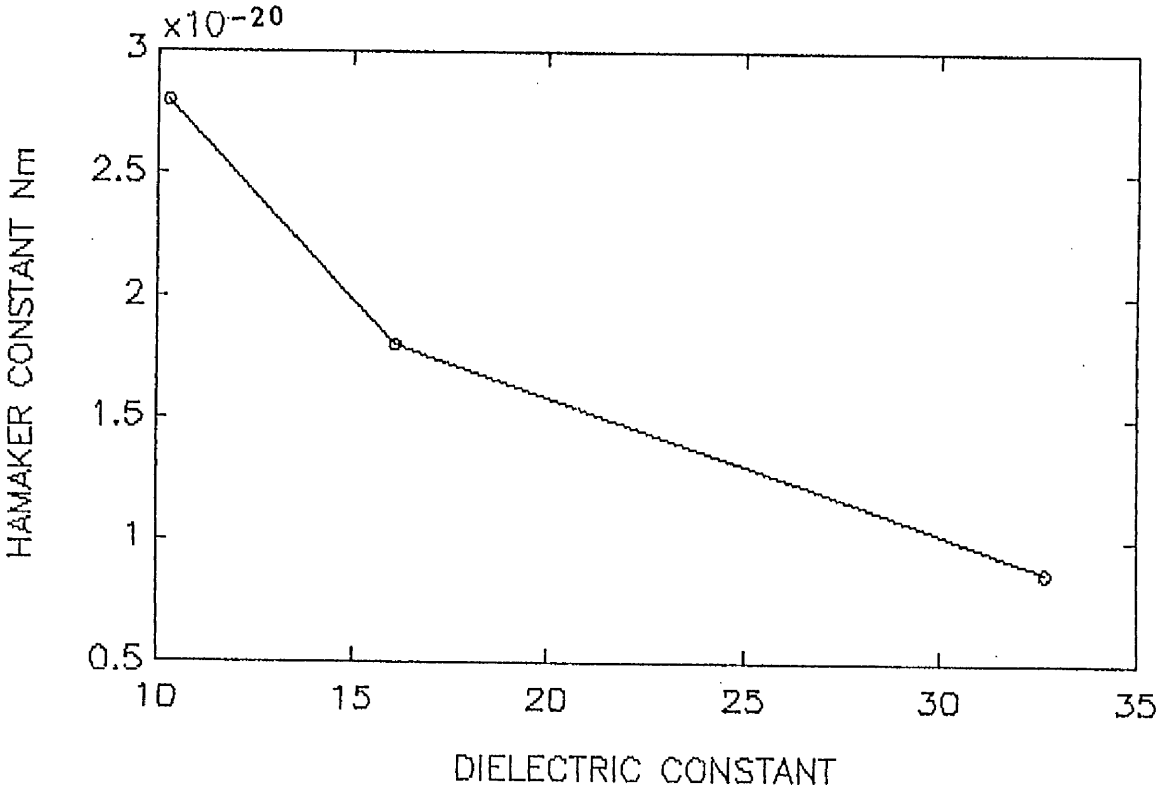

FIG. 3.8 RELATIONSHIPS BETWEEN CHANGES IN TENSILE STRENGTH AND HAMAKER CONSTANT TO CHANGES IN DIELECTRIC CONSTANT FOR PMMA

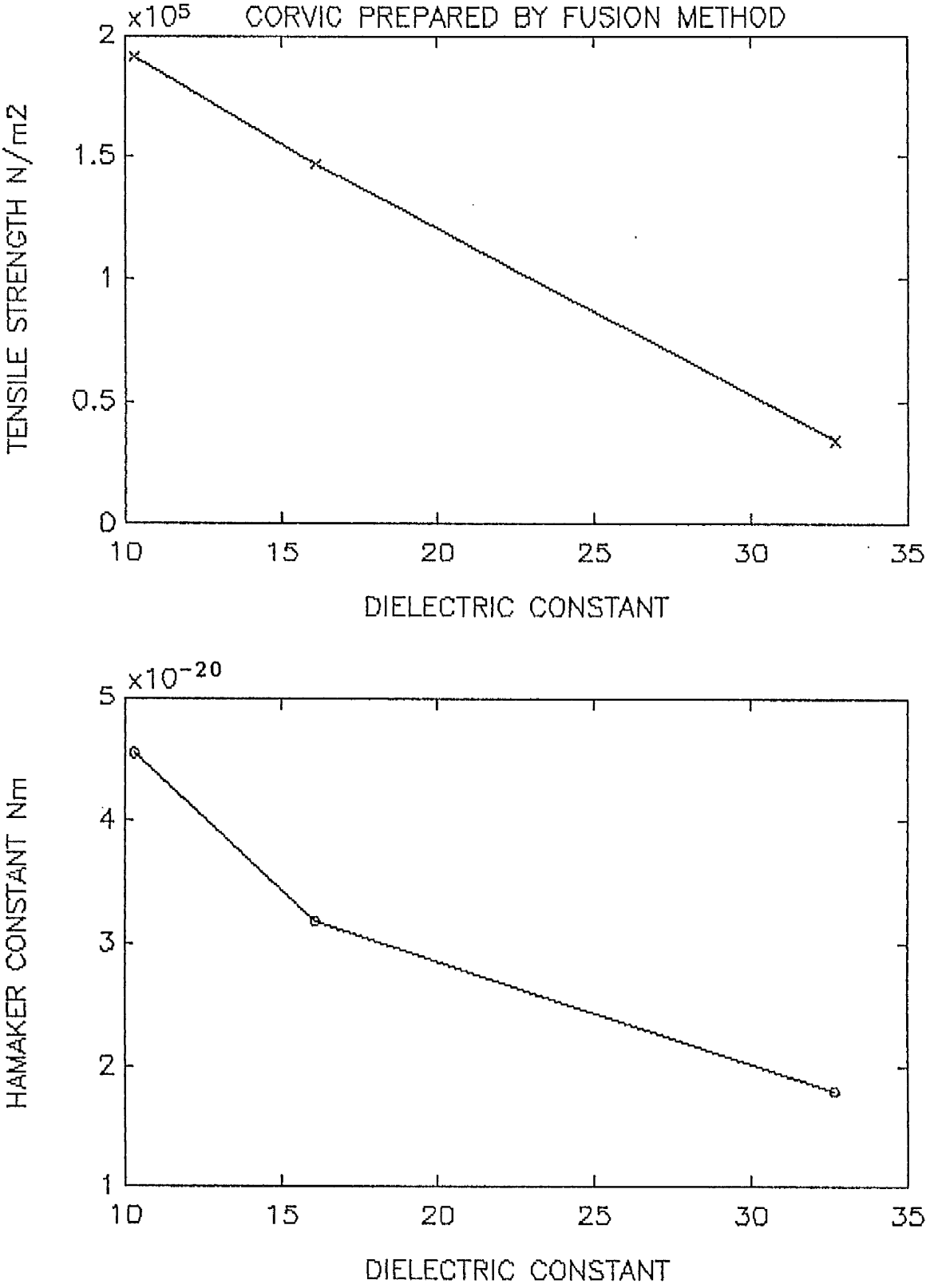

FIG. 3.9 RELATIONSHIPS BETWEEN CHANGES IN TENSILE STRENGTH AND HAMAKER CONSTANT TO CHANGES IN DIELECTRIC CONSTANT FOR CORVIC PREPARED BY FUSION METHOD

TABLE 3.7

TENSILE STRENGTH, $\sigma \times 10^5$ N/m^2 AND HAMAKER CONSTANT, $A \times 10^{-20}$ N.m FOR PTFE COMPACTS FORMED BY COMPRESSION WITH AND WITHOUT HEATING

Dielectric constants	Hamaker constants	Tensile strength	
		no heat	heat
32.7	0.23	5.62	5.56
16.1	0.19	4.84	5.26
5.8	0.16	4.46	5.01
AIR	0.87	6.66	6.75

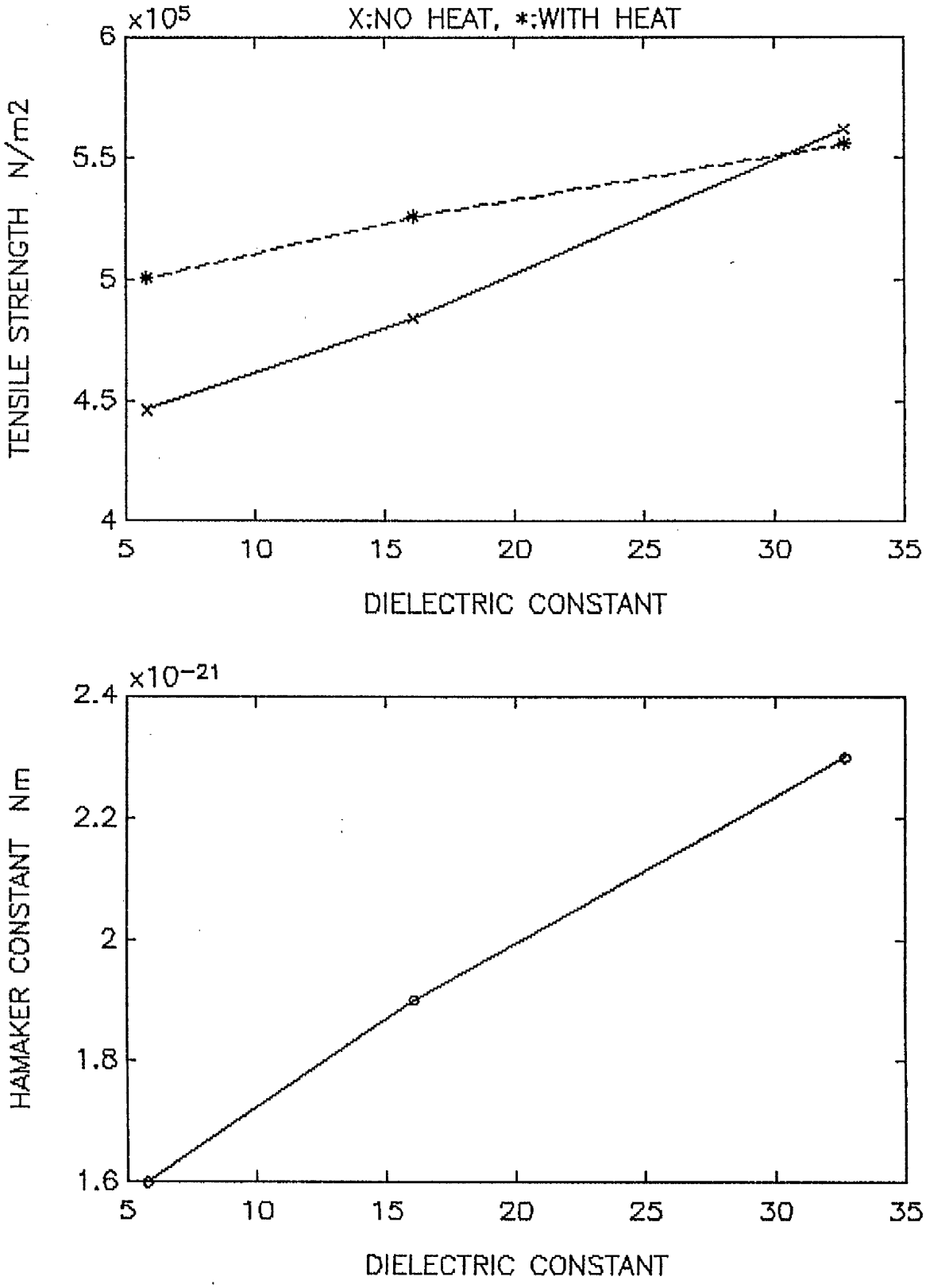

FIG. 3.10 RELATIONSHIPS BETWEEN CHANGES IN TENSILE STRENGTH AND HAMAKER CONSTANT TO CHANGES IN DIELECTRIC CONSTANT FOR PTFE POWDER WITH AND WITHOUT HEATING BEFORE COMPRESSION

Tensile strengths and Hamaker constants have dropped drastically in an intervening medium compared to air. A similar agreement showing a reduction of the Hamaker constants in the liquid medium was obtained by Israelachivilli (1985) and Visser (1972). Carre and Schultz (1984) also found a decrease in separation strength between aluminum and an adhesive in a series of alcohols such as methanol, ethanol and butanol. This decrease, as explained by Sato (1954) is due to the decrease of breaking stress which is a function of surface energies of solid in air and of interfacial energies in a liquid. This weakening effect is brought about by the changing of solid forces to liquid forces leading to a defect in the solid surface, followed by the transition of nearby molecules to fill in this defect, resulting in a dislocation phenomenon. Therefore, the strength in the liquid media is weaker than in air (tables 3.4-3.6).

The disintegration test is one of the general tests used to measure drug bioavailability. Disintegration tests were carried out in the series of alcohols used in the previous study. Table 3.8 shows the disintegration times, tensile strengths and Hamaker constants for PVC, Corvic and PTFE. There is a direct relationship between tablet strength and disintegration time. Plots of this relationship are shown in Figs.3.11-3.13. The bonds were disrupted at the faster rate (shorter time) in methanol than hexanol for PVC and Corvic since they give a lower A value in methanol than in hexanol, hence weaker bonds were formed. A similar agreement was found in the

TABLE 3.8

TENSILE STRENGTH, $\sigma \times 10^5$ N/m^2 AND HAMAKER CONSTANT, $A \times 10^{-20}$ N.m AND DISINTEGRATION TIME (MINS.) FOR PVC, CORVIC AND PTFE

Liquids	Dielect. const.	PVC			Corvic			PTFE		
		σ	A	time	σ	A	time	σ	A	time
Methanol	32.7	0	1.91	0.5	0	1.79	4.0	5.73	0.23	2.9
Ethanol	24.5	0	2.25	1.0	0.21	2.18	15.0	5.13	0.16	2.5
Hexanol	13.3	0.41	3.12	138	1.12	3.18	105.0	4.88	0.16	1.6
2 methyl-butan-2-ol	5.8	0.52	3.60	>300	–	–	-	4.55	0.16	1.8

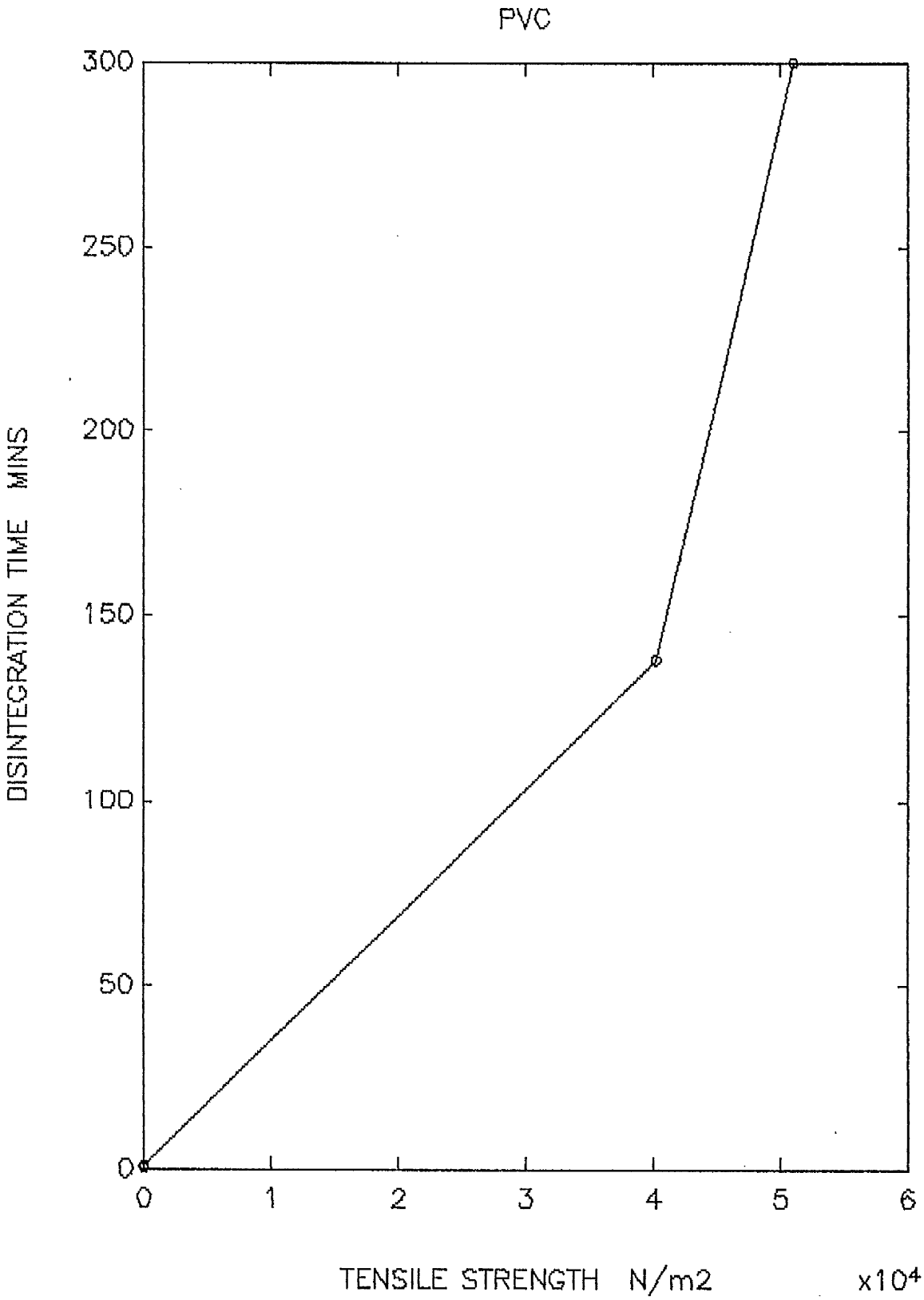

FIG. 3.11 **RELATIONSHIPS BETWEEN TENSILE STRENGTH AND DISINTEGRATION TIME FOR PVC**

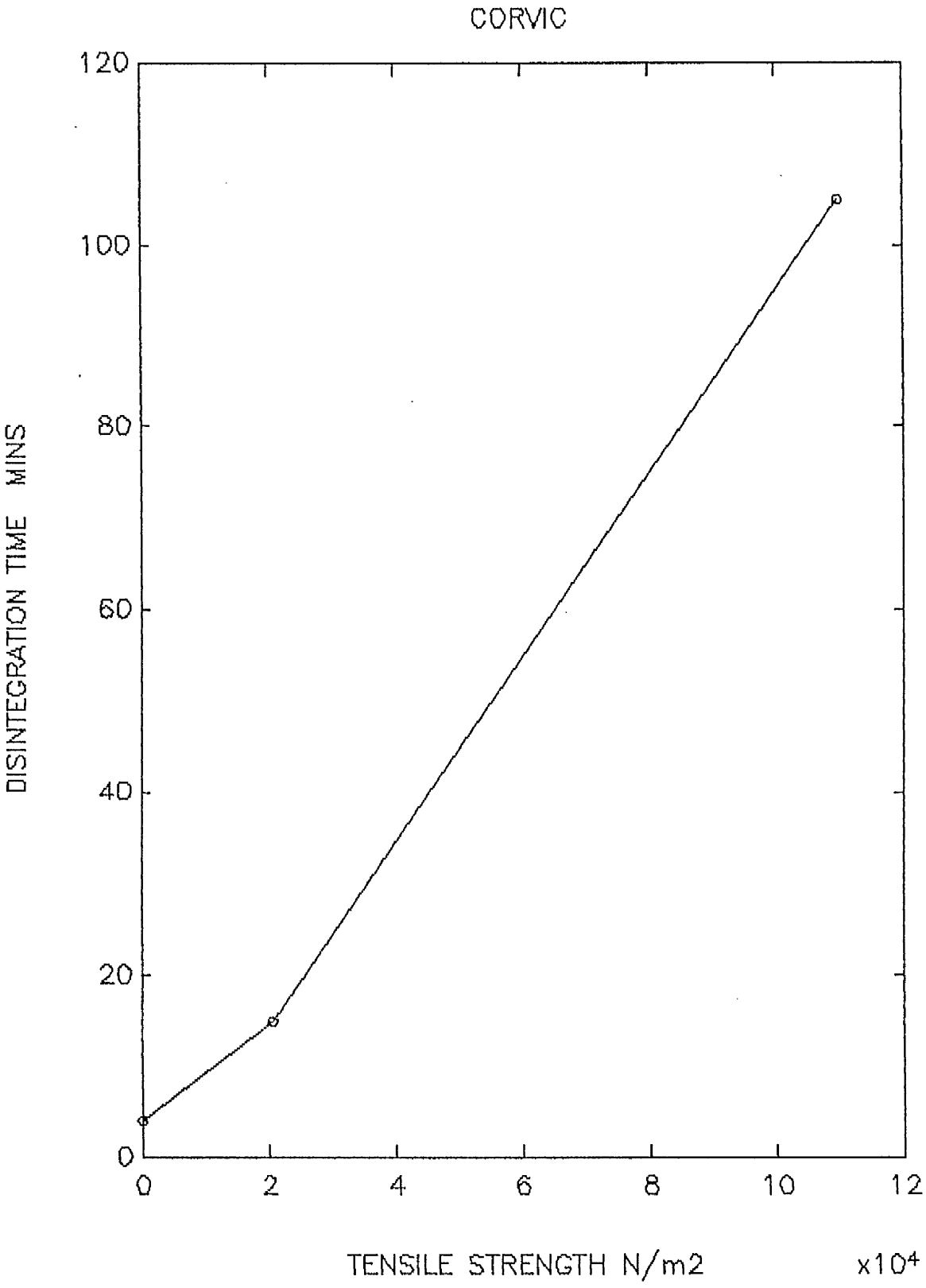

FIG. 3.12 RELATIONSHIPS BETWEEN TENSILE STRENGTH AND DISINTEGRATION TIME FOR CORVIC

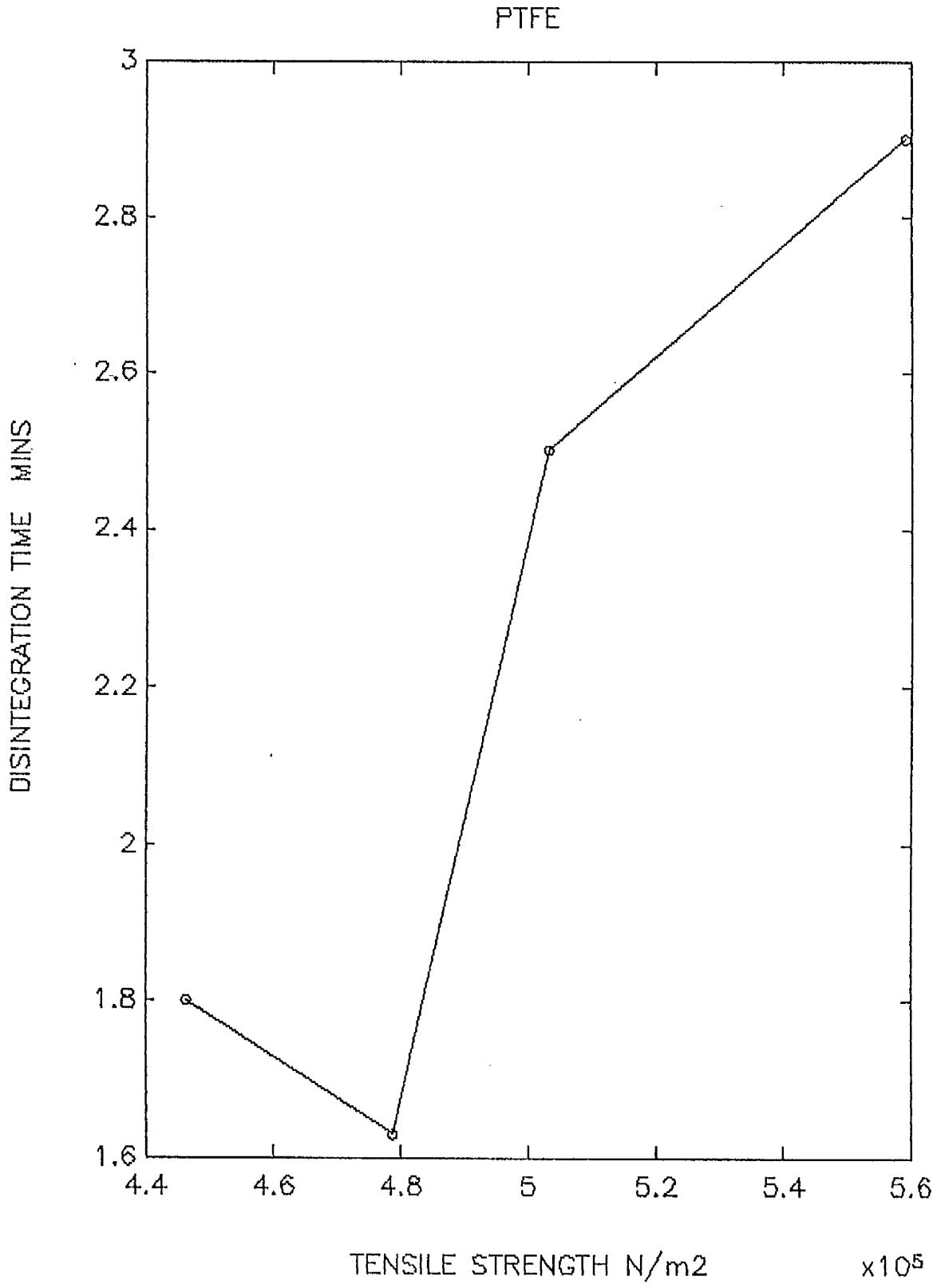

FIG. 3.13 RELATIONSHIPS BETWEEN TENSILE STRENGTH AND DISINTEGRATION TIME FOR PTFE

work of Reier and Shangraw (1966) when a shorter disintegration time of microcrystalline cellulose was obtained in a higher polarity liquid. For PTFE an inverse effect was observed.

The results obtained ,hitherto, lead to a conclusion that there is a relationship between the estimated strength and measured strength. Therefore, the bonding mechanisms of these compacts either formed by compression or fusion methods are Van der Waals forces. The disintegration time also shows a good correlation to tensile strength and hence Hamaker constant. Therefore a prediction of bonding strength of any material can be achieved from a knowledge of surface free energies.

3.2 COMBINING RULE

According to equation 1.28, the effective Hamaker constant of two similar particles in an intervening media depends on the difference between the surface free energies of the solid and liquid phases, and it is always attractive. If this is the case, these compacts should not respond to changes in dielectric constants as all the test liquids have the same magnitude of surface tension, and the Hamaker constant would therefore be consistent in every liquid. In fact all the test materials responded to the change of alcohol. Hamaker constants for the

materials under test calculated on the basis of combining rules tends to be zero as the forces between the phases are of the same degree. Therefore, the tensile strength of PTFE tablets should tend to zero in the various liquids, since its surface energy is of the same magnitude as liquids.

The misunderstanding which is also suggested by Neumann et al (1982) results from the misinterpretation of Berthelot's equation The equation derived from combining rules, therefore, is not suitable, and equations 1.18 and 1.19 are applicable instead.

3.3 BONDING STRENGTH OF MIXTURES

Bonding forces between individual particles contribute to the strength of tablets. In a binary mixture, containing particles of both components interactions may occur. The possibilities of the interaction are shown in Fig. 3.14 suggested by Luenberger (1982). A linearity is obtained when there is no interaction between the two components (Fig. 3.14a). The other two cases (fig. 3.14 b,c) show a positive or negative interactions. Three different types of mixtures were chosen to study different aspects of bonding mechanisms using a knowledge of Hamaker constants. These mixtures were PEM and Corvic, PVC and PTFE and magnesium carbonate and Emcompress.

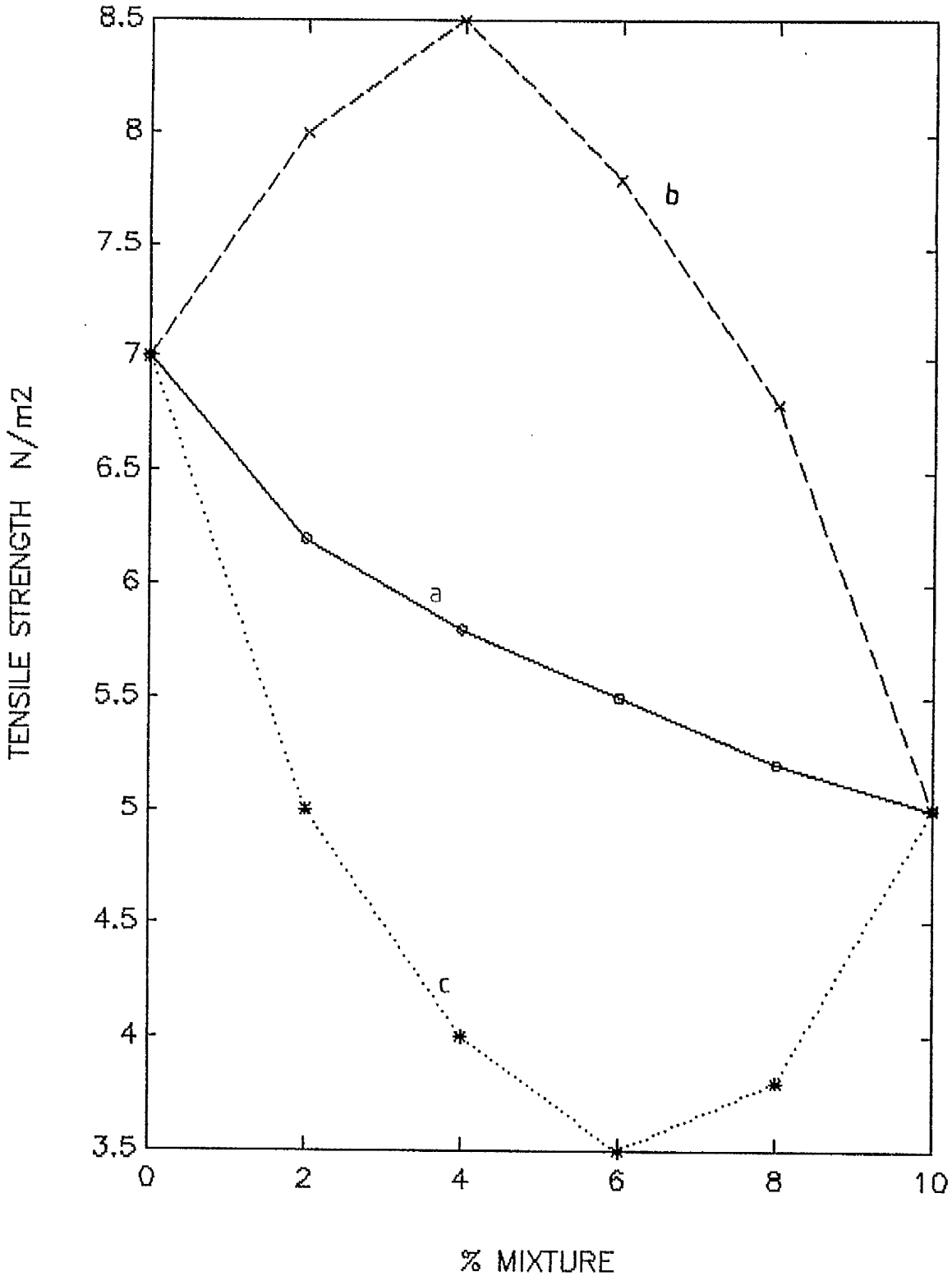

FIG. 3.14 THREE POSSIBILITIES OF TENSILE STRENGTH FOR BINARY MIXTURES

a) NO INTERACTION

b) POSITIVE INTERACTION

c) NEGATIVE INTERACTION

The powders were selected because:

1. Similar size fractions in each mixture can be obtained, since tensile strength varies with different particle sizes (Sheikh -Salem and Fell, 1982; Alderborn and Nystrom, 1982a; Duberg and Nystrom, 1982).

2. These powders provide an ideal system for the tensile strength test due to their similar consolidation mechanisms in each mixture. Mixtures of PEM and Corvic and PVC and PTFE exhibit plastic flow while magnesium carbonate and Emcompress undergo fragmentation.

3. Particles of PEM and Corvic are spherical in shape allowing a constant powder bed structure to be maintained throughout a range of mixtures. Alderborn and Nystrom (1982b) found that different shapes of particles give different tensile strengths.

4. PVC and PTFE represents a mixture of a hydrophilic and a hydrophobic powder whereas PEM and Corvic, and magnesium carbonate and Emcompress, are mixtures between hydrophilic powders.

Table 3.9 shows tensile strength and Hamaker constants of every mixture. The Hamaker constants of the mixtures were calculated according to equation 1.11 and 1.21, assuming the component 1 has x particles and 2 has 1-x particles. Therefore equation 3.1 is given:

$$A = 2x(1-x)[(\gamma_1^d \gamma_2^d)^{1/2} + (\gamma_1^p \gamma_2^p)^{1/2}]*12\pi d_0^2 \quad \ldots 3.1$$

TABLE 3.9

TENSILE STRENGTH, $\sigma \times 10^5$ N/m^2 AND HAMAKER CONSTANT, $A \times 10^{-20}$ N.m OF PEM AND CORVIC, PVC AND PTFE AND MAGNESIUM CARBONATE AND EMCOMPRESS

Mixtures	Tensile strength	Hamaker constant
PEM:Corvic		
100:0	1.17	9.99
80:20	1.30	1.38
50:50	1.48	2.15
20:80	1.97	1.38
0:100	2.32	8.99
PVC:PTFE		
100:0	12.07	11.49
75:25	11.65	1.18
50:50	17.88	1.57
25:75	19.20	1.18
10:90	11.00	0.56
0:100	6.79	4.50
Mg:Emcompress		
100:0	23.64	11.02
75:25	21.58	2.15
50:50	19.33	2.86
25:75	17.95	2.15
0:100	8.53	12.09

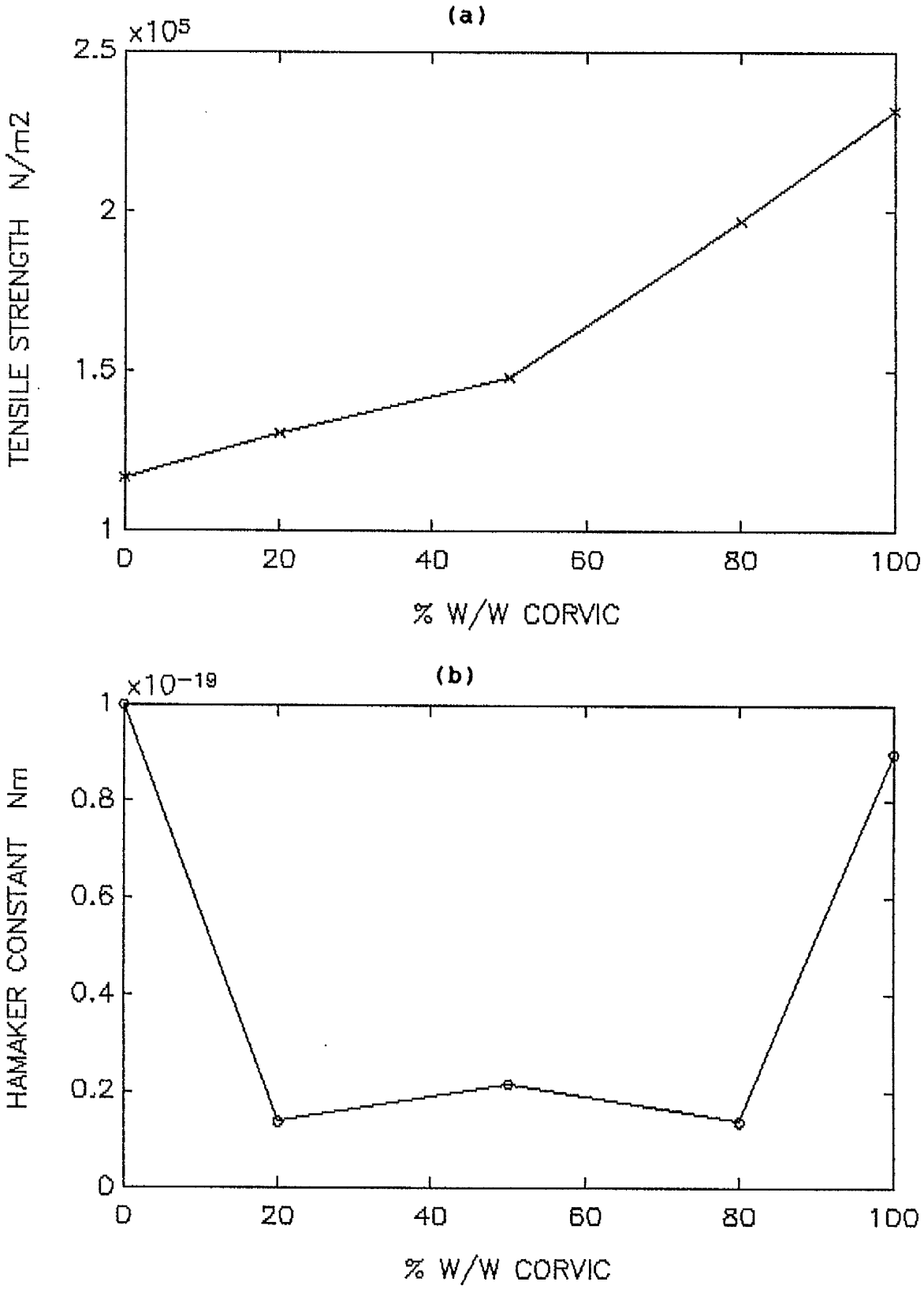

FIG. 3.15 RELATIONSHIPS BETWEEN CHANGES IN TENSILE STRENGTH AND HAMAKER CONSTANT TO CHANGES IN DIELECTRIC CONSTANT FOR MIXTURE OF PEM AND CORVIC

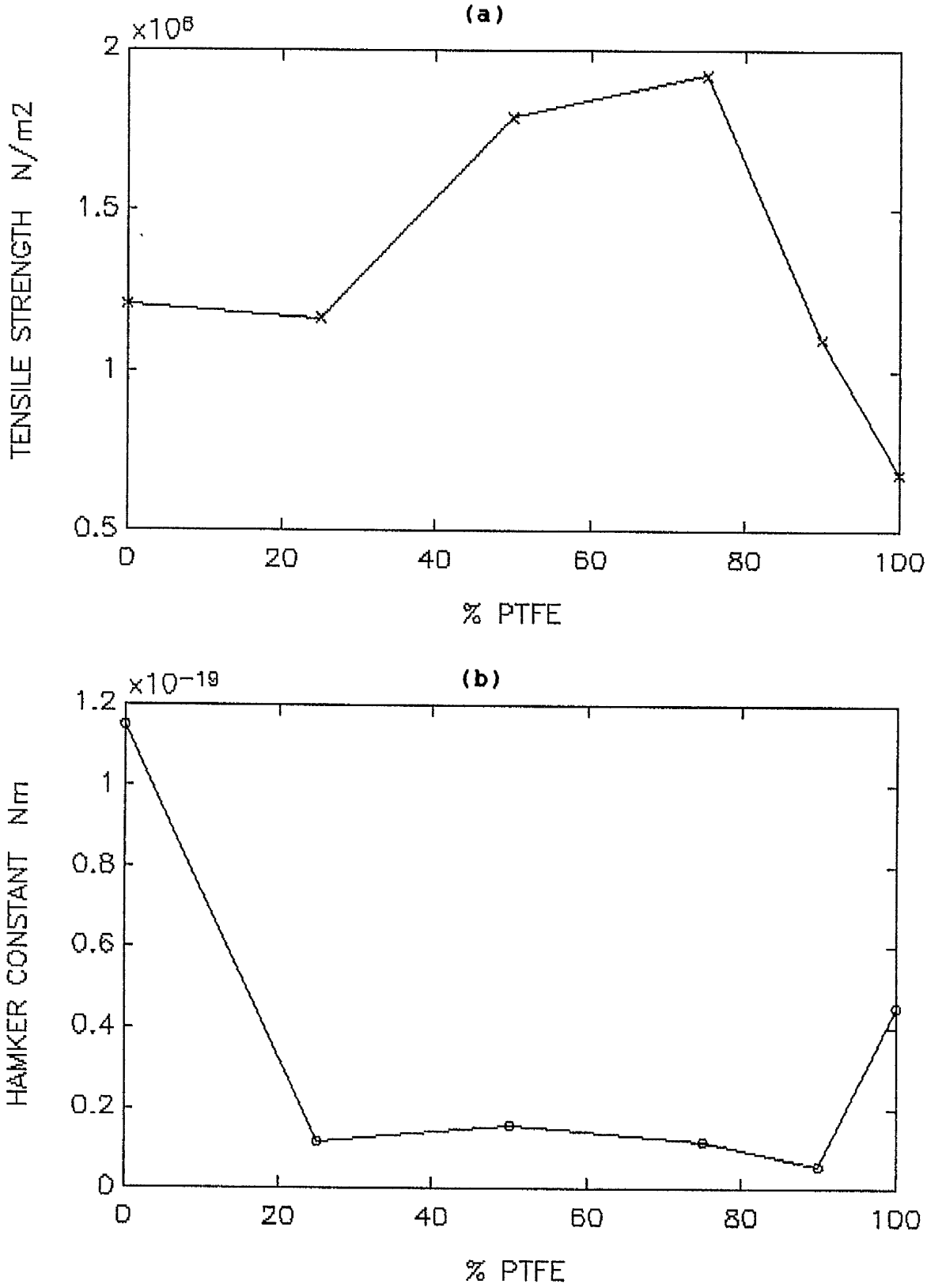

FIG. 3.16 RELATIONSHIPS BETWEEN CHANGES IN TENSILE STRENGTH AND HAMAKER CONSTANT TO CHANGES IN DIELECTRIC CONSTANT FOR MIXTURE OF PVC AND PTFE

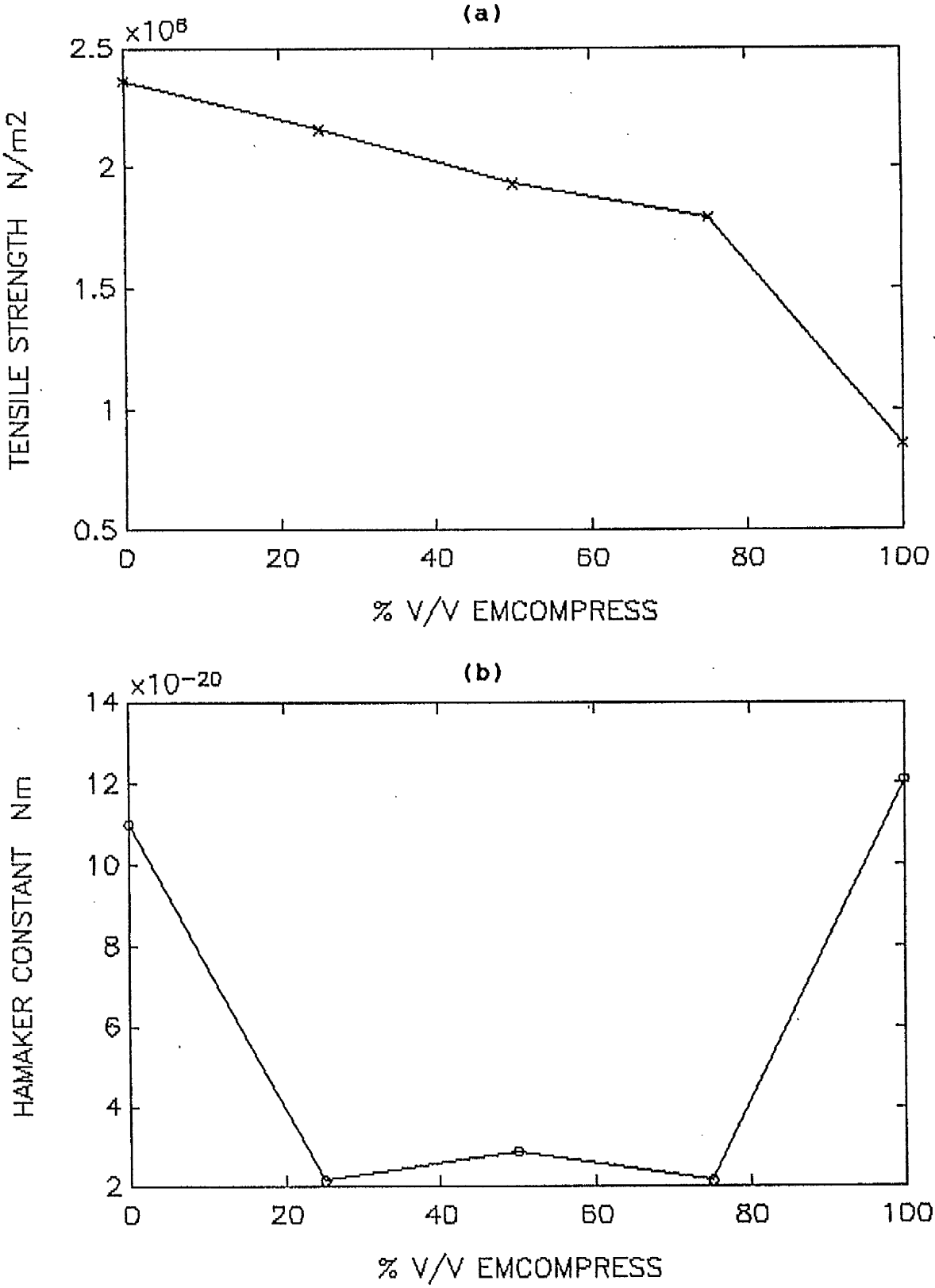

FIG. 3.17 RELATIONSHIPS BETWEEN CHANGES IN TENSILE STRENGTH AND HAMAKER CONSTANT TO CHANGES IN DIELECTRIC CONSTANT FOR MIXTURE OF MAGNESIUM CARBONATE AND EMCOMPRESS

Plots of tensile strength and Hamaker constant against mixture composition are shown in Figs. 3.15-3.17. Unlike pure materials, an agreement between both trends was not obtained. The predicted strengths gave a negative interaction in all compositions for each mixtures. However, the experimental results (tensile strength test) show no interaction in the first and last pairs while the mixtures of PVC and PTFE exhibit a positive interaction. The disagreement in behaviour are due to properties of the materials themselves which is further considered below:

1. MIXTURE OF PEM AND CORVIC

Table 3.10 shows the tensile strength of the mixture of each composition at different pressures. Each value was the average of five tablets. The appplication of pressure to a powder bed within the confines of a punch and die system, results in a reduction of the porosity and thickness of every mixture, and increases the tensile strength. The applied pressure brings particles closer together due to the processes of rearragement and plastic deformation, the contact area is increased, hence a stronger compact is formed. The results obtained are in agreement with the work of Fell and Newton (1968), Newton and Grant (1974), Newton et al. (1977), Groves and Alkan (1979) and Sheikh-Salem and Fell (1981,1982). The relationship between tensile strength and applied pressure at different compositions is shown in Fig 3.18. All the curves are

linear, the higher is the pressure, the stronger tablets. Higher tensile strength are observed for higher ratios of Corvic. An agreement is also observed in a plot of mixture compositions and the tensile strength at different pressures (Fig 3.15a and Fig. 3.19). The addition of Corvic results in an increase in the tensile strength at all compaction pressures. This increased tensile strength is due to the decrease in porosity as can be seen in Fig. 3.20 since Corvic powders can flow more readily than PEM powders. This results in particles becoming closer together, an increase in contact area and consequently more bonds are formed. The work is in accordance with Vromans and Lerk (1988) who suggested that the increase in strength is a result of increasing densification.

A correction factor $(1/1-\epsilon_v)$ was suggested for tensile strength values since the tensile strength was measured on tablets of different porosities (Newton et al.1971). The tensile strength equation after correction is given as:

$$\sigma = \frac{2P}{\Pi dT(1-\epsilon_v)} \qquad \ldots 3.2$$

Plots of tensile strength after correction against pressures or the ratios of Corvic are shown in Fig 3.21 and 3.22. Incorporation of this factor does not change the general shapes of the curves. Therefore, the tensile strength value determined by diametral compression test is a function of pore structure.

TABLE 3.10

TENSILE STRENGTH, $\sigma \times 10^5$ N/m^2 OF MIXTURE OF PEM AND CORVIC AT FOUR COMPACTION PRESSURES (MN/m^2)

Compaction Pressure	PEM:COR. w/w	Thickness cm.	Porosity	Tensile strength	$\sigma/(1-\varepsilon_v)$
77.41	100:0	0.4795	0.3521	0.39	0.61
	80:20	0.4615	0.3259	0.54	0.80
	50:50	0.4462	0.3349	0.81	1.22
	20:80	0.3890	0.2630	1.03	1.40
	0:100	0.3757	0.2550	1.46	1.96
116.11	100:0	0.4430	0.2980	0.52	0.74
	80:20	0.4370	0.2850	0.73	1.02
	50:50	0.4180	0.2870	0.77	1.07
	20:80	0.3800	0.2480	1.20	1.59
	0:100	0.3700	0.2430	1.59	2.10
154.82	100:0	0.4250	0.2620	0.78	1.06
	80:20	0.4260	0.2780	0.94	1.31
	50:50	0.3950	0.2520	1.23	1.64
	20:80	0.3600	0.2040	1.71	2.14
	0:100	0.3520	0.2020	1.85	2.32

193.52	100:0	0.4280	0.2640	1.17	1.59
	80:20	0.4050	0.2450	1.30	1.72
	50:50	0.3920	0.2350	1.48	1.94
	20:80	0.3620	0.1990	1.97	2.46
	0:100	0.3480	0.1840	2.32	2.84

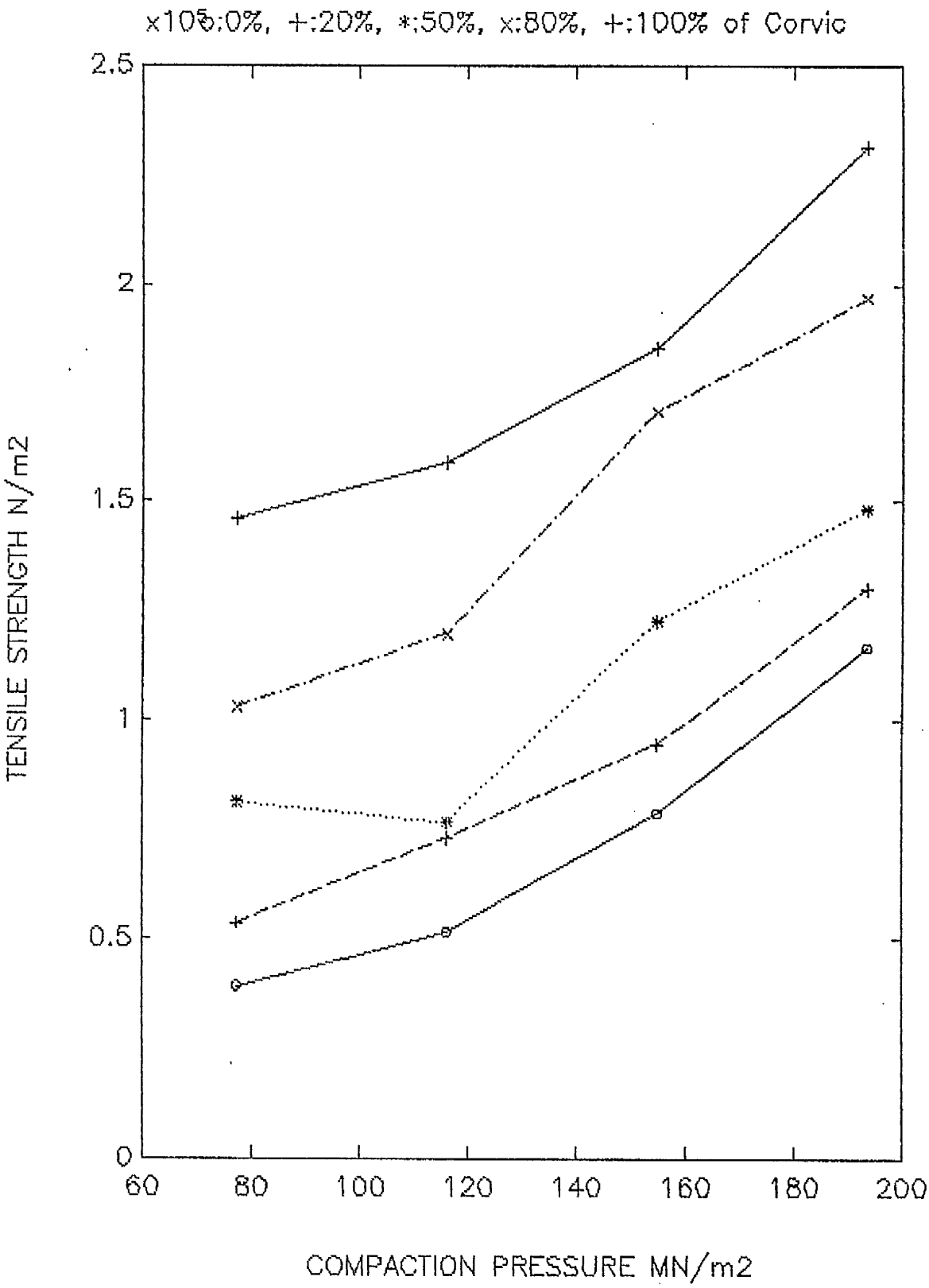

FIG. 3.18 **THE RELATIONSHIP BETWEEN TENSILE STRENGTH AND APPLIED PRESSURE AT DIFFERENT COMPOSITION OF MIXTURE OF PEM AND CORVIC**

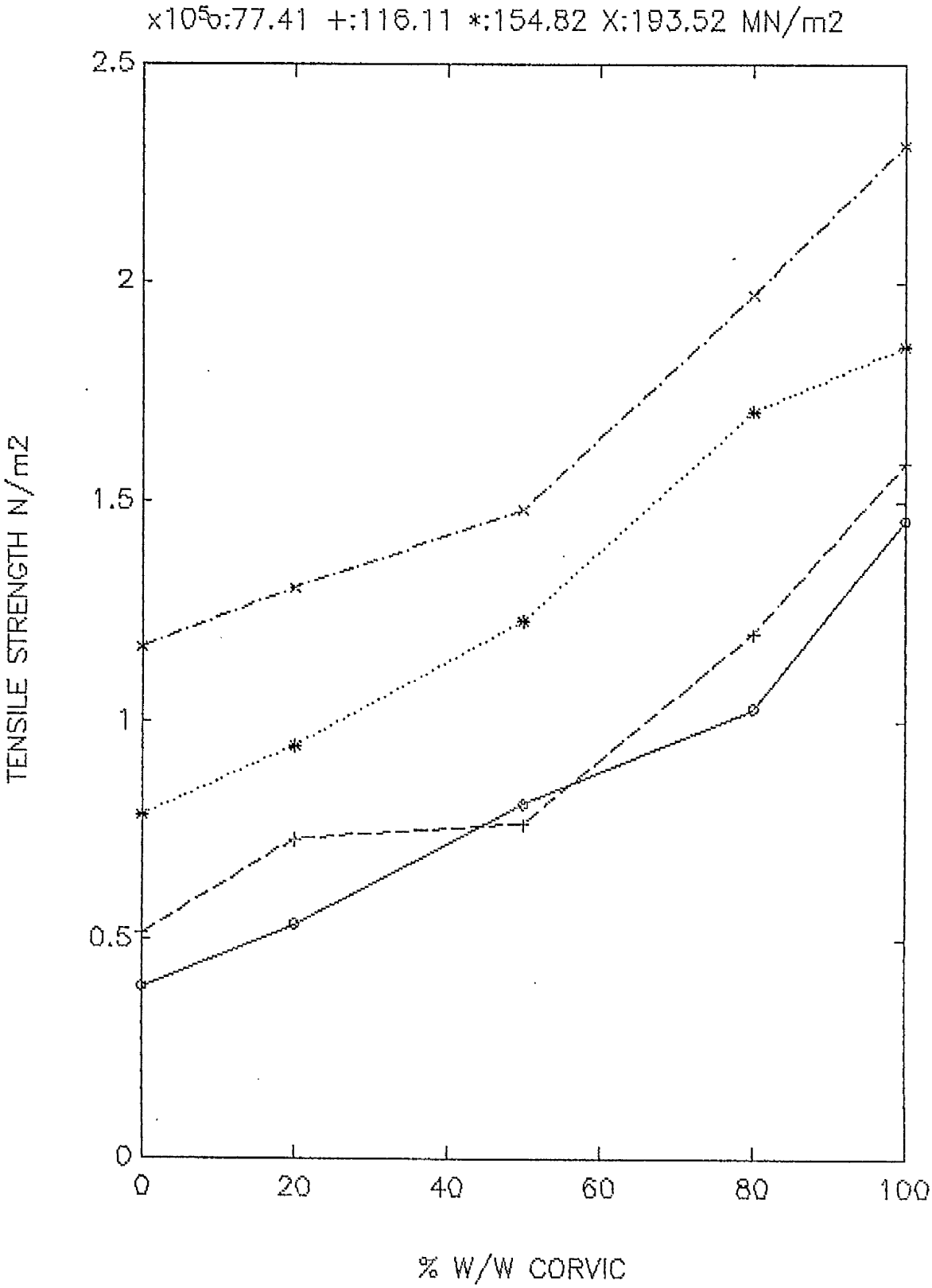

FIG. 3.19 THE RELATIONSHIP BETWEEN TENSILE STRENGTH AND COMPOSITION OF MIXTURE OF PEM AND CORVIC AT DIFFERENT PRESSURES

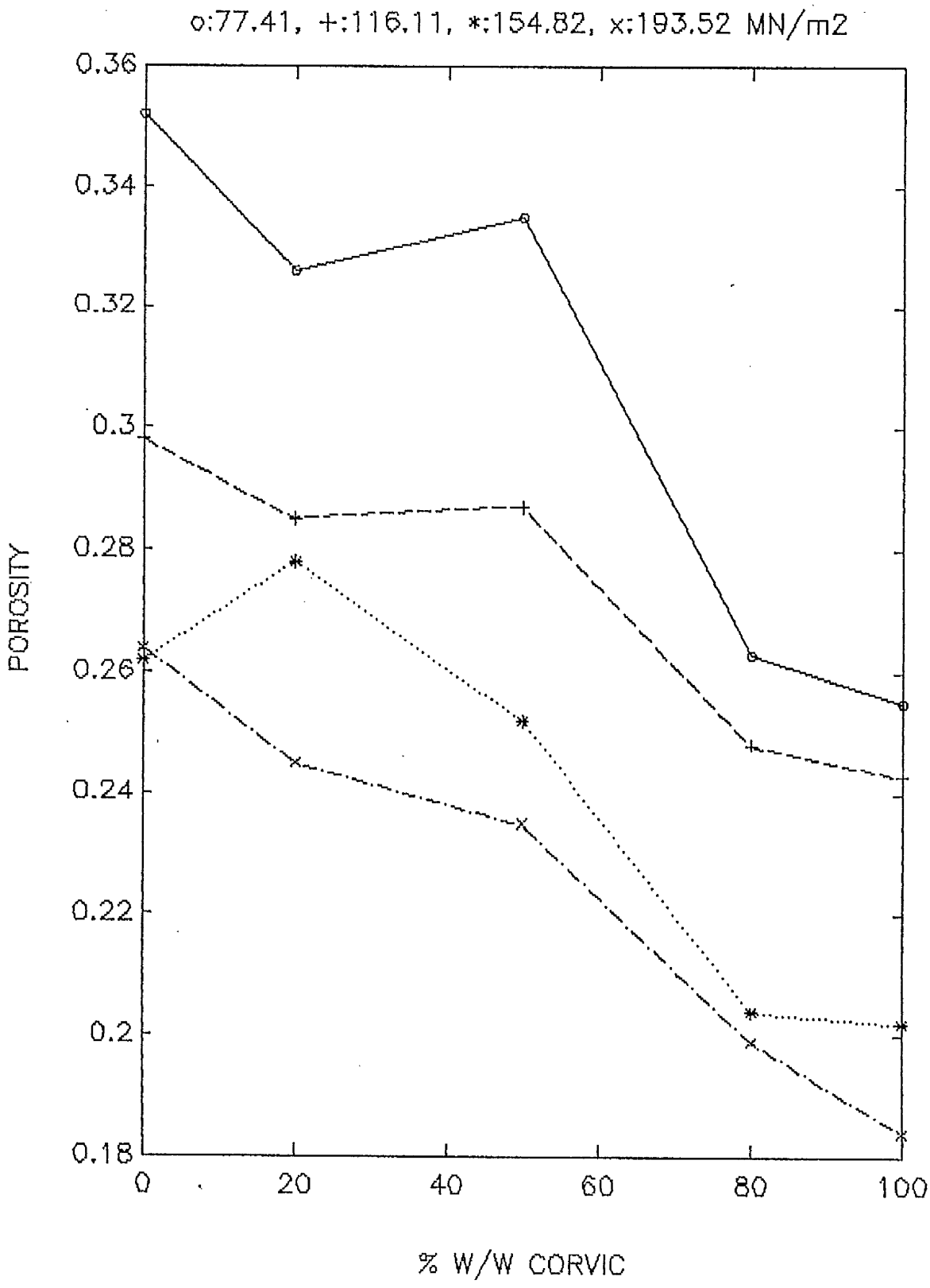

FIG. 3.20 THE RELATIONSHIP BETWEEN POROSITY AND COMPOSITIONS OF MIXTURE OF PEM AND CORVIC

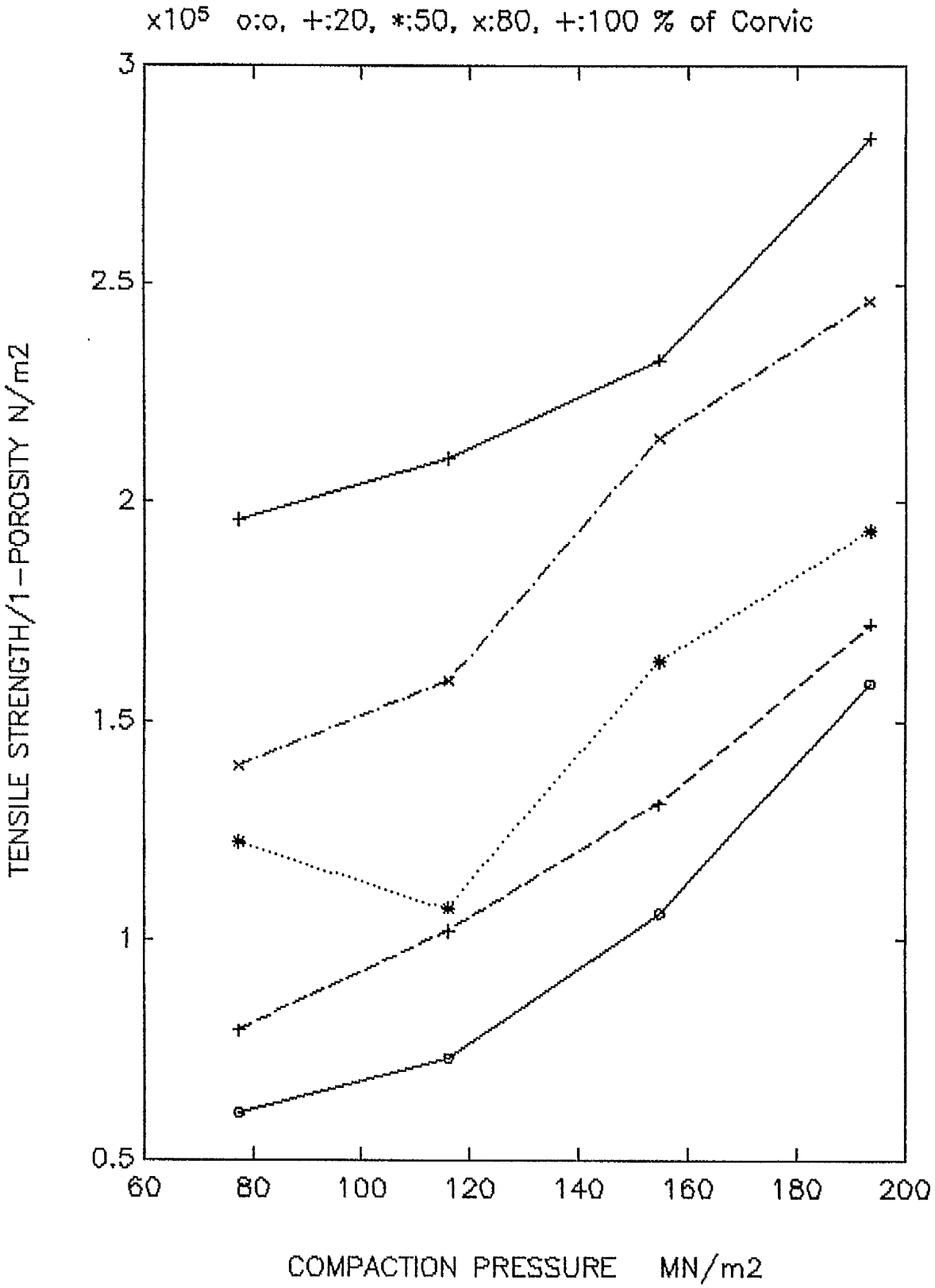

FIG. 3.21 THE RELATIONSHIP BETWEEN TENSILE STRENGTH AFTER APPLYING A CORRECTION FACTOR AND COMPACTION PRESSURE AT DIFFERENT COMPOSITIONS OF MIXTURE PEM AND CORVIC

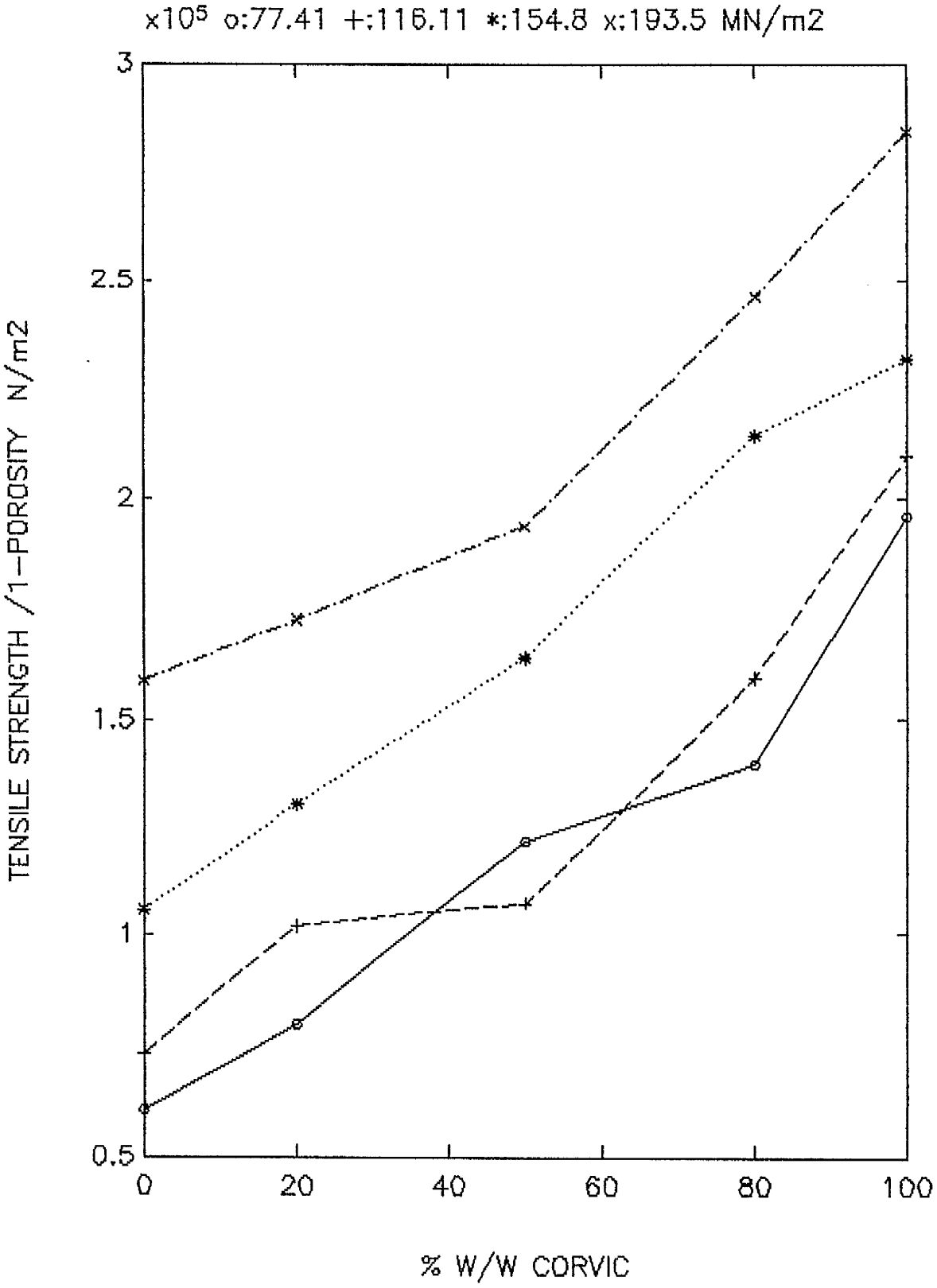

FIG. 3.22 THE RELATIONSHIP BETWEEN TENSILE STRENGTH AFTER APPLYING A CORRECTION FACTOR AND COMPOSITION OF MIXTURE OF PEM AND CORVIC AT DIFFERENT PRESSURES

2 MIXTURE OF PVC AND PTFE

Fig. 3.16 shows the different trends of experimental and predicted strength obtained. The disagreement might be due to the work of densification, as with the mixture of PEM and Corvic.

Table 3.11 gives the properties of PVC/PTFE mixtures and their tensile strengths. The thickness and porosity decrease as the ratio of PTFE increases. The relationship between the porosity and the composition of the mixture is given in Fig 3.23. The increase in densification is observed when the amount of PTFE increases. It indicates that PTFE particles rearrange themselves by plastic flow into a closer compact than PVC tablets and the bonds between PTFE particles are probably stronger than PVC-PVC bonds. This suggestion is confirmed from the scanning electron micrographs. Figs. 3.24-3.25 show the scanning electron micrographs of PTFE and PVC before and after compaction respectively. Both powders exhibit plastic deformation, PVC particles keep their individuality and neatly fit together to a tight packing whereas PTFE particles readily fuse together, losing their individuality. Therefore, the highest tensile strength was expected from PTFE tablets. However, a higher tensile strength was found in the mixtures than that of the individual materials themselves. The highest strength was observed in tablets containing 75% PTFE (Fig.3.16a). The presence of a higher strength than predicted suggested that

TABLE 3.11

PROPERTIES OF MIXTURE OF PVC AND PTFE POWDERS

PVC:PTFE	weight (gm.)	thickness (mm)	diameter (mm)	density g/cm^3	porosity
0:100	0.5328	2.0240	12.6880	2.3880	0.1286
25:75	0.5352	2.3560	12.8000	2.1133	0.1650
50:50	0.5336	2.7140	12.7700	1.8470	0.1692
75:25	0.5285	3.1960	12.7800	1.7466	0.2622
100:0	0.5336	3.8560	12.7950	1.6544	0.3497

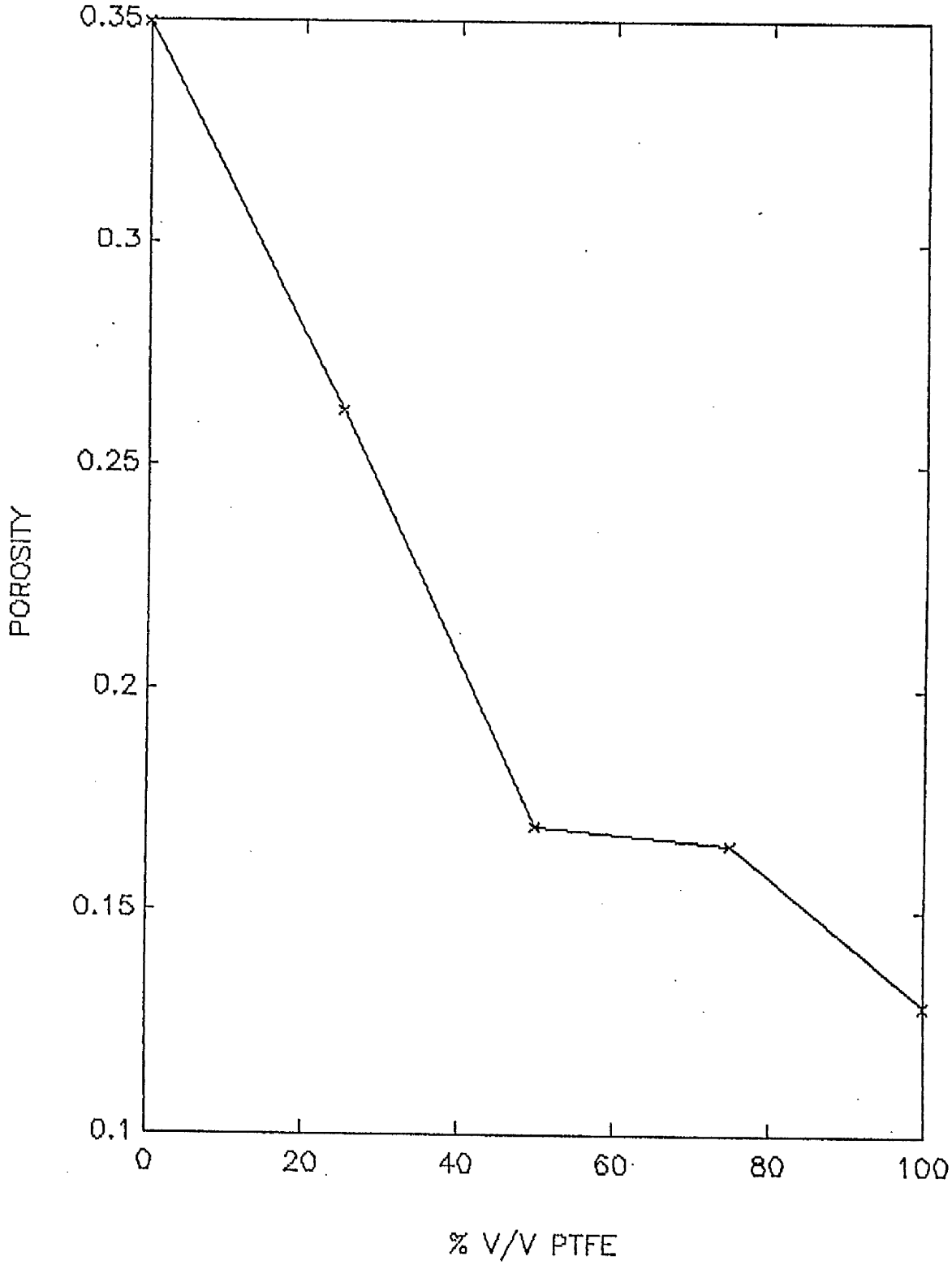

FIG. 3.23 THE RELATIONSHIP BETWEEN POROSITY AND COMPOSITIONS OF MIXTURE OF PVC AND PTFE

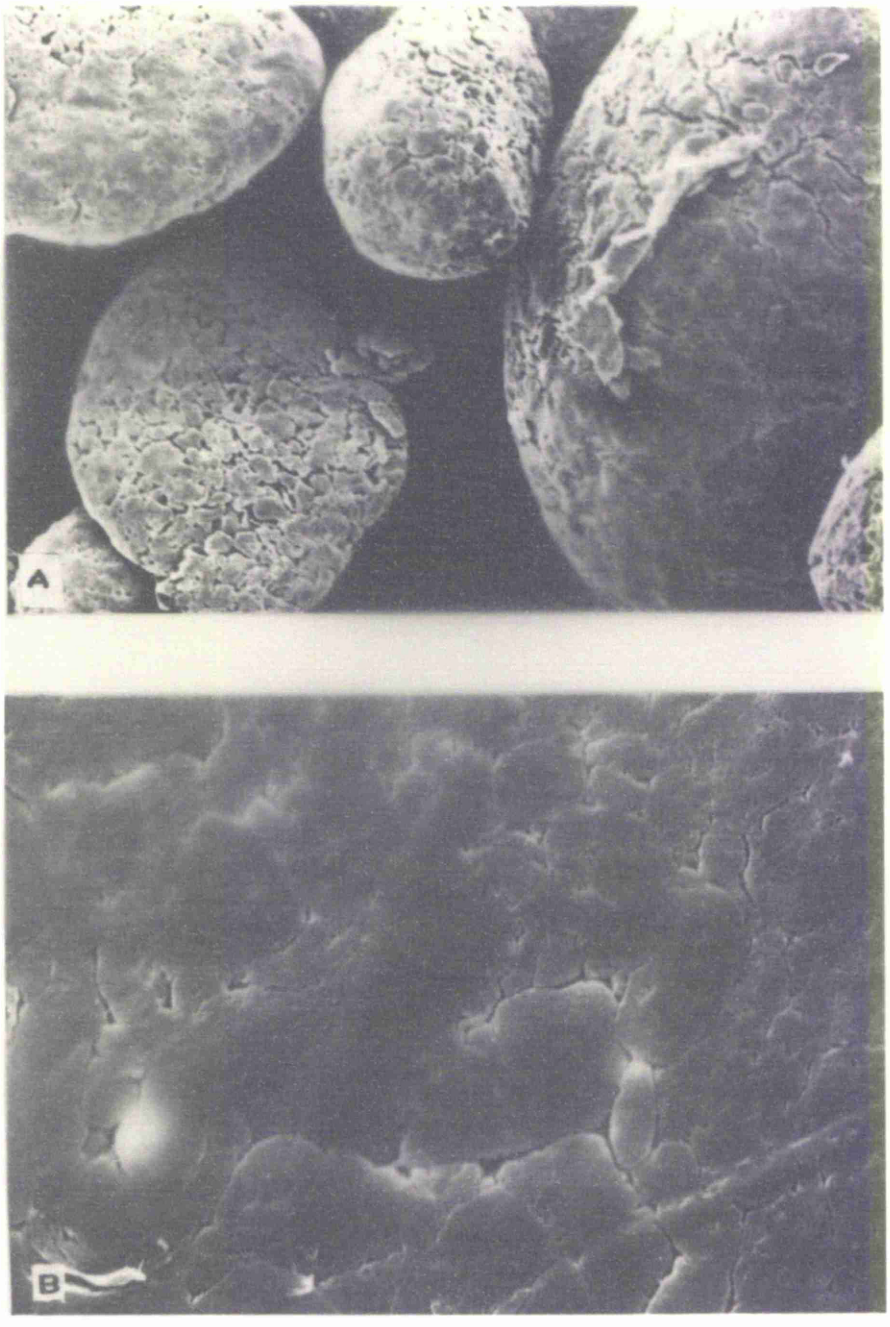

FIG. 3.24 SCANNING ELECTRON MICROGRAPHS OF PTFE POWDER BEFORE (A, MAGNIFIED BY 200) AND AFTER COMPACTION (B , MAGNIFIED BY 2000)

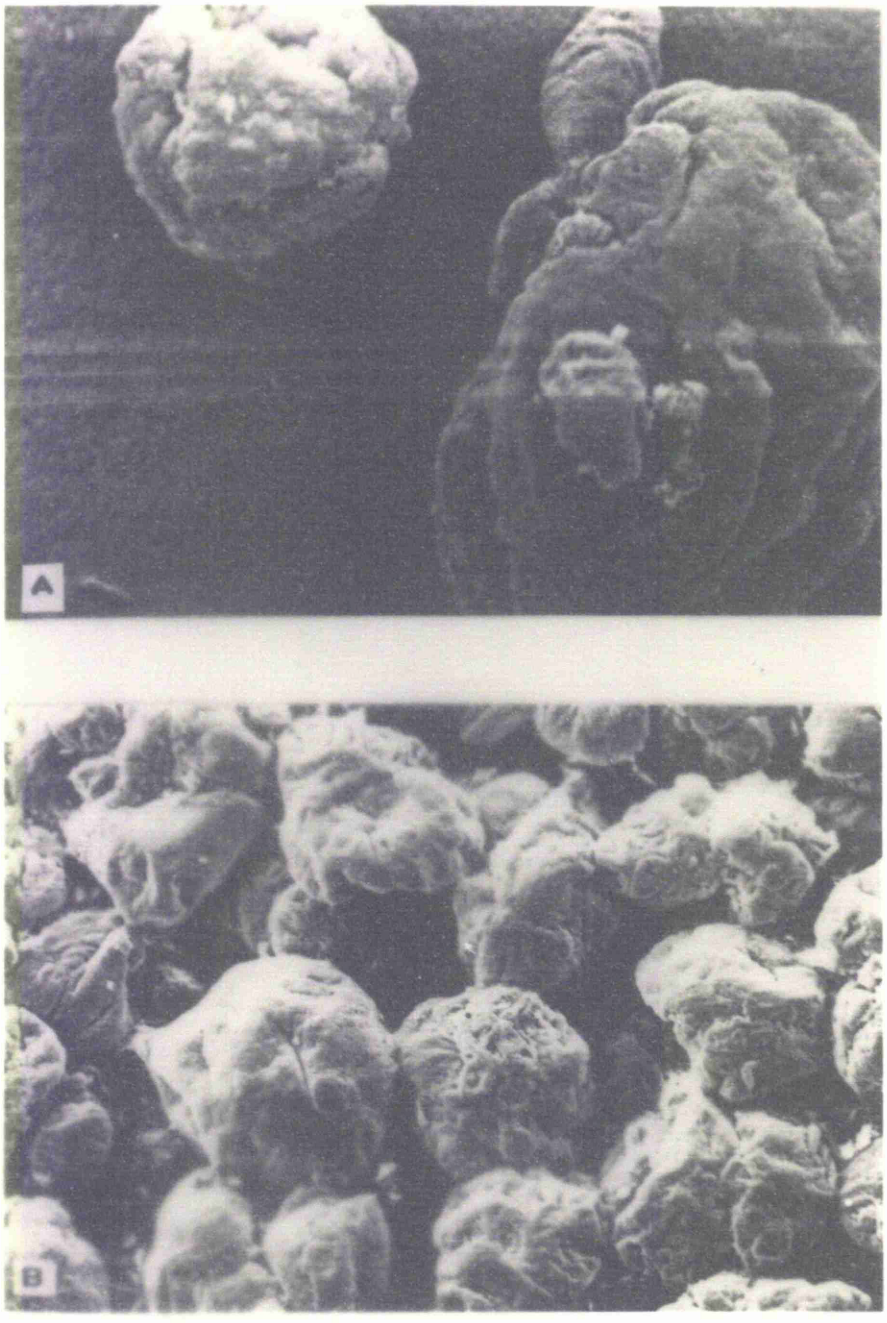

FIG. 3.25 SCANNING ELECTRON MICROGRAPHS OF PVC POWDER BEFORE (A, MAGNIFIED BY 500) AND AFTER COMPACTION (B, MAGNIFIED BY 200)

there is a positive interaction and the bonds between the differing materials might be formed preferentially rather than that between the individual material themselves. Therefore stronger bonds are formed. Similar results were found in the work of Newton et al. (1977) and Cook et al. (1975) for mixtures of phenacetin and dicalcium phosphate and of Emcompress and phenacetin respectively. Cook and Summers (1985) also found that the strength of mixtures of Emcompress and Aspirin were stronger than the individual materials themselves and a change of strength did not relate to a change of porosity. However, the evidence from the scanning electron micrograph of the surface of the 75% PTFE tablets shown in Fig. 3.26 is that bonding between PVC and PTFE did not occur. This suggests that an increase in the strength is a result of other mechanisms, presumably linked to the structure of the tablet which influences the failure and crack propagation during the test (Gordon, 1976). Kinloch and Young (1981) indicated that fracture of polymers tends to initiate along Van der Waals bonds rather than bonds within particles provided that the cracks are not prevented by their structures.

Since the surface structure of tablets could have been affected by the upper punch, the surface of fracture of 75% PTFE and a PTFE tablet were examined by scanning electron microscopy as shown in Fig. 3.27 and 3.28 respectively. Examination of electron micrographs shows that failure of PTFE occurs mainly across the particles indicating the strength

between particles is stronger than within the particle whereas the failure of PVC occurs around the particles indicating their weaker intermolecular bonds. Shotton and Ganderton (1960a,b) suggested that fracture across particles indicating bonds between adjacent particles is at least as strong as bonding forces in the particles. The highest strength obtained at 75% PTFE is due to the prevention of cracks by the small amount of PVC particles. Since PVC bonds are weaker the addition of higher proportions of PVC at 50 and 75% reduces the strength compared to that at 25% PVC.

The bonding mechanism of these compacts are Van der Waals forces. This can be confirmed in a similar manner to the studies of pure materials in a various liquids. A programme for the calculation of Hamaker constants of mixtures in an intervening media based on the equation 1.16 is given in appendix 1. Table 3.12 gives calculated results and tensile strengths of various compositions of the test liquids. Plots between changes in dielectric constant to Hamaker constant and tensile strength are shown in Figs. 3.29-3.32. In every composition the curves of strength and Hamaker constant have the same trends indicating that the bonding mechanism of these mixtures is Van der Waals forces.

The tensile strength of each compact in an intervening media is smaller than in air. The decreased effect can be explained in the same manner as for the pure materials.

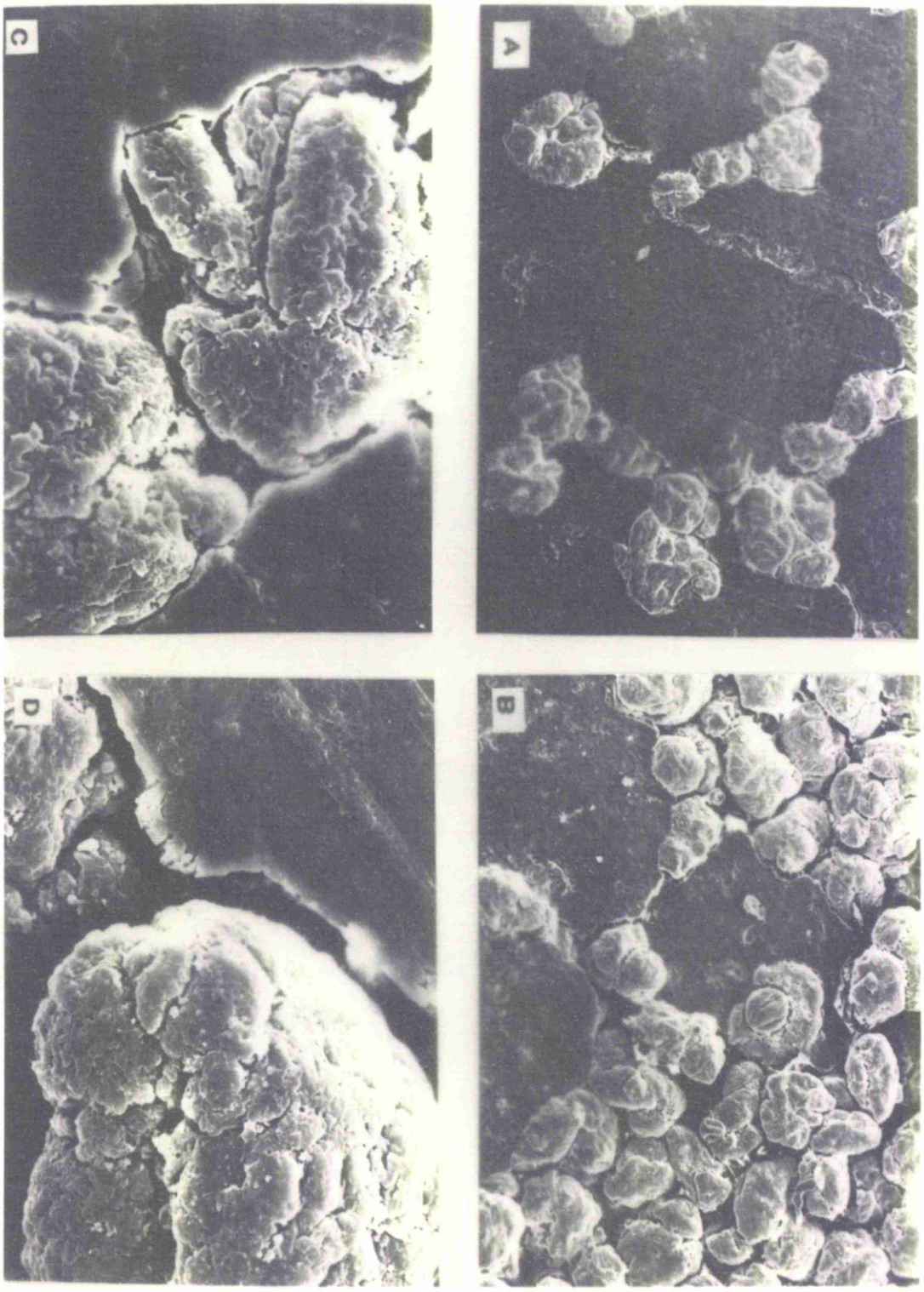

FIG. 3.26 SCANNING ELECTRON MICROGRAPHS OF MIXTURE OF 25 % PVC AND 75% PTFE TABLET AT MAGNIFICATION OF 100 X (A,B) AND OF 1000X (C,D)

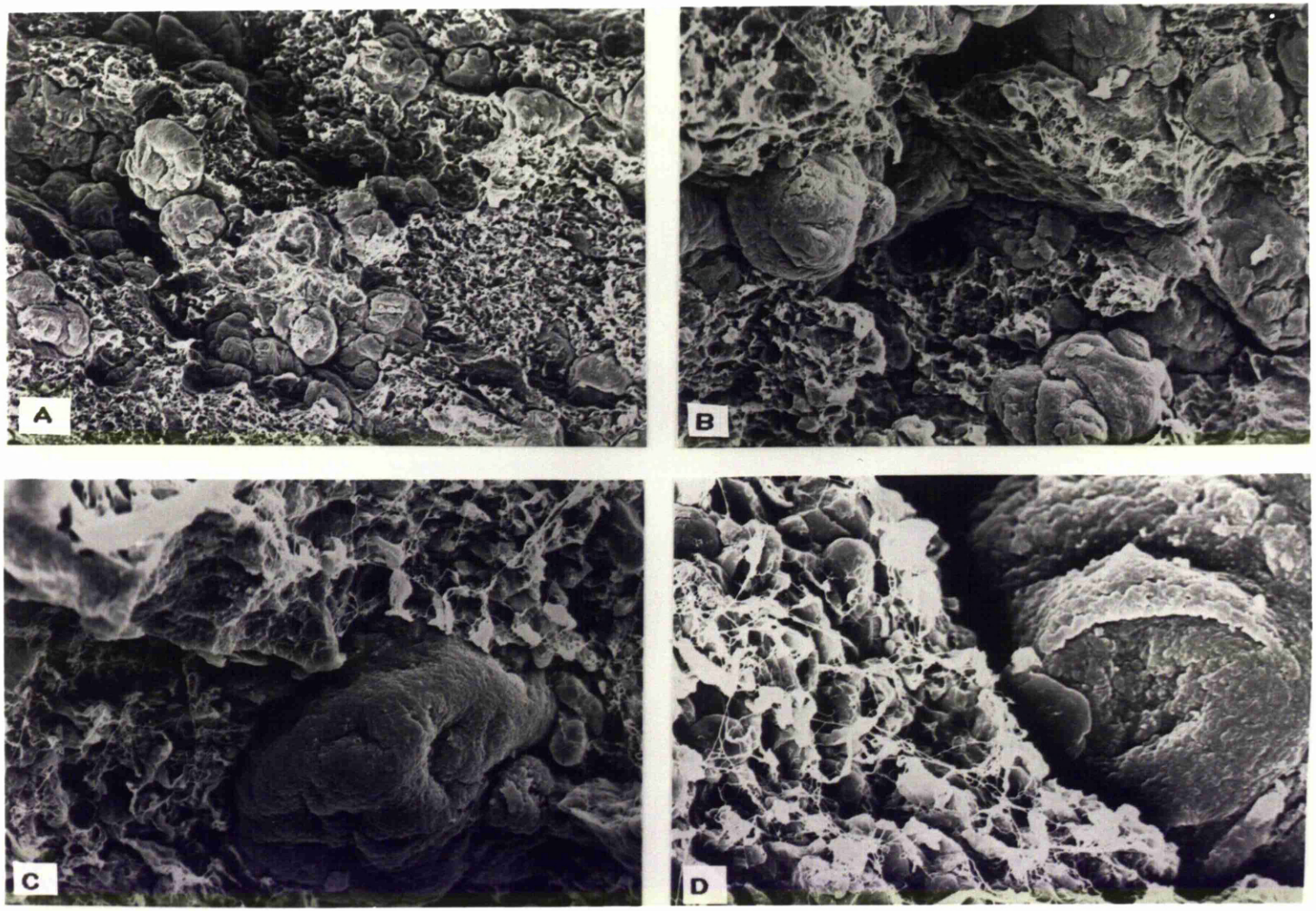
A
B
C
D

FIG. 3.28 SCANNING ELECTRON MICROGRAPHS OF THE FRACTURE SURFACE OF PTFE TABLET (A,B, MAGNIFIED BY 100 AND 200)

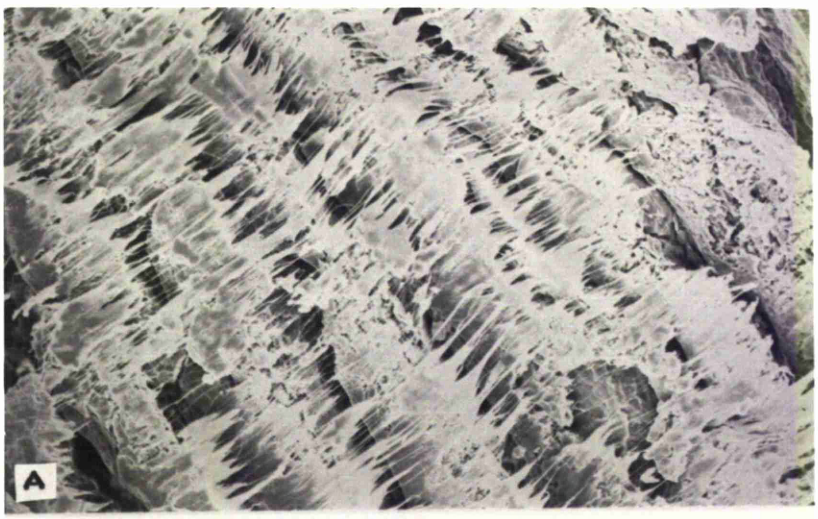
A

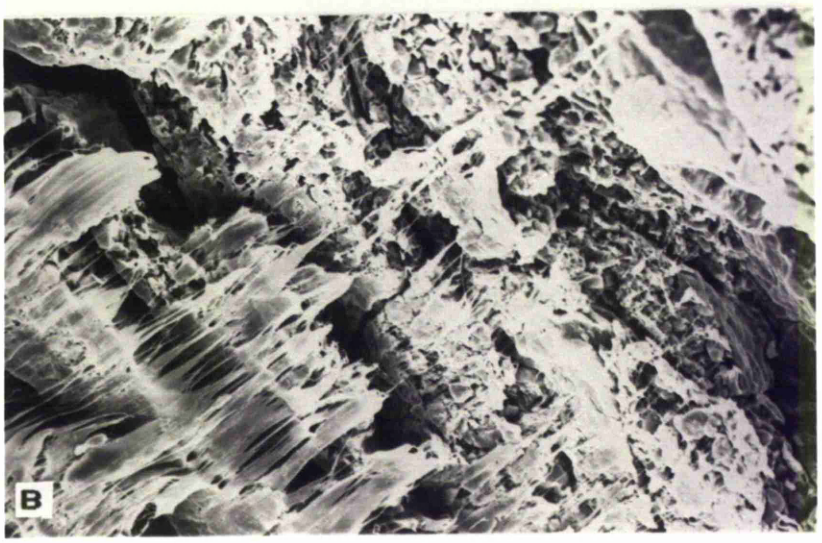
B

TABLE 3.12

TENSILE STRENGTH, $\sigma \times 10^{5}$ N/m^{2} AND HAMAKER CONSTANT, $A \times 10^{-20}$ N.m OF PVC AND PTFE IN AIR AND TEST LIQUIDS

Liquids	0:100		10:90		25:75		50:50		75:25		100:0	
	σ	A	σ	A	σ	A	σ	A	σ	A	σ	A
Methanol	5.62	0.23	8.46	1.13	10.95	1.34	4.59	1.07	0.47	0.01	0	1.91
Ethanol	5.03	0.16	7.21	1.11	11.26	1.35	5.37	1.13	0.97	0.13	0	2.25
Propanol	4.67	0.10	6.75	1.01	11.25	1.29	8.04	1.12	4.86	0.17	0.98	2.60
Hexanol	4.78	0.16	7.85	1.34	12.05	1.65	9.33	1.54	7.21	0.65	5.49	3.12
2methyl-2 butanol	4.46	0.16	6.86	1.29	10.68	1.64	9.45	1.58	7.53	0.75	9.71	3.60
Air	6.79	4.50	11.00	.56	19.20	1.18	17.8	1.57	11.6	1.18	12.1	11.4

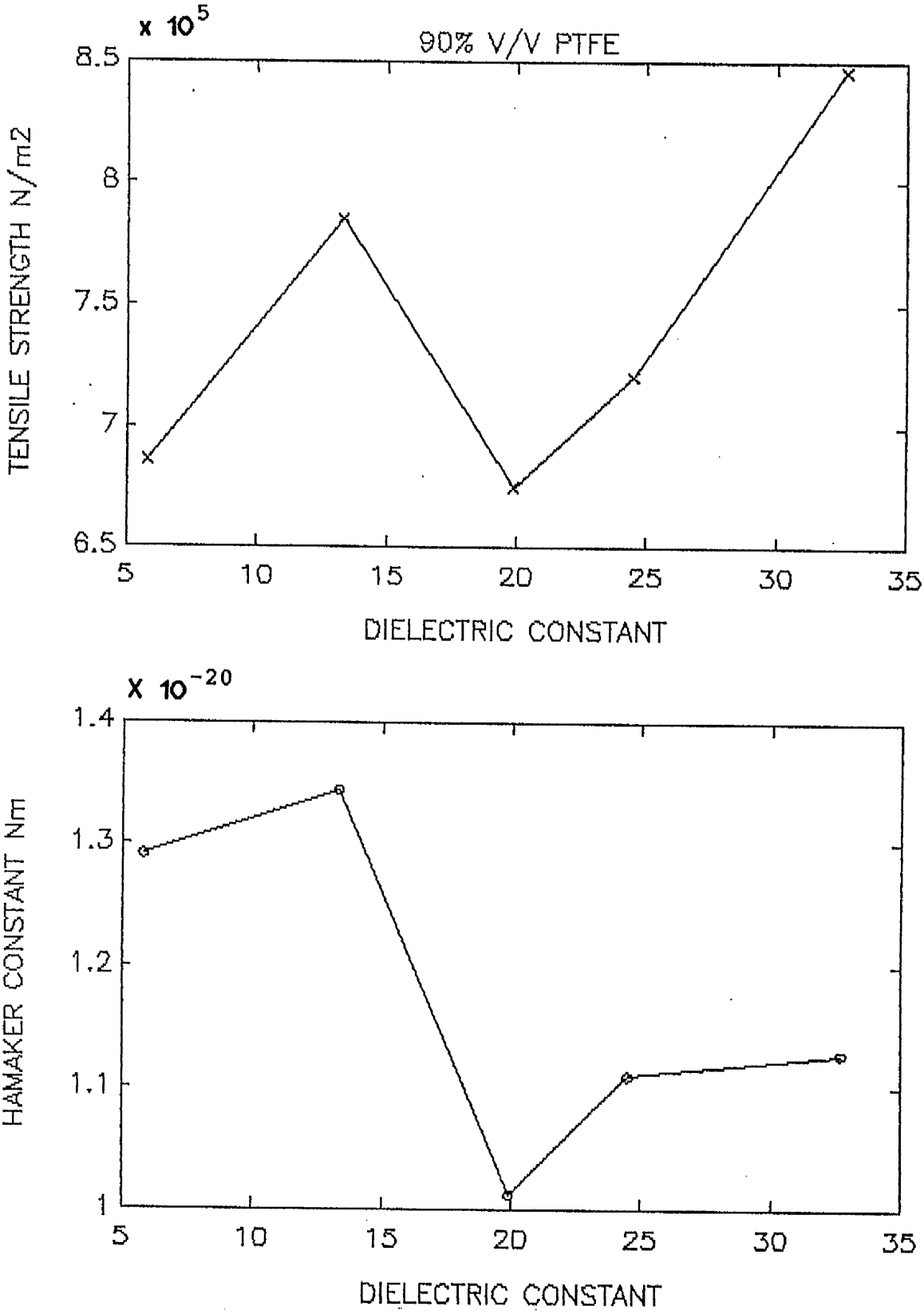

FIG. 3.29 RELATIONSHIPS BETWEEN CHANGES IN TENSILE STRENGTH AND HAMAKER CONSTANT TO CHANGES IN DIELECTRIC CONSTANT FOR 90 % PTFE TABLET

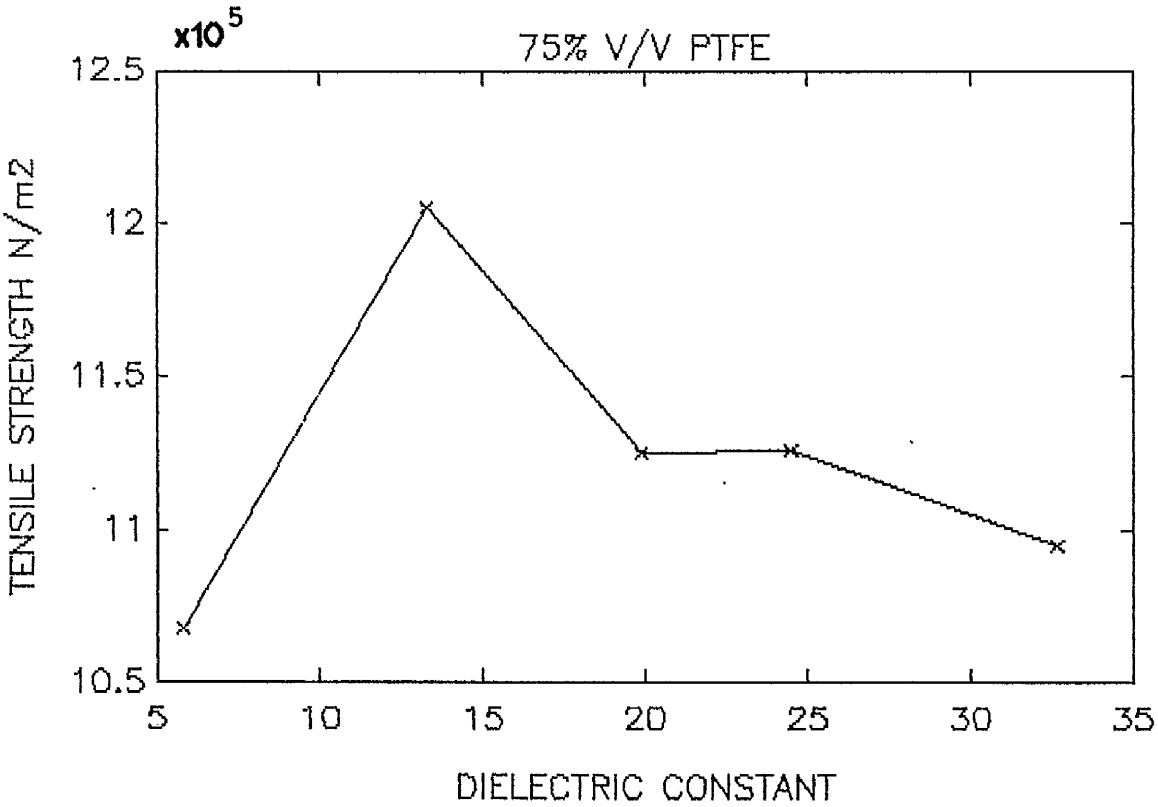

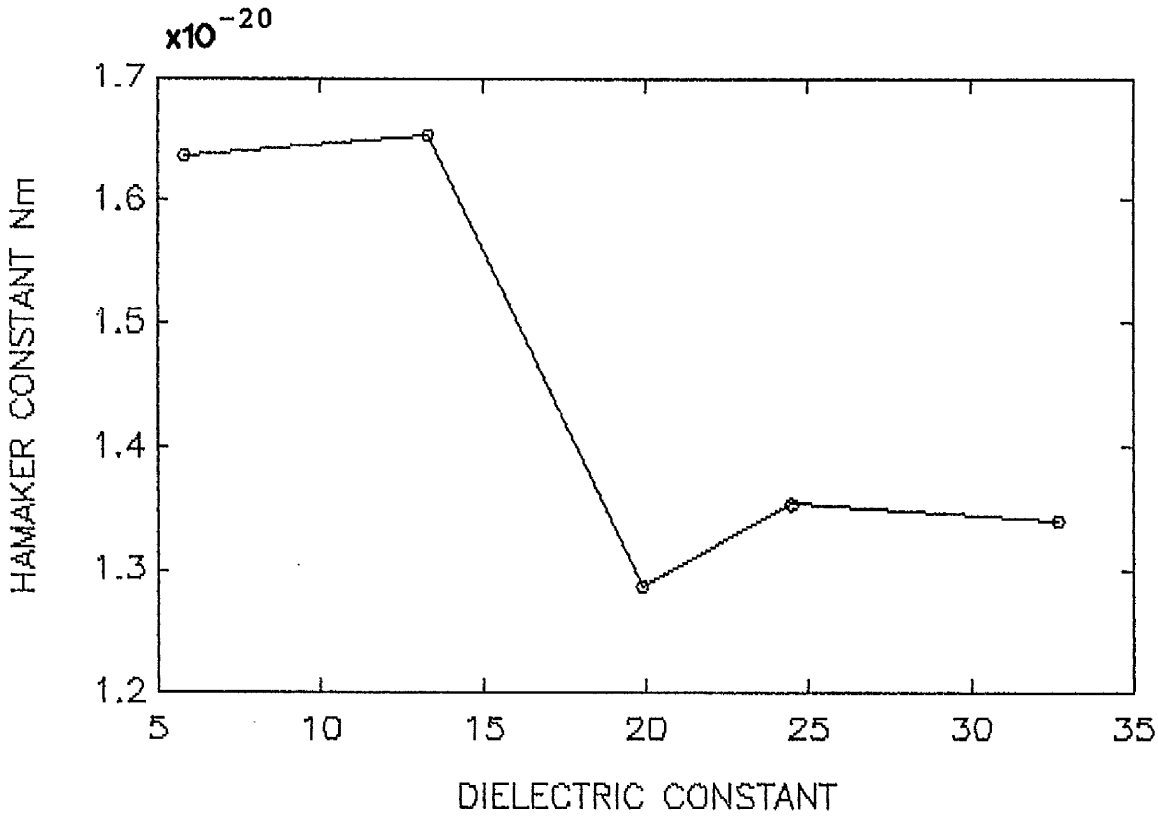

FIG. 3.30 RELATIONSHIPS BETWEEN CHANGES IN TENSILE STRENGTH AND HAMAKER CONSTANT TO CHANGES IN DIELECTRIC CONSTANT FOR 75 % PTFE TABLET

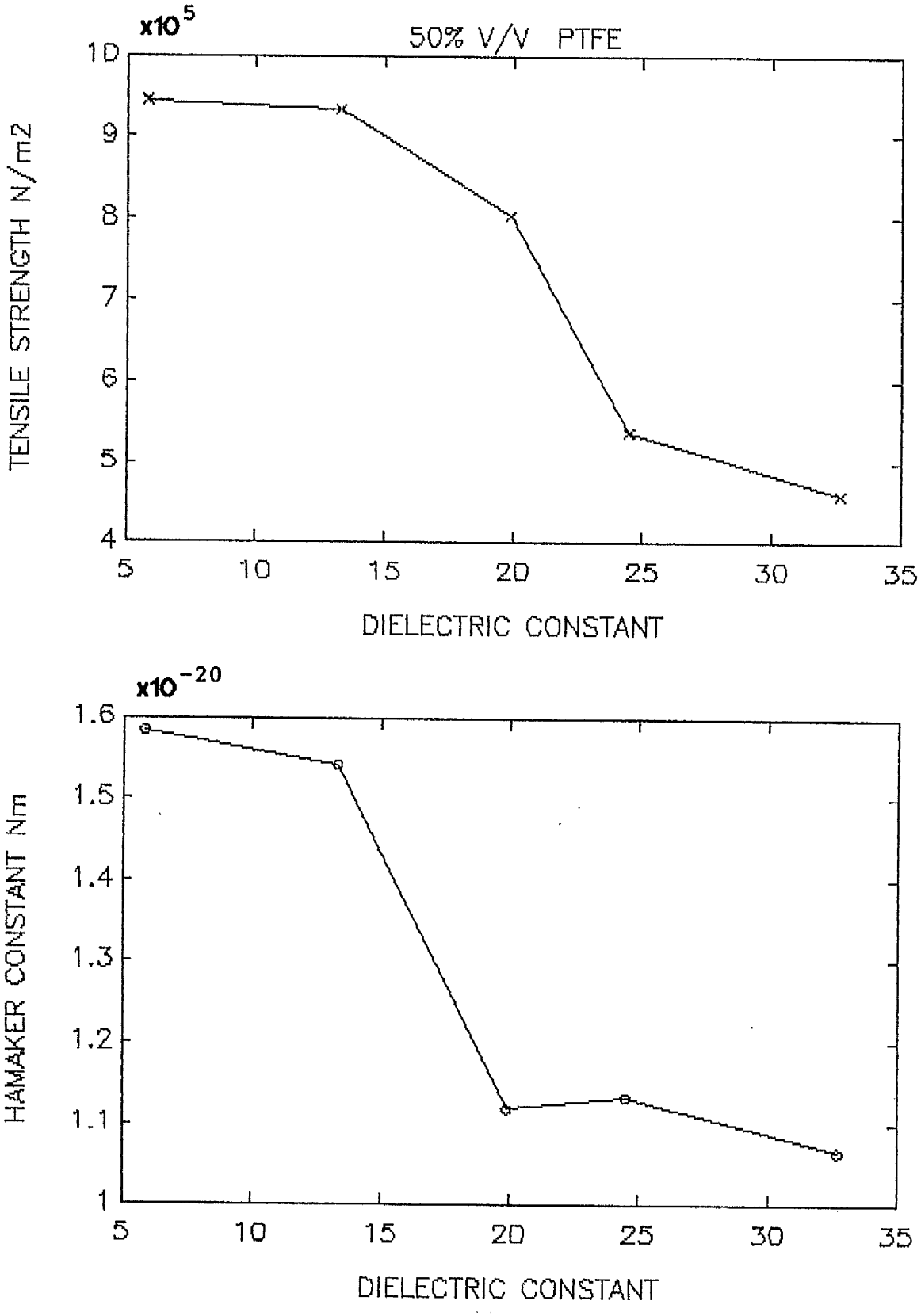

FIG. 3.31 RELATIONSHIPS BETWEEN CHANGES IN TENSILE STRENGTH AND HAMAKER CONSTANT TO CHANGES IN DIELECTRIC CONSTANT FOR 50 % PTFE TABLET

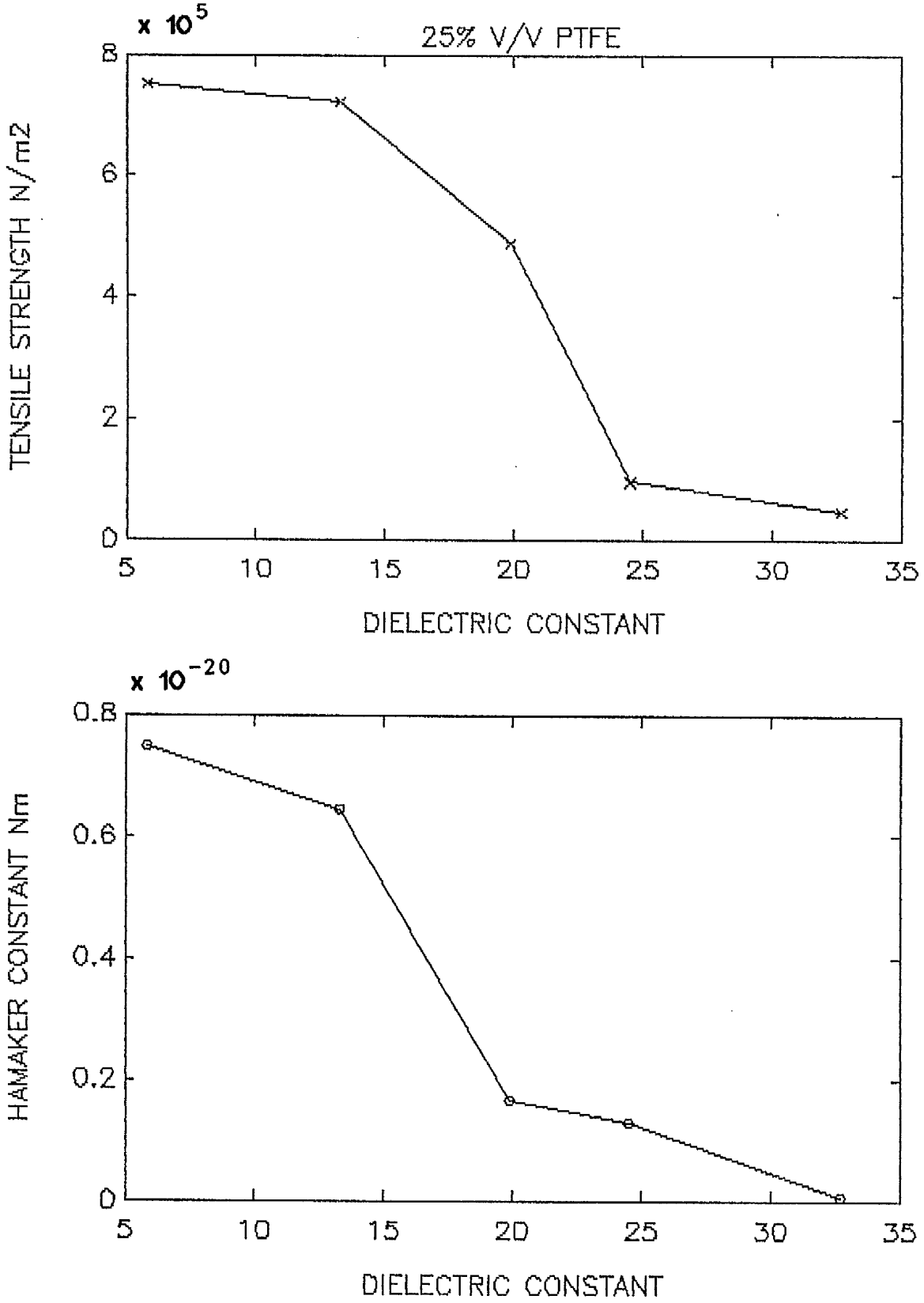

FIG. 3.32 RELATIONSHIPS BETWEEN CHANGES IN TENSILE STRENGTH AND HAMAKER CONSTANT TO CHANGES IN DIELECTRIC CONSTANT FOR 25 % PTFE TABLET

3 THE MIXTURE OF MAGNESIUM CARBONATE AND EMCOMPRESS

Table 3.13 shows the properties of mixtures of magnesium carbonate and Emcompress, their thicknesses, porosities and tensile strengths. A plot of the relationship between porosity and composition is shown in Fig. 3.33. As an increasing amount of Emcompress results in a reduction of porosity, a stronger compact was expected. However, the opposite effect was observed (Fig. 3.17 and table 3.9). The tensile strength increases when the porosity increases. A higher tensile strength was obtained when the composition of magnesium carbonate increased. This result might be due to the highly extensive fragmentation of Emcompress. The fragmaentation of this powder is well recognized (Duberg and Nystrom, 1985). The adition of magnesium carbonate reduces the magnitude of fragmentation and increases the energy within the tablet since magnesium carbonate is less fragmented, therefore it gives a higher stress relaxation energy which results in a stronger compact being formed. The result is in accordance with the work of Humbert-Drotz (1983) who found that the addition of Avicel powder into Emcompress reulted in an increased tensile strength.

TABLE 3.13

PROPERTIES OF MIXTURES OF MAGNESIUM CARBONATE AND EMCOMPRESS

MAG:EMC.	weight (gm.)	thickness (mm)	diameter (mm)	density g/cm^3	porosity
100:0	0.5725	3.0740	12.8520	2.1777	0.3410
75:25	0.5698	2.8420	12.8120	2.2995	0.3193
50:50	0.5694	2.6840	12.8260	2.3425	0.2993
25:75	0.5691	2.5120	12.8160	2.4019	0.2688
0:100	0.5676	2.3520	12.7860	2.5677	0.2680

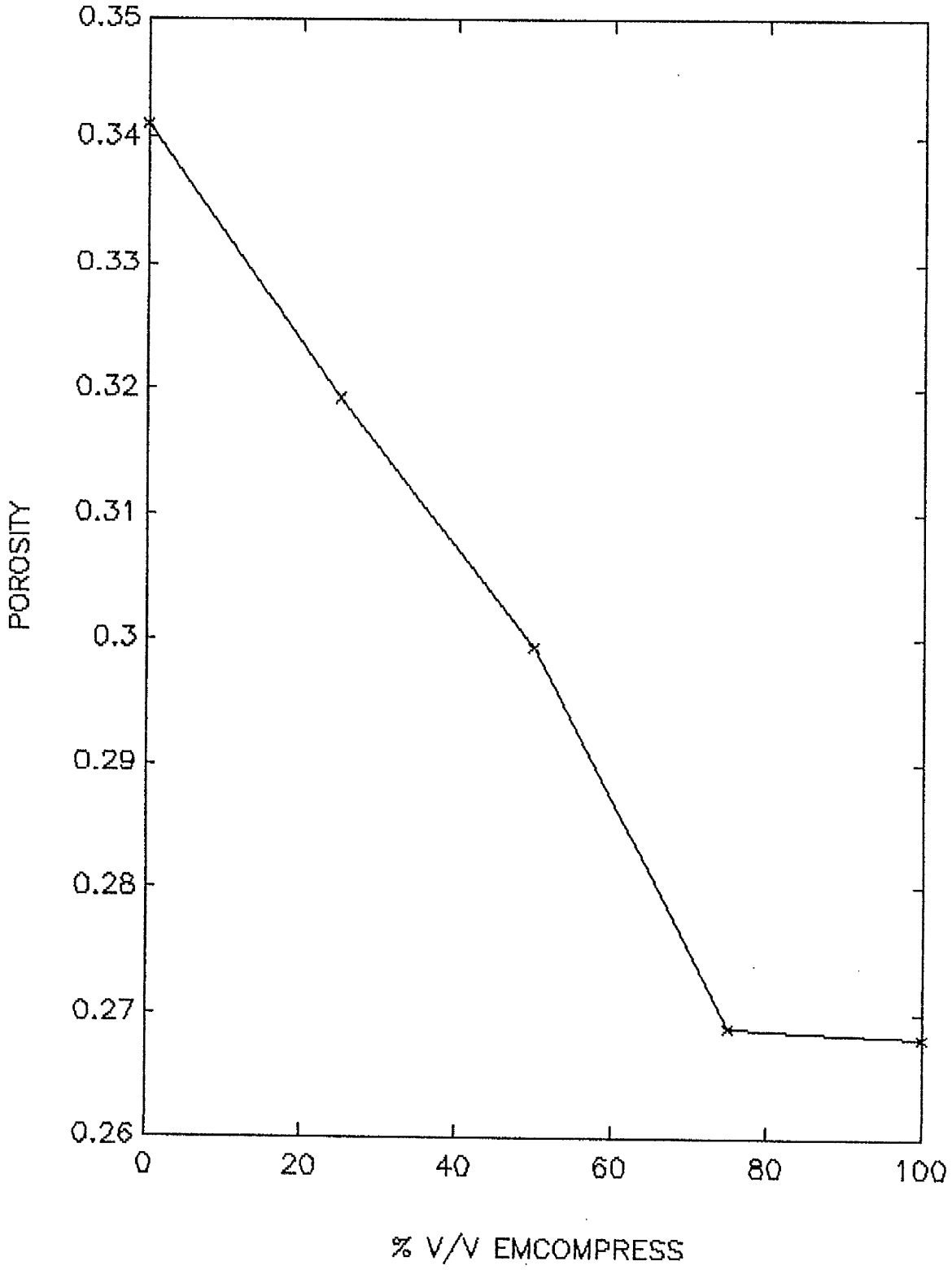

FIG. 3.33 THE RELATIONSHIP BETWEEN POROSITY AND COMPOSITIONS OF MIXTURE OF MAGNESIUM CARBONATE AND EMCOMPRESS

CHAPTER 4

CONCLUSIONS

Results obtained from the calculation of Hamaker constants in a series of alcohols show a change in Hamaker constant with dielectric constants for every powder. These changes are in accordance with tensile strength values. Plots between the dielectric constant and tensile strengths or Hamaker constant exhibit similar trends,indicating a relationship between both terms. Since the tensile strength measurement is obtained from a fracture along a bonding line between particles (Butcher et al., 1974), the bonding in these compacts can largely be accounted for by Van der Waals forces.

The results were then applied to binary systems. Agreement between predicted strength and measured strength was not observed. The magnitude of bond strengths could not be predicted from a knowledge of Hamaker constant, unless a careful consideration of tablet structure was taken into account. However, the studies of strength changes in mixtures of PVC and PTFE in a series of alcohols exhibit a relationship between tensile strength and Hamaker constant for every proportion. Therefore , the studied compacts are formed by bonds due to Van der Waals forces.

A relationship between tensile strength and disintegration time was also found. Therefore the Hamaker constant can be used to predict relative disintegration times.

GENERAL CONCLUSION

The surface energy of a solid is a fundamental characteristic, a knowledge of which would be of advantage in the understanding of many pharmaceutical processes. As well as conventional pharmaceutical processes such as tabletting and adsorption altered surface properties may result in a change in distribution of a particulate system in the body giving rise to the possibilities of targetting. The work described in the thesis has examined the measurement of surface free energies for powder systems and has defined the condition required to obtain reliable results. The values can hence be ultilised to gain an deeper understanding of pharmaceutical processes involving solid surfaces.

Compressed tablets are the most commonly used pharmaceutical dosage form. Conventional tablets are required to be strong enough to withstand subsequent processing and handling and yet be such that they disintegrate readily when exposed to fluids. Both tablet strength and disintegration are a function of bonds formed during the tabletting process.

Although many studies have been directed towards understanding the tabletting process and the formulation of tablet is no longer purely empirical, it is still not possible to "design" a tablet formulation. Of all the areas in the tabletting process that have been examined, studies on the bonding between particles during compression has been neglected. The work described in this thesis has attempted to elucidate

bonding mechanisms through the use of surface energy measurements. The approach is similar to that of Rowe (1988 a,b, c) but instead of using solubility parameters, attractive forces are described in terms of Hamaker constants derived from surface energy values.

It has been shown that the strength and disintegration of tablets of single components could be accounted for by Van der Waals forces but that extrapolation of these results to binary mixtures was not simple. The approach is of value in that it attempts to account for strength and disintegration properties of tablets in terms of a fundamental material characteristic and should enable logical predictions to be made. Future work could be directed towards appying the concepts to more familiar pharmaceutical materials and to a deeper study of mixtures.

REFERENCES

Adam, N.K.

The chemical structure of solid surfaces as deduced from contact angles

Advances in Chemistry Series 43, American Chemical Society, Washington P 52-56 (1964)

Addinall, E. and Hackett, P.

The effect of platen conditions on the tensile strengths of rock-like materials

Civil engineering and public work review 59, 1250-1253 (1964)

Alderborn, G. and Nystrom, C.

Studies on direct compression of tablets

IV. The effect of particle size on the mechanical strength of tablets

Acta. Pharm. Suec. 19, 381-390 (1982a)

Alderborn, G. and Nystrom, C

Studies on direct compression of tablets

III The effect on tablet strength of changes in particle shape and texture obtained by milling

Acta. Pharm. Suec. 19, 147-156 (1982b)

Alderborn, G. and Nystrom, C.

Radial and axial tensile strength and strength variability of paracetamol tablets

Acta. Pharm. Suec., 21, 1-8 (1984)

Alderborn, G., Pasanen, K. and Nystrom, C.
Studies on direct compression of tablets XI
Characterization of particle fragmentation during compaction by permeametry measurements of tablets
Int. J. Pharm. 23, 79-86 (1985)

Alderborn, G., Lang, P.O., Sagstron, A. and Kristensen, A.
Compression characteristics of granulated materials
I. Fragmentation propensity and compactability of some granulations of a high dosage drug
Int. J. Pharm. 37, 155-161 (1987)

Andrews, E.H. and King, N.E.
Surface energetics and adhesion
Polymer surface, Clark, D.T. and Feast, W.T. ed., Willey, New York
P 47-63 (1978)

Ayala, R.E., Casassa, E.Z. and Parfitt, G.D.
A study of the applicability of the capilary rise of aqueous solutions in the measurements of contact angle in powder systems
Powder Tech. 51, 3-14 (1987)

Bartell, F.E. and Osterhof, H.J.
Determination of the wettability of a solid by a liquid
Ind. and Eng. Chem. 19, 1277-1280 (1927)

Bartell, F.E. and Zuidema, H.H.
Wetting characteristics of solids of low surface tension such as Talc, Waxes and Resins
J. Amer. Chem. Soc. 58, 1449-1454 (1936)

Brook, D.B. and Marshall, K.
Crushing strength of compressed tablets I
Comparison of testers
J. Pharm. Sci. 57, 481-484 (1968)

Buckton, G.
Assessment of the wettability of powders
Ph.D. Thesis , University of London (1985)

Buckton, G. and Newton, J.M.
Assesment of the wettability and surface energy of a pharmaceutical powder by liquid penetration
J. Pharm. Pharmac. 37, 605-609 (1985)

Buckton, G. and Newton, J.M.
Assessment of the wettability of powders by use of compressed powder disc
Powder Tech. 46, 201-208 (1986)

Busscher, H.J., Van Pelt, A.W.J., de Jong, H.P. and Arends, J.
Effect of spreading pressure on surface free energy determinations by means of contact angle measurements
J. Col. Int. Sci. 95(1), 23-27 (1983)

Butcher, A.E., Fell, J.T. and Newton, J.M.
Tensile failure planes of powder compacts
Powder Tech. 9, 57-59 (1974)

Cain, J.B., Francis, D.W. and Venter, R.D. and Neumann, A.W.
Dynamic contact angles on smooth and rough surfaces
J. Col. Int. Sci. 94(1), 123-130 (1983)

Capes, C.E.
Handbook of powder technology particle size enlargement
Williams, J.C. and Allen, T. ed., Elsevier, Amsterdam (1980)

Carli, F. and Simioni, L.
Permeability and penetrability of solid beds in dosage form design and development
Drug Dev. and Ind. Pharm. 3(1), 1-21 (1977)

Carli, F. and Simioni, L.
Limitations of the Washburn equation in quantifying penetration rates
J. Pharm. Pharmac. 31, 128 (1979)

Carli, F., Colombo, I., Simioni, L. and Bianchini, R.
The effect of compression on the capillary microstructure of tablets
J. Pharm. Pharmac. 33, 129-135 (1981)

Carneiro, F.L.L.B. and Barcellos, A.
Concrete tensile strength
R.I.L.E.M. Bulletin 13, 97-107 (1953)

Carre, A. and Schultz, J.

Polymer-Aluminium adhesion

III Effect of a liquid environment

J. adhesion, 18, 171-184 (1984)

Cassie, A.B.D., Baxter, S.

Wettability of porous surfaces

Trans. Faraday Soc. 40, 546-551 (1944)

Chowhan, I.T. and Chow, Y.P.

Compression behaviour of pharmaceutical powders

Int. J. Pharm. 5, 139-148 (1980)

Cole, E.T., Rees, J.E. and Hersey, J.A.

Relations between compaction data for some crystalline pharmaceutical materials

Pharm. Acta. Helv. 50, 28-32 (1975)

Cook, D., Hone, C. and Newton, J. M.

The tensile strength of tablets of mixed components

J. Pharm. Pharmac. 27, 81P (1975)

Cook, G.D. and Summers, M.P.

The tensile strength of Aspirin-Emcompress tablets

J. Pharm. Pharmac. 37, 29P (1985)

Cooper, A.R. and Eaton, L.E.

Compaction behaviour of several ceramic powders

J. Amer. Cer. Soc. 45, 97-101 (1962)

Danjo, K. and Otsuka M.

The effect of temperature on diametral compression strength of δ-phenylbutazone and Barbital (formII) tablets

Chem. Pharm. Bulletin 36(2), 763-768 (1988)

Dann, J.R.

Forces involved in the adhesive process

I Critical surface tension of polymeric solids as determined with polar liquids

J. Col. Int. Sci. 32(2), 302-320, (1970a)

Dann, J.R.

Forces involved in the adhesive process

II Nondispersion forces at solid liquid interfaces

J. Col. Int. Sci. 32(2), 321-331 (1970b)

David, S.T. and Augsburger, L.L

Flexure test for determination of tablet tensile strength

J. Pharm. Sci. 63(6), 933-936 (1974)

David, S.T. and Augsburger, L.L

Plastic flow during compression of directly compressible fillers and its effect on tablet strength

J. Pharm. Sci. 66, 155-159 (1977)

de Boer ,A.H. ,Bolhius, G.K. and Lerk, C.F.

Bonding characteristics by scanning electron microscopy of powders mixed with magnesium stearate

Powder Tech. 20, 75-82 (1978)

Duberg, M. and Nystrom, C.
Studies on direct compression of tablets
VI. Evaluation of methods for the estimation of particle fragmentation during compaction
Acta. Pharm. Suec. 19, 421-436 (1982)

Duberg, M. and Nystrom, C.
Studies on direct compression of tablets
XII The consolidation and bonding properties of some pharmaceutical compounds and their mixture with Avicel 105
Int. J. Pharm. Tech. and Prod. Mfr. 6(2), 17-25 (1985)

Efentakis, E.
An investigation of the wettability of pharmaceutical powders
Ph.D. Thesis, Manchester University (1979)

Elliott, G.E.P. and Riddiford, A.C.
Dynamic contact angles
I The effect of impresses motion
J. Col. Int. Sci. 23, 389-398 (1967)

El-Shimi, A. and Goddard, E.D.
Wettability of some low energy surfaces
I air /liquid /solid interface
J. Col. Int. Sci. 48(2), 242-248 (1974)

Endicott, C.J., Lowenthal, W. and Gross, H.M.
New instrument and method for evaluating tablet fracture resistance
J.Pharm. Sci. 50 ,343-34 (1961)

Fell, J.T. and Newton, J.M.
The tensile strength of lactose tablets
J. Pharm. Pharmac. 20, 657-658 (1968)

Fell, J.T. and Newton, J.M.
The prediction of the tensile strength of tablets
J. Pharm. Pharmac. 22, 247-248 (1970a)

Fell, J.T. and Newton, J.M.
Determination of tablet strength by the diametral compression test
J. Pharm. Sci. 59, 688-691 (1970b)

Fell, J.T. and Effentakis, E.
The wetting of powders of acetylsalicylic acid, salicylic acid, phenacetin and paracetamol
J. Pharm. Pharmac. 30, 538-541 (1978)

Fell, J.T. and Effentakis, E.
Contact angle determinations on pharmaceutical powders:
A comparison of two methods
Int. J. Pharm. 4, 153-157 (1979)

Fraser, D.R.
An investigation of some factors influencing tablets strength
Proceedings of the first international conference on the compaction and consolidation of particulate matter, Goldberg, A.S., Powder Advisory Centre, London, p 149-154 (1973)

Fowkes, F.M.

Determination of interfacial tensions, contact angles and dispersion forces in surface by assuming additivity of intermolecular interaction in surface

J. Phys. Chem. 66, 382 (1962)

Fowkes, F.M.

Attractive forces at interfaces

Ind. Eng. Chem. 56(12), 40-52 (1964)

Fox, H.M. and Zisman, W.A.

The spreading of liquids on low energy surfaces

I. Polytetrafluoroethylene

J. Col. Int. Sci. 5, 541-531 (1950)

Fukuoka, E., Kimura, S. and Yamazaki, M.

The role of penetration of liquid into tablets

Chem. Pharm. Bull. 29(1), 205-212 (1981)

Fukuoka, E., Kimura, S. and Yamazaki, M.

The rate of penetration of liquid into tablet II influence of second ingredient and mixing ratio

Chem. Pharm. Bull. 31(1), 1030-1039, (1983)

Ganderton, D,

The effect of distribution of magnesium stearate on the penetration of a tablet by water

J. Pharm. Pharmac. supp. 21, 9S-18S (1969)

Ganderton, D. and Selkirk, B.
The effect of granule properties on the pore structure of tablets of sucrose and lactose
J. Pharm. Pharmac. 22, 345-353 (1970)

Ganderton D. and Fraser, D.R.
Some observations of the penetration and disruption of tablets by water
J. Pharm. Pharmac. 22S, 95S-103S (1970)

Girifalco, L.A. and Good, R.J.
A theory for the estimation of surface and interfacial energies
I. derivation and application to interfacial tension
J. Phys. Chem. 61, 904-909 (1957)

Good, R.J.
Theory for the estimation of surface and interfacial energies
VI surface energies of some fluorocarbon surface from contact angle measurements
Contact angles wettability and adhesion, Advances in Chemistry series 43, American Chemical Society, Washington, 1964

Gordon, J.E.
The new science of strong materials, Penguin books, Middlesex, England (1976)

Groves, M.J. and Alkan, M.H.
A note on the collapse of disintegrating tablets under laminar flow conditions
Int. J. Pharm. 3, 81-86 (1979)

Hamaker, H.C.
The London-Van der Waals attraction between spherical particles
Physica IV 10, 1058-1072 (1937)

Hansen, R.S. and Miotto, M.
Relaxation phenomena and contact angle hysteresis
J. Am. Chem. Soc. 79, 1765 (1957)

Hanus, E.J. and King, L.D.
Thermodynamic effects in the compression of solids
J. Pharm. Sci. 57,677-684 (1968)

Hansford, D.T., Grant, D.J.W. and Newton, J.M.
The influence of processing variables on the wetting properties of a hydrophobic powders
Powder Tech. 26, 119-126 (1980)

Harkins W.D. and Brown F.E.
The determination of surface tension and the weight of falling drops: The surface tension of water and benzene by the capillary heihgt method
J. Amer. Chem. Soc. 41, 499-524 (1919)

Heckel, R.W.
An analysis of powder compaction phenomena
Trans. Metall. Soc. AIME. 221, 1001-1008 (1961)

Heimenz, P.C.

Van der Waals attraction and floculation

Principles of colloid and surface chemistry 2nd ed., Marcel Dekker Inc., New york, P.611-676 (1986)

Hersey, J.A., Cole, E.T. and Rees, J.E.

Deformation of particles during briqueting

Nature Phys. Sci., 230 (12), 96 (1971)

Hersey, J.A., Cole, E.T. and Rees, J.E.

Powder consolidation during compaction

Proceedings of the first international conference on the compaction and consolidation of particle matter, Goldberg, A.S. ed., Powder advisory centre, London, p 165, 1972

Huntington, A.K.

The concentration of metallifrons sulphides by flotation

Trans. Fara. Soc., 1, 345 (1906)

Humbert-Droz, P., Gurny, R., Mordier, D. and Doelker, E.

Densification behaviour of drug presenting availability problems

Int. J. Pharm. Tech. and Prod. Mfr., 4(2), 29-35 (1983a)

Humbert-Droz, P., Mordier, D. and Doelker, E.

Densification behaviour of powder mixtures

Acta Pharm. Tech. 29(2), 69-73 (1983b)

Israelachvili, J.N.

Van der Waals dispersion force contribution to works of adhesion and contact angles on the basis of macroscopic theory

J. Chem. Soc. Faraday trans 2, 1729-1738 (1973)

Israelachvili, J.N.

Intermolecular and surface forces, Academic press, London (1985)

Jaycock, M.J. and Parfitt, G.D.

Introduction to interface and the forces involved in their formation

Chemistry of interface,Ellis Horwood Ltd., Chichester p11-21 (1981)

Johnson, R.E., Dettre, R.H.

Contact angle hysteresis

I Study of an idealized rough surface

Advances in Chemistry Ser. 43, American Chemical Society, Washington 112-145 (1964a)

Johnson, R.E., Dettre, R.H.

Contact angle hysteresis

III Study of an idealized heterogenous surface

J. Phys. Chem., 68, 1744-1749 (1964b)

Johnson, R.E., Dettre, R.H.

Wettability and contact angles

Surface and colloid science, vol. 2, Matijevic, E. ed., Wiley, New York , 85-153, (1969)

Kaelble, D.H.
Dispersion polar surface tension properties of organic solids
J. adhesion, 2, 66-81 (1970)

Kinloch, A.J. and Young, R.J.
Fracture behaviour of polymers, Elsevier Applied Science, England, p 43-73 (1985)

Kossen, N.W.F. and Hertjes, P.M.
The determination of the contact angle for systems with a powder
Chem. Eng. Sci., 20, 593-599 (1965)

Krupp, H.
Particle adhesion theory and experiment
Advanc. Col. Int. Sci., 1 ,111-239 (1967)

Lerk, C.F., Schoonen, A.J.M. and Fell, J.M.
Contact angles and wetting of pharmaceutical powders
J. Pharm. Sci., 65, 843-847 (1976)

Lerk, C.F., Lagas, M., Boelstra, J.P. and Broersma, P.
Contact angles of pharmaceutical powders
J. Pharm. Sci.,66(2), 1480-1481 (1978)

Lerk, C.F., Bolhuis, G.K. and de Boer, A.H.
Effect of microcrystalline cellulose on liquid penetration in and disintegration of directly compressed tablets
J. Pharm. Sci., 68, 205-210 (1979)

Leuenberger, H.

The compressibility and compactability of powder systems

Int. J. Pharm., 12, 41-55 (1982)

Liao, W.C. and Zatz, J.L.

Critical surface tension of pharmaceutical solids

J. Pharm. Sci., 68(4), 488-494 (1979)

Lifshitz, E.M.

The theory of molecular attractive forces between solids

Soviet Phys. JETP, 2, 73-83 (1956)

Lowe A.C. and Riddiford A.C.

An assessment of introduction at the polytetrafluoroethylene water interface from dynamic contact angle studies

J. Chem. Soc.(D), 387-388 (1970)

Luangtana-Anan, M.

Surface free energy determination on powders

Powder Tech., 52, 215-218 (1987)

Mack, G.L.

The determination of contact angles from measurements of the dimensions of small bubbles and drops I

J. Phys. Chem., 40(2), 159-167 (1936)

Mahanty, J. and Ninham, B.W.

Dispersion forces

Colloid Science , Ottiwill R.H. and Rowell, R.L. ed., Academic press, London (1976)

Mitchell, N.B.

The indirect tension test for concrete

Materials research and standards, 1, 780-788 (1961)

Matsunaga, T.

Surface free energy analysis of polymers and its relation to surface composition

J. App. Poly. Sci., 21, 2847-2854 (1977)

Mohammad, H.A.H.

Studies on the wettability of pharmaceutical powders

Ph.D. Thesis, Manchester, (1983)

Mohammad, H.A.H. and Fell J.T.

Contact angles of powder mixtures consisting of spherical particles

Int. J. Pharm., 11, 149-154 (1982)

Mohammad, H.A.H. and Fell J.T.

Surface free energy characteristics of mixtures

Int. J. Pharm., 17, 39-46 (1983)

Murphy, W.J., Roberts, M.W. and Ross, R.H.

Contact angle studies of some low energy polymer surfaces

J. Chem. Soc. Faraday Trans., 68, 1190-1199 (1972)

Nagami, H., Nagai, T. and Fukuoka, E.
Disintegration of the aspirin tablets containing potato starch and microcrystalline cellulose in various concentration
Chem. Pharm. Bull., 17, 1450-1455 (1969)

Nelson, E.
Tensile strength tests for compressed tablets
Drug standards, 24, 1-5 (1956)

Neumann, A.W.
Contact angles and their temperature dependence:
Thermodynamic status, measurement, interpretation and application
Adv. Col. Int. Sci., 4, 105-191 (1974)

Neumann, A.W., Omenyi, S.N. and Van Oss, C.J.
Negative Hamaker coefficients
I. Particle engulfment or rejection at solidification fronts
Col. Poly. Sci., 257, 413-419 (1979)

Neumann, A.W., Omenyi, S.N. and Van Oss, C.J.
Attraction and repulsion of solid particles by solidification fronts 3. Van der Waals interactions
J. Phys. Chem., 86, 1267-1270 (1982)

Newton, J.M., Rowley, G., Fell, J.T. Peacock, D.G. and Ridgway,K.
Computers analysis of the relation between tablet strength and compaction pressure
J. Pharm. Pharmac., 23S, 195S-201S (1971)

Newton, J.M. and Grant, D.J.W.
The relation betwen the compaction pressure porosity and tensile strength of compacted powders
Powder Tech., 9, 295-297 (1974)

Newton, J.M., Cook, D. and Hollebon, C.
The strength of tablets of mixed components
J. Pharm. Pharmac., 29, 247-248 (1977)

Nystrom, C. Alex, W. and Malmqvist, K.
A new approach to tensile strength measurement of tablets
Acta Pharm. Suec, 14, 317-320 (1977)

Nystrom C.
Axial tensile strength of tablets
Acta Pharm. Suec, 18, 84 (1981)

Nystrom, C. Malmqvist, K. and Mazur, J.
Measurement of axial and radial tensile strength of tablets and their relation to capping
Acta Pharm. Suec , 15, 226-232 (1978)

Nystrom, C. Mazur, J. and Sjogren, J.
Studies on direct compression of tablets II
The influence of the particle size of a dry binder on the mechanical strength of tablets
Int. J. Pharm., 10, 209-218 (1982)

Nystrom, C. and Karehill, P.G.

Studies on direct compression of tablets

XVI The use of surface area measurements for the evaluation of bonding surface area in compressed powders

Powder Tech., 47, 201-209 (1986)

Ohm, A. and Lippold, B.C.

Surface tension of solid drugs and its correlation with solubility

Int. J. Pharm. tech. and Prod. Mfr., 6(4), 1-6 (1985)

Padday, J.F.

A new method for measuring the spreading coefficient of a liquid on a solid surface

Second international congress of surface activity III, Butterworths Scientific publication, London, p 136 (1957)

Pease, D.C.

the significance of the contact angle in relation to the solid surface

J. Phys. Chem., 49, 107-110 (1945)

Phillips, M.C. and Riddiford, A.C.

Dynamic contact angles

II Velocity and relaxation effect for various liquids

J. Col. Int. Sci., 41(1), 77-85 (1972)

Poynting, J.H. and Thomson, J.J.
Properties of matter, Textbook of Physics, Griffin & Cy. Ltd., London, p 156 (1905)

Ratner, B.D. and Hoffman, A.S.
Characterization of hydrophilic hydrophobic polymeric surfaces by contact angle measurements
J. Col. Int. Sci., 82(1), 25-37 (1981)

Ray, B.R. and Bartell, F.E.
Hysteresis of contact angle of water on paraffin effect of surface roughness and of purity of paraffin
J. Col. Int. Sci., 8, 214-223 (1953)

Reir, G.E. and Shangraw, R.F.
Microcrystalline cellulose in tableting
J. Pharm. Sci., 55(5), 510-514 (1966)

Ridgway, K.
Aspects of pharmaceutical engineering testing tablets by diametral crushing
Pharm. J., 26, 709-712 (1970)

Rowe, R.C.
Adhesion of film coating to tablet surfaces-a theoretical approach based on solubility parameter
Int. J. Pharm., 41, 219-222 (1988a)

Rowe, R.C.
Interaction of lubricants with microcrystalline cellulose and anhydrous lactose: A solubility parameter approach
Int. J. Pharm., 41, 223-226 (1988b)

Rowe, R.C.
Interactions in the ternary powder system microcrystalline cellulose, magnesium stearate and colloidal silica:
A solubility parameter approach
Int. J. Pharm. 45, 259-261 (1988c)

Rudnick, A., Hunter, A.R. and Holden, F.C.
An analysis of the diametral-compression test
Materials research and standards, 1, 283-289 (1963)

Rumpf, H.
The strength of granules and agglomeration, Knapper, W.A. ed.,
Interscience, New York, 379-418 (1962)

Sato, M.
Studies on the wetting effect and the surface tension of solids
A formular for determining surface tension of solids
Proc. Japan Acad., 30, 193-198 (1954)

Seelig, R.P. and Wulff, J.
Pressing operation in fabrication of articles by powder metallurgy
Trans. Am. Inst. Mining met. Engrs., 166, 492-504, discussion, 504-505 (1946)

Shaw, J.

Colloid stability

Introduction to colloid and surface chemistry 3rd.edn.,p 183-212

Butterworths, London, (1986)

Sheikh-Salem, M. and Fell, J.T.

Compaction characteristics of mixtures of materials with dissimilar compaction mechanisms

Int. J. Pharm. Tech. and Prod. Mfr., 21(1), 19-22 (1981)

Sheikh-Salem, M. and Fell, J.T.

The tensile strength of tablets of lactose, sodium choride and their mixtures

Acta Pharm Suec., 19, 391-396 (1982)

Shotton, E. and Ganderton, D.

The strength of compressed tablets

PartI The measurement of tablet strength and its relation to compression forces

J. Pharm. Pharmac., 12S, 87T-92T (1960)

Shotton, E. and Ganderton, D.

PartII the bonding of granules during compression

J. Pharm. Pharmac. 12S, 92T-96T (1960)

Stamm, A., Gissinger, D., Boymond, C.

Quantitative evaluation of the wettability of powders

Drug Dev. Ind. Pharm., 10, 381-408 (1984)

Stockdale, G.f., Tooley, F.V. and Ying, C.W.
Changes in the tensile strength of glass caused by water immersion treatment
J. Am. Cer. Soc., 34(4), 116-121 (1951)

Studebaker, M.L. and Snow, C.W.
The influence of ultimate composition upon the wettability of carbon blacks
J. Phys. Chem., 59, 973-976 (1955)

Tabor, D.
Attractive surface forces
Colloidal dispersions, Goodwin, J.W. , Henry Ling Ltd., Dorset Press, Dorset, P 23-46 (1982)

Travers, D.N. and Merriman, M.P.H.
Temperature changes occurring during the compression and recompression of solids.
J. Pharm. Pharmac., 22S, 11S-16S (1970)

Van Kamp,H.V. Bolhius, G.K. and Kussendrager, K.D. and Lerk, C.F.
Studies on tableting properties of lactose IV dissolution and disintegration properties of different types of crystalline lactose
Int, J. Pharm., 28, 229-238 (1986a)

Van Kamp, H.V., Bolhius, G.K. de boer, A.H. Lerk, C.F. and Huen,L.
The role of water uptake on tablet disintegration
Pharm. Acta. Helv.,6(1), 22-29 (1986b)

Van Oss, C.J., Absolom, D.R. and Neumann, A.W.
The hydrophobic effect: Essentially a Van der Waals interaction
Col. Poly. Sci., 258, 424-427 (1980)

Van Oss, C.J and Visser, J.
The concept of negative Hamaker Coefficient II Thermodynamics, experimental evidence and applications
Advan. Col. Int. Sci., 18, 133-148 (1983)

Van Oss, C.J. and Good, R.J.
The equilibrium distance between two bodies immersed in a liquid
Col. Surf., 8(4), 373-381 (1984)

Visser, J.
On Hamaker constants: A comparison between Hamaker constants and Lifshitz-Van der Waals constants
Advan. Col. Int. Sci., 3, 331-363 (1972)

Vromans, H. Bolhius, G.K. and Lerk, C.F.
Magnesium stearate susceptibility of direct compressible materials as an indication of fragmentation properties
Powder Tech., 54, 39-44 (1988)

Vromans, H. and Lerk, C.F.
Densification properties and compactability of mixtures of pharmaceutical excipients with and without magnesium stearate
Int. J. Pharm., In press (1988)

Wan, L.S.C. and Choong, Y.L.
The effect of excipient on the penetration of liquid into tablets
Pharm. Acta. Helv., 61, 150-156 (1986)

Washburn, E.W.
The dynamic of capillary flow
Physical review, 17, 273-283 (1921)

Wenzel, R.N.
Resistance of solid surfaces to wetting by water
Ind. Eng. Chem., 28(8), 988-994 (1936)

Witvoet, ω.
Enige aspecten van het dispergeerproces
Ph.D. Thesis, Netherland (1971)

Wood, J.A. and Harder, S,W.
The adhesion of film coating to the surfaces of compressed tablets
Canadian J. of Pharm. Sci., 5(1), 18-23 (1970)

Wu, S.
Calculation of interfacial tension in polymer systems
J. Polym. Sci. part C, 34, 19-30 (1971)

Yang, Y.W. and Zografi, G.
Use of the Washburn-Rideal equation for studying capillary flow in porous media
J. Pharm. Sci., 75, 719-721 (1986)

York, P. and Pilpel, N.

The tensile strength and compression behaviour of lactose, four fatty acids and their mixtures in relation to tableting

J. Pharm. Pharmac., 25S, 1P-11P (1973)

Zisman, W.A.

Influence of constitution on adhesion

Ind. Eng. Chem., 55 (10), 19-38 (1963)

Zografi, G.

Surface effects in the design of solid dosage forms

Compilation of Symposium papers 5th National meeting

A.Ph.A. Academy of Pharmaceutical Science, Washington, D.C. P190 (1968)

Zografi, G. and Tam, S.

Wettability of pharmaceutical solids: estimation of solid surface polarity

J. Pharm. Sci., 65(8), 1145-1149 (1976)

Zografi, G. and Johnson, B.

Effect of surface roughness on advancing and receding contact angles

Int. J. Pharm., 22, 159-176 (1984)

APPENDIX 1

```
function res=manicalb
disp('interfacial forces for mix. of PVC,PTFE')
        g1=18.;g2=46.;gd1=16.;gd2=20.;gp1=2.;gp2=26.;
        x=[.9 .75 .5 .25];
for i=1:4
        for n=1:5
                if n==1
                        g3=23.7;
                        gd3=18.2;
                        gp3=5.5;
                end
                if n==2
                        g3=23.7;
                        gd3=19.3;
                        gp3=4.4;
                end
                if n==3
                        g3=23.0;
                        gd3=19.5;
                        gp3=3.5;
                end
                if n==4
                        g3=25.24;
                        gd3=22.75;
                        gp3=2.49;
                end
                if n==5
                        g3=24.62;
                        gd3=22.89;
                        gp3=1.73;
                end

s1=x(i)*g1+(1-x(i))*g2;
s2=-2*x(i)*(1-x(i))*(sqrt(gp1*gp2)+sqrt(gd1*gd2));
s3=x(i)*g1+g3-2*x(i)*(sqrt(gp1*gp3)+sqrt(gd1*gd3));
s4=(1-x(i))*g2+g3-2*(1-x(i))*(sqrt(gp2*gp3)+sqrt(gd2*gd3));
s=-((s1+s2-s3-s4)*12*pi*1.82^2);

res(i,n)=s;
% disp('X1 value is : ');disp(x(i));
% disp('N  value is : ');disp(n);
% disp('S  calculated : ');disp(s);
% pause(3);
end;
end
```